EUROPEAN ORGANISATION FOR NUCLEAR RESEARCH (CERN)

Submitted to: JHEP

CERN-EP-2023-063
16th May 2023

Search for direct production of winos and higgsinos in events with two same-charge leptons or three leptons in pp collision data at $\sqrt{s} = 13$ TeV with the ATLAS detector

The ATLAS Collaboration

A search for supersymmetry targeting the direct production of winos and higgsinos is conducted in final states with either two leptons (e or μ) with the same electric charge, or three leptons. The analysis uses 139 fb^{-1} of pp collision data at $\sqrt{s} = 13$ TeV collected with the ATLAS detector during Run 2 of the Large Hadron Collider. No significant excess over the Standard Model expectation is observed. Simplified and complete models with and without R-parity conservation are considered. In topologies with intermediate states including either Wh or WZ pairs, wino masses up to 525 GeV and 250 GeV are excluded, respectively, for a bino of vanishing mass. Higgsino masses smaller than 440 GeV are excluded in a natural R-parity-violating model with bilinear terms. Upper limits on the production cross section of generic events beyond the Standard Model as low as 40 ab are obtained in signal regions optimised for these models and also for an R-parity-violating scenario with baryon-number-violating higgsino decays into top quarks and jets. The analysis significantly improves sensitivity to supersymmetric models and other processes beyond the Standard Model that may contribute to the considered final states.

1 Introduction

Experimental searches for signals of physics beyond the Standard Model (SM) at colliders have long exploited the signature of a pair of isolated light leptons (electrons or muons) with same-sign (SS) electric charges. In the SM, the production of such lepton pairs is rare and originates mainly from pairs of weak-boson decays. In proton–proton (pp) collisions at $\sqrt{s}$ = 13 TeV, the inclusive cross section of same-sign lepton pair production is of the order of one pb [1, 2], i.e. it is suppressed by more than three orders of magnitude relative to the production of opposite-sign lepton pairs. On the other hand, heavy particles beyond the SM (BSM) could decay into multiple massive SM bosons or top quarks, which subsequently decay into jets and same-sign leptons, thus involving a relatively low SM background. Examples of such BSM states include supersymmetric (SUSY) particles [3, 4], SS top-quark pairs [5, 6], scalar gluons (sgluons) [7, 8], heavy scalar bosons of extended Higgs sectors [9, 10], Majorana heavy neutrinos [11, 12], and vector-like top quarks [13].

At the Large Hadron Collider (LHC) [14], the ATLAS [15] and CMS [16] experiments have extensively probed possible SM extensions in the same-sign dilepton channel. Among these theoretical proposals, SUSY [17–23] remains a compelling framework as it provides solutions to the gauge hierarchy problem [24–27] without the need for large fine-tuning of fundamental parameters [28, 29], offers gauge coupling unification [24–27], and contains weakly interacting particles that can contribute to the dark matter [30, 31].

Charginos, $\tilde{\chi}^{\pm}_{1,2}$, and neutralinos, $\tilde{\chi}^{0}_{1,2,3,4}$, collectively referred to as 'electroweakinos', are the ordered mass eigenstates formed from the linear superposition of the higgsinos, winos, and binos, which are the SUSY partners of the Higgs and electroweak gauge bosons, respectively. A discrete multiplicative symmetry, R-parity [32], is often introduced in SUSY models to avoid rapid proton decay. In R-parity-conserving (RPC) models, the lightest supersymmetric particle (LSP) is stable and is required to be neutral and colourless to evade observation as a dark matter candidate [33]. It would therefore also be invisible in a hadron collider experiment, only manifested through large missing transverse momentum, $E_{\mathrm{T}}^{\mathrm{miss}}$. Models of R-parity-violating (RPV) SUSY [34] are also well-motivated, while introducing more parameters to constrain. In RPV SUSY, a $\tilde{\chi}^{0}_{1}$ LSP would decay into SM particles and, due to its Majorana nature, it may give rise to SS-lepton final states.

In this article, the search described in Ref. [35] is extended to more signal models using the full data set of pp collisions at $\sqrt{s}$ = 13 TeV recorded by the ATLAS detector during Run 2 of the LHC, corresponding to an integrated luminosity of 139 fb^{-1}. The selection is based on final states with two SS leptons or three leptons accompanied by large $E_{\mathrm{T}}^{\mathrm{miss}}$ and a number of hadronic jets, possibly containing b-hadrons and tagged as 'b-jets'. This search provides the first ATLAS result from a two-SS-lepton selection targeting direct chargino and neutralino production. Such production may be dominant at the LHC according to naturalness considerations [28, 29], which suggest that the lightest electroweakinos have masses near the electroweak scale while the superpartners of the gluon and quarks can be heavier than a few TeV. This search covers so-far unconstrained kinematic regions, not yet excluded by previous three-lepton analyses. The smaller background faced by SS-lepton analyses allows looser kinematic requirements to be imposed, e.g. on $E_{\mathrm{T}}^{\mathrm{miss}}$ or on the momenta of jets and leptons, which provides sensitivity to scenarios with small mass splittings between the superpartners [36–38]. In addition to directly exploring such scenarios, the analysis aims to provide signal regions orthogonal to others targeting different final states, thus improving the overall sensitivity through future statistical combinations. The event selection is optimised to target four models: (i, ii) simplified models of winos and binos with on-shell WZ or Wh boson pairs as intermediate states;

(iii) higgsino production with bilinear R-parity-violating (bRPV) terms; and (iv) higgsino production with R-parity-violating decays to top quarks via baryon-number-violating (BNV) UDD couplings.

All prior searches for SS lepton pairs and several three-lepton searches carried out by ATLAS [35, 39–43] and CMS [44–46] focused on strong production of superpartners, on electroweak SUSY production with low hadronic activity, or on slepton resonant production [47]. Other analyses with three-lepton selections focused on direct electroweakino production in events without jets [48–56] or with trilepton resonances [57].

Simplified models with $\tilde{\chi}_1^{\pm}\tilde{\chi}_2^0$ production and Wh bosons in the decay chain have been explored by ATLAS in fully hadronic [58], semileptonic [40], photon [59], and multilepton [43] final states with large $E_{\mathrm{T}}^{\mathrm{miss}}$. CMS has constrained this scenario by combining a variety of leptonic signatures, including SS dileptons and τ-leptons [46, 60]. Intermediate decays to WZ bosons have been probed previously in ATLAS assuming the presence of boosted hadronically decaying bosons [58], two [61] or three leptons [56] in the final state. CMS has investigated this channel in searches for multileptons [60], two SS leptons or three leptons [46], and soft leptons [38].

ATLAS has set limits on bRPV models assuming strong superpartner production [62]. Minimal Supergravity [63–65] with bilinear terms has been constrained in events with one lepton [66, 67], one τ [68], or two SS leptons [39], and in their combination [69]. A reinterpretation of a SS-lepton analysis [39] set bounds [70] in a 'natural' bRPV scenario [28, 29] within the phenomenological Minimal Supersymmetric Standard Model (pMSSM) [71, 72].

Baryonic UDD operators have been probed by the ATLAS [58, 73–78] and CMS [45, 79–83] experiments in multijet final states and by ATLAS in events with at least one lepton [84]. Models with $\tilde{\chi}_1^0 \to tbs$ have been constrained in gluino and top-squark production in a wide range of λ''_{323} couplings, by reinterpreting several ATLAS searches optimised for RPC and RPV SUSY models [85].

The paper is structured as follows. Section 2 is dedicated to the targeted signal models. Details of the ATLAS detector are described in Section 3, with the utilised data set and simulation samples listed in Section 4. The object definitions and the event categorisation are discussed in Section 5 and Section 6, respectively. The background modelling and validation is given in Section 7. Systematic uncertainties are discussed in Section 8, and the results and interpretations are presented in Section 9 and Section 10, respectively. The conclusions are summarised in Section 11. In addition, the UDD RPV model analysis, which provides a relatively small improvement in this search, is discussed in Appendix A.

2 Signal models

The models targeted in this analysis can be divided into two main scenarios: directly produced wino-like electroweakinos with a bino-like LSP in RPC SUSY, shown in Figure 1, and higgsino-like electroweakinos with RPV terms, shown in Figure 2.

2.1 Wino–bino $\tilde{\chi}_1^{\pm}\tilde{\chi}_2^0$ production with Wh or WZ bosons

Simplified models [86–88] involving the direct production of a lightest chargino, $\tilde{\chi}_1^{\pm}$, and a next-to-lightest neutralino, $\tilde{\chi}_2^0$, are considered. The $\tilde{\chi}_1^{\pm}$ and the $\tilde{\chi}_2^0$ are assumed to be mass-degenerate. The $\tilde{\chi}_1^{\pm}/\tilde{\chi}_2^0$ are

wino-like, i.e. superpartners of the $SU(2)_L$ gauge fields, whilst the $\tilde{\chi}_1^0$ is bino-like, i.e. the superpartner of the $U(1)_Y$ gauge field [2]. The $\tilde{\chi}_1^\pm$ is assumed to decay into an on-shell, leptonically decaying W and $\tilde{\chi}_1^0$. For the $\tilde{\chi}_2^0$, two decay cases are examined: (i) a SM Higgs boson and (ii) a leptonically decaying Z boson. The Higgs boson decay is dominant for many choices of MSSM parameters as long as the mass-splitting between the two lightest neutralinos is larger than the Higgs boson mass and the higgsinos are heavier than the winos. All possible decays of the Higgs boson which ultimately result in a single lepton and jets (mostly via intermediate states) are taken into account. This is indicated by the grey-filled dot in the Higgs decay in Figure 1(a). In the case of the leptonically decaying Z boson, this is produced on-shell and leads to the diagram of Figure 1(b).

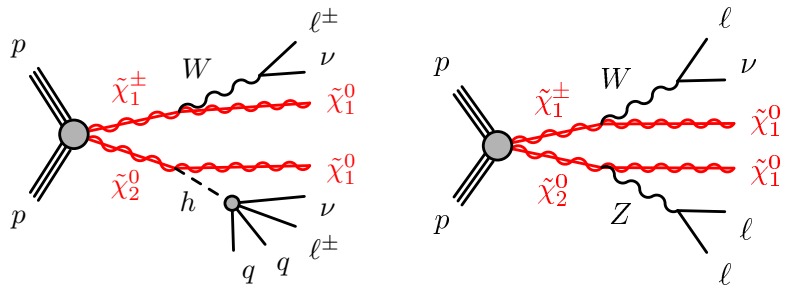

Figure 1: Diagrams of the targeted RPC simplified models with intermediate gauge vector and Higgs boson production.

2.2 Higgsino-like electroweakinos in RPV scenarios

The RPV component of the generic superpotential can be written as [34]:

$$W_{\not R_p} = \frac{1}{2}\lambda_{ijk} L_i L_j \bar{E}_k + \lambda'_{ijk} L_i Q_j \bar{D}_k + \epsilon_i L_i H_2 + \frac{1}{2}\lambda''_{ijk} \bar{U}_i \bar{D}_j \bar{D}_k, \tag{1}$$

where $i, j, k = 1, 2, 3$ are generation indices. The L_i, Q_i represent the lepton and quark $SU(2)_L$ doublet superfields, whereas H_2 is the Higgs superfield. The $\bar{E}_j$, $\bar{D}_j$, and $\bar{U}_j$ are the charged lepton, down-type quark, and up-type quark $SU(2)_L$ singlet superfields, respectively. The Yukawa couplings are λ, λ', and λ'', whilst ϵ is a dimensionful mass parameter. Two RPV scenarios are explored, the first from bilinear lepton-number-violating terms LH_2, and the second from BNV terms UDD, in Eq. (1).

RPV SUSY through bilinear terms is strongly motivated by its inherent connection with neutrino physics [89–91]. Sneutrino vacuum expectation values (VEVs) introduce a mixing between neutrinos and neutralinos, leading to a see-saw mechanism that gives mass to one neutrino at tree level, with the other two neutrino masses being induced by loop effects [92, 93]. The same VEVs are also involved in the decay of the LSP, which is thus constrained by experimental neutrino measurements.

The model considered features pair production of light higgsinos, $\tilde{\chi}_2^0$, $\tilde{\chi}_1^\pm$ and $\tilde{\chi}_1^0$, decaying into all possible final states allowed by the bRPV couplings – it is primarily inspired by naturalness arguments [28, 29]. The dominant production processes are $\tilde{\chi}_1^\pm\tilde{\chi}_1^0$, $\tilde{\chi}_1^\pm\tilde{\chi}_2^0$, $\tilde{\chi}_1^0\tilde{\chi}_2^0$, and $\tilde{\chi}_1^\pm\tilde{\chi}_1^\mp$. The first three processes can lead to a two-SS-lepton or three-lepton final state. The dominant decays are $\tilde{\chi}_1^\pm \to W^\pm\nu$, $\tilde{\chi}_{1,2}^0 \to W^\pm\ell^\mp, W^\pm\tau^\mp$, and $\tilde{\chi}_2^0 \to \tilde{\chi}_1^\pm\pi^\mp$. Higgsino mass splittings of less than 2 GeV [94] are targeted. A ratio of Higgs doublet VEVs

of $\tan\beta = 5$ is chosen to primarily favour light leptons, thus suppressing the $\tilde{\chi}^0_{1,2} \to W^\pm\tau^\mp$ decays, which are preferred at high $\tan\beta \sim 50$ with a branching ratio of more than 90%. At $\tan\beta = 5$, the branching ratio for $\tilde{\chi}^0_{1,2} \to W^\pm\tau^\mp$ drops to less than 50%, while for $\tilde{\chi}^0_2 \to \tilde{\chi}^\pm_1\pi^\mp$ it is ~20%.

Example diagrams are given in Figure 2(a) and Figure 2(b). The decay modes are partly determined by a fit to neutrino oscillation experimental data [95], leading to flavour non-universality of lepton decays, with more details given in Section 4. The bRPV couplings are large enough to ensure prompt higgsino decays. All possible allowed higgsino decays are considered in the analysis.

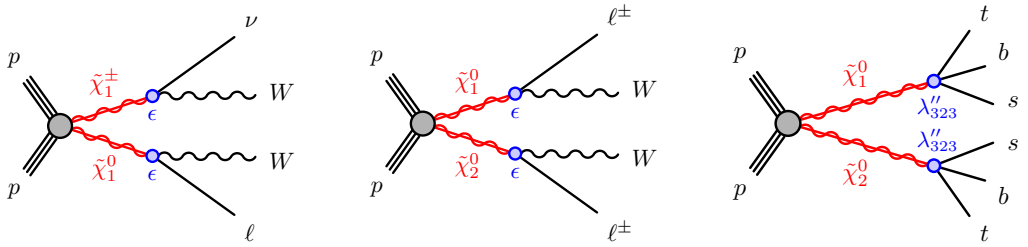

Figure 2: Diagrams of the targeted RPV models. Diagrams (a) and (b) serve as examples, since inclusive bRPV production is considered. The *UDD* RPV scenario with BNV terms in diagram (c) is a simplified model.

Besides SUSY with *UDD* terms in Eq. (1) [34, 96, 97], baryon-number violation is featured in BSM scenarios such as grand unified theories [98] and models with black holes [99]. Moreover, in a universe with initially equal amounts of baryonic and anti-baryonic matter, BNV is necessary to describe the observed baryon asymmetry [100].

In the simplified topology considered, higgsino $\tilde{\chi}^0_1\tilde{\chi}^0_2$ pairs are produced directly and undergo prompt RPV decays as shown in the diagram of Figure 2(c). The UDD-type BNV coupling λ''_{323}, defined in Eq. (1), is chosen to be non-vanishing, as it is predicted to be dominant under the minimal flavour violation hypothesis [97]. Its value is chosen to be $O(10^{-3})$ to $O(10^{-2})$, which guarantees prompt decays for electroweakino masses down to 180 GeV. The $\tilde{\chi}^0_2$ next-to-LSP (NLSP) and the $\tilde{\chi}^0_1$ LSP are mass degenerate and decay with a 100% branching ratio into tbs, thus possibly leading to a final state with two SS leptons and at least six jets, of which at least four are b-jets. Other electroweakino production modes do not lead to the final states targeted by this search.

3 ATLAS detector

The ATLAS detector [15] is a multipurpose particle detector with a forward–backward symmetric cylindrical geometry and a near 4π coverage in solid angle.[1] It consists of an inner tracking detector surrounded by a thin superconducting solenoid providing a 2 T axial magnetic field, electromagnetic and hadronic calorimeters, and a muon spectrometer. The inner tracking detector (ID) covers the pseudorapidity range

[1] ATLAS uses a right-handed coordinate system with its origin at the nominal interaction point (IP) in the centre of the detector and the z-axis along the beam pipe. The x-axis points from the IP to the centre of the LHC ring, and the y-axis points upwards. Cylindrical coordinates (r, ϕ) are used in the transverse plane, ϕ being the azimuthal angle around the z-axis. The pseudorapidity is defined in terms of the polar angle θ as $\eta = -\ln\tan(\theta/2)$. Angular distance is measured in units of $\Delta R \equiv \sqrt{(\Delta\eta)^2 + (\Delta\phi)^2}$.

$|\eta| < 2.5$. It consists of silicon pixel, silicon microstrip, and transition radiation tracking detectors. An additional layer of silicon pixels, the insertable B-layer [101, 102], was installed closer to the beamline before Run 2. Lead/liquid-argon (LAr) sampling calorimeters provide electromagnetic (EM) energy measurements with high granularity. A steel/scintillator-tile hadron calorimeter covers the central pseudorapidity range ($|\eta| < 1.7$). The endcap and forward regions are instrumented with LAr calorimeters for both the EM and hadronic energy measurements up to $|\eta| = 4.9$. The muon spectrometer surrounds the calorimeters and is based on three large superconducting air-core toroidal magnets with eight coils each. The field integral of the toroids ranges between 2.0 and 6.0 T m across most of the detector. The muon spectrometer (MS) includes a system of precision chambers for tracking and fast detectors for triggering. A two-level trigger system is used to select events. The first-level trigger is implemented in hardware and uses a subset of the detector information to accept events at a rate below 100 kHz. This is followed by a software-based trigger that reduces the accepted event rate to 1 kHz on average depending on the data-taking conditions. An extensive software suite [103] is used in data simulation, in the reconstruction and analysis of real and simulated data, in detector operations, and in the trigger and data acquisition systems of the experiment.

4 Data set and simulated event samples

This paper analyses proton–proton collision data collected by the ATLAS detector between 2015 and 2018. In this period, the LHC delivered colliding beams with a peak instantaneous luminosity reaching $2.1 \times 10^{34}\,\text{cm}^{-2}\,\text{s}^{-1}$, achieved in 2018, and an average number of pp interactions per bunch crossing, $\langle\mu\rangle$, of 33.7. After the application of beam, detector, and data-quality criteria [104], the total integrated luminosity of the data set is 139 fb^{-1} with a combined uncertainty of 1.7% [105], obtained using the LUCID-2 detector [106] for the primary luminosity measurements.

Events with $E_{\text{T}}^{\text{miss}} < 250$ GeV were selected using dilepton triggers [107, 108], with lepton p_{T} thresholds increasing during the Run 2 data-taking period to a maximum of 24 GeV for triggers requiring two electrons, 22 GeV for the leading-p_{T} muon in triggers requiring two muons, and 17 GeV (14 GeV) for the electron (muon) in different-flavour dilepton triggers. For events with $E_{\text{T}}^{\text{miss}} > 250$ GeV, a logical OR of these triggers and $E_{\text{T}}^{\text{miss}}$ triggers [109] was used. The above strategy was chosen to maximise the trigger efficiency, while selecting events relevant to the targeted final states [35]. The selection thresholds are defined such that the trigger efficiencies are constant throughout the lepton p_{T} and $E_{\text{T}}^{\text{miss}}$ range considered in the analysis.

Signal and background events produced in pp collisions were simulated with various Monte Carlo (MC) generators. They include the effect of multiple pp interactions in the same and neighbouring bunch crossings ('pile-up'), which was modelled by overlaying each simulated hard-scattering interaction with simulated inelastic pp events generated by Pythia 8.186 [110, 111] with the NNPDF2.3lo set of parton distribution functions (PDF) [112] and a set of tuned parameter values called the A3 tune [113]. The simulated events were weighted to reproduce the $\langle\mu\rangle$ distribution observed in the data. The EvtGen [114] program was used to simulate the b- and c-flavoured hadron decays.

The detector response was simulated using either the full ATLAS detector description [115] based on Geant4 [116], or a fast simulation based on a parameterisation of the performance of the electromagnetic and hadronic calorimeters and Geant4 for the other parts of the detector [117]. The generated events are reconstructed in the same manner as the data.

4.1 Signal samples

The signal samples for the targeted models were generated using MadGraph5_aMC@NLO 2.2.3 [1, 118] interfaced to Pythia 8.186 with the A14 tune [119] for the modelling of the parton showering (PS) [120], hadronisation and underlying event. The matrix element (ME) calculation was performed at tree level, including the emission of up to two additional partons. The PDF set used for the generation was NNPDF2.3lo [112]. The ME–PS matching was carried out using the CKKW-L prescription [121, 122], with a matching scale set to one quarter of the pair-produced superpartner mass. For the bRPV model, the RPV parameters (together with the mass spectra and the decay modes) were determined by a fit to neutrino experimental data performed by the SPheno [123, 124] spectrum calculator produced by the Sarah [125, 126] package.

Signal cross sections were calculated to next-to-leading order (NLO) in the strong coupling constant, adding the resummation of soft gluon emission at next-to-leading-logarithm (NLL) accuracy (NLO+NLL) using Resummino 2.0.1 [127–131]. The nominal cross section and its uncertainty were taken from an envelope of cross-section predictions using different PDF sets and factorisation and renormalisation scales [132, 133]. Production cross sections range between $O(10^{-3}$ pb) and $O(1$ pb).

4.2 Irreducible-background samples

Production of WZ and $W^{\pm}W^{\pm}$ represents the dominant irreducible background in most signal regions. Samples of fully leptonic, semileptonic and loop-induced VV ($V = W, Z$) processes and electroweak $VVjj$ processes were simulated. The associated production of a vector gauge boson with a $t\bar{t}$ pair, $t\bar{t}$+V, is also an important background. Depending on the targeted signal model, considerable background contributions come from $t\bar{t}$+H, tribosons and rare top processes, with the last including tWZ, tZq and samples with three or four top quarks. Higgs boson production via vector-boson fusion (VBF) and in association with a vector boson (VH) was also simulated, whereas production via gluon–gluon fusion and decay into two vector bosons was not simulated separately since the events are included in the diboson processes.

Samples of diboson final states VV were simulated with the Sherpa 2.2.2 [134] generator, including off-shell effects and Higgs boson contributions where appropriate. Fully leptonic final states and semileptonic final states, where one boson decays leptonically and the other hadronically, were generated using MEs at NLO accuracy in QCD for up to one additional parton and at leading-order (LO) accuracy for up to three additional parton emissions. Samples for the loop-induced processes $gg \rightarrow VV$ were generated using LO-accurate MEs for up to one additional parton emission for both the cases of fully leptonic and semileptonic final states. The ME calculations were matched and merged with the Sherpa PS based on Catani–Seymour (CS) dipole factorisation [135, 136] using the MEPS@NLO prescription [137–140]. The virtual QCD corrections were provided by the OpenLoops library [141–143]. The NNPDF3.0nnlo set of PDFs was used [144], along with the dedicated set of tuned PS parameters developed by the Sherpa authors.

Electroweak diboson production in association with two jets, $VVjj$, was simulated with the Sherpa 2.2.2 generator. The LO-accurate MEs were matched to the PS based on CS dipole factorisation using the MEPS@LO prescription. Samples were generated using the NNPDF3.0nnlo PDF set, along with the dedicated set of tuned PS parameters developed by the Sherpa authors.

The production of $t\bar{t}+V$ events was modelled using the MadGraph5_aMC@NLO 2.3.3 [1] generator at NLO with the NNPDF3.0nlo [144] PDF. The events were interfaced to Pythia 8.210 [111], which used the A14 tune and the NNPDF2.3lo [144] PDF set.

Higgs bosons produced in association with a $t\bar{t}$ pair, $t\bar{t}+H$, were generated using the Powheg Box v2 [145–149] generator at NLO with the NNPDF3.0nlo PDF set. The events were interfaced to Pythia 8.230 [111], which used the A14 tune [119] and the NNPDF2.3lo PDF set.

Triboson (VVV) event production was simulated with the Sherpa 2.2.1 [134] generator. MEs accurate to LO in QCD for up to one additional parton emission were matched and merged with the Sherpa PS based on CS dipole factorisation using the MEPS@LO prescription. Samples were generated using the NNPDF3.0nnlo PDF set, along with the dedicated set of tuned PS parameters developed by the Sherpa authors.

The production of rare top events was modelled using the MadGraph5_aMC@NLO 2.3.3 generator, which provides MEs at NLO in the strong coupling constant α_s, with the NNPDF3.1nlo [144] PDF. The functional form of the renormalisation and factorisation scales was set to $0.25\times\sum_i\sqrt{m_i^2+p_{\mathrm{T},i}^2}$, where the sum runs over all the particles generated by the ME calculation, following Ref. [150]. Top quarks were decayed at LO using MadSpin [151, 152] to preserve all spin correlations. The events were interfaced with Pythia 8.230 [111] for the PS and hadronisation, using the A14 tune and the NNPDF2.3lo PDF set.

Higgs boson production was simulated with Powheg Box v2 [146–148, 153] and interfaced with Pythia 8 [111] for the PS and non-perturbative effects. The Powheg Box prediction is accurate to NLO and uses the PDF4LHC15nlo PDF set [133] and the AZNLO tune [154] of Pythia 8 [111]. The loop-induced $gg\to ZH$ process was generated separately at LO. The MC prediction was normalised to cross sections calculated at next-to-NLO (NNLO) in QCD with NLO electroweak corrections for $q\bar{q}/qg\to VH$ and at NLO and NLL in QCD for $gg\to ZH$ [155–161]. The VBF production sample was normalised to an approximate-NNLO QCD cross section with NLO electroweak corrections [162–164]. The normalisation of all Higgs boson samples accounts for the decay branching ratio calculated with HDECAY [165–167] and Prophecy4f [168–170].

4.3 Reducible-background samples

Even though they do not share the same final state as the signal, some SM processes are possible sources of background due to misidentification of leptons or their charges. These *reducible* backgrounds, discussed in detail in Section 7, are estimated with data-driven techniques. They include V+jets and electroweak VBF Vjj, as well as top-quark pairs and single-top events.

The production of V+jets was simulated with the Sherpa 2.2.1 [134] generator using NLO MEs for up to two partons, and LO MEs for up to four partons, calculated with the Comix [135] and OpenLoops [141–143] libraries. They were matched with the Sherpa parton shower [136] using the MEPS@NLO prescription [137–140] and the set of tuned parameters developed by the Sherpa authors. The NNPDF3.0nnlo set of PDFs [144] was used and the samples were normalised to a NNLO prediction [171].

Electroweak VBF Vjj production leading to $\ell\ell jj$, $\ell\nu jj$ and $\nu\nu jj$ final states was simulated with Sherpa 2.2.11 [134] using LO MEs with up to one additional parton emission. The MEs were merged with the Sherpa PS [136] following the MEPS@LO prescription [139] and using the set of tuned parameters developed by the Sherpa authors. The NNPDF3.0nnlo set of PDFs [144] was employed. The samples

were produced in the VBF approximation, which avoids overlap with semileptonic diboson topologies by requiring a t-channel colour-singlet exchange. The starting conditions of the CS shower were set according to the large-N_c amplitudes supplied by Comix [172] to achieve the correct VBF-appropriate radiation pattern.

The production of $t\bar{t}$ events was modelled using the Powheg Box v2 [145–148] generator at NLO with the NNPDF3.0nlo [144] PDF set and the h_{damp} parameter[2] set to $1.5\,m_{\text{top}}$ [173]. The events were interfaced to Pythia 8.230 [111] to model the PS, hadronisation, and underlying event, with parameter values set according to the A14 tune [119] and using the NNPDF2.3lo set of PDFs [112].

The associated production of a top quark and a W boson (tW) and production of single-top in the s-channel (t-channel) were modelled using the Powheg Box v2 [146–148, 174, 175] generator at NLO in QCD in the five-flavour (four-flavour) scheme with the NNPDF3.0nlo [144] PDF set. For tW production, the diagram removal scheme [176] was used to remove interference and overlap with $t\bar{t}$ production. The events were interfaced with Pythia 8.230 [111], which used the A14 tune [119] and the NNPDF2.3lo PDF set.

5 Object identification and reconstruction

Leptons and jets selected for analysis are categorised as 'baseline' (BL) or 'signal' (Sig) according to various quality and kinematic selection criteria. The baseline objects are used in the computation of the missing-transverse-momentum vector $\mathbf{p}_{\text{T}}^{\text{miss}}$ and its magnitude $E_{\text{T}}^{\text{miss}}$, defined below, and to resolve ambiguities between closely spaced analysis objects.

Each electron candidate is reconstructed from a cluster of energy deposits in the EM calorimeter matched to an ID track. Baseline electrons are required to satisfy the `Loose` identification [177] and to have $p_{\text{T}} > 10\,\text{GeV}$ and $|\eta| < 2.47$, excluding the barrel-to-endcap transition region $1.37 < |\eta| < 1.52$ in the EM calorimeter. The electron track's transverse impact parameter d_0, measured from the beamline with uncertainty $\sigma(d_0)$, must satisfy $|d_0/\sigma(d_0)| < 5$, and its longitudinal impact parameter z_0, the z-distance from the primary vertex[3] to the point where d_0 is measured, must satisfy $|z_0 \sin(\theta)| < 0.5\,\text{mm}$. Baseline electrons that satisfy the tighter `Medium` identification [177] and satisfy both a track-based and a calorimeter-based isolation criterion are selected as signal electrons. Track-based isolation requires the summed scalar p_{T} of nearby ID tracks not to exceed 6% of the electron p_{T}. Similarly to the isolation variables defined in Ref. [178], these nearby tracks must lie within in a cone of $p_{\text{T}}(e)$-dependent size $\Delta R = \sqrt{(\Delta\eta)^2 + (\Delta\phi)^2} = \min\{0.2, 10\,\text{GeV}/p_{\text{T}}(e)\}$ around the electron, and must be associated with the primary vertex to limit sensitivity to pile-up. Calorimeter-based isolation requires the sum of the transverse energies of the calorimeter energy clusters in a cone of $\Delta R = 0.2$ around the electron (excluding its own energy) to be less than 6% of the electron's energy. Only signal electrons with $|\eta| < 2.0$ are considered, since this suppresses contributions from electrons having misidentified charge, and these are further rejected by exploiting information related to the electron track reconstruction and its compatibility with the primary vertex and the electron's energy cluster [177].

Muon candidates are reconstructed [178] in the region $|\eta| < 2.5$ from MS tracks matching ID tracks. Baseline muons satisfy $p_{\text{T}} > 10\,\text{GeV}$, $|\eta| < 2.5$, $|z_0 \sin(\theta)| < 0.5\,\text{mm}$ and a set of `Medium` requirements [179] on the quality of the tracks. Signal muons are defined as baseline muons that also satisfy the requirement

[2] The h_{damp} parameter is a resummation damping factor and one of the parameters that controls the matching of Powheg MEs to the PS and thus effectively regulates the high-p_{T} radiation against which the $t\bar{t}$ system recoils.

[3] The primary vertex is defined as the vertex with the largest sum of track p_{T}^2.

$|d_0/\sigma(d_0)| < 3$ and pass track-based isolation requirements that are robust against pile-up and similar to those for electrons, but with the maximal cone size increased to 0.3.

Jets are reconstructed from particle-flow energy deposits using the anti-k_t algorithm [180] with four-momentum recombination and distance parameter $R = 0.4$. The reconstructed jets are then calibrated by the application of a jet energy scale derived from 13 TeV data and simulation [181]. Jets with $p_{\mathrm{T}} > 20$ GeV and $|\eta| < 4.5$ are used as baseline jets in the analysis and are also used in computing the $E_{\mathrm{T}}^{\mathrm{miss}}$. Signal jets are selected as jets satisfying the requirements of $p_{\mathrm{T}} > 20$ GeV and $|\eta| < 2.8$. To suppress jets originating from pile-up, additional track-based criteria are applied by using the `Tight` working point of the jet vertex tagger [181, 182].

Signal jets containing b-hadrons, referred to as b-jets, are identified (b-tagged) by the `DL1r` algorithm [183, 184] via a multivariate discriminant combining information from the impact parameters of displaced tracks with topological properties of secondary and tertiary decay vertices reconstructed within the jet. The chosen working point has a b-jet tagging efficiency of 70% and rejection factors of 6 and 134 for charm-jets and light-flavour jets, respectively. Additionally, the selected b-jets must satisfy $|\eta| < 2.5$.

To avoid the double counting of analysis baseline objects, a procedure to remove reconstruction ambiguities is applied as follows:

- Electron candidates within $\Delta R' = \sqrt{(\Delta y)^2 + (\Delta\phi)^2} = 0.01$ of a muon are removed.[4] Softer electron candidates are removed if they are within $\Delta R' = 0.05$ of other electron candidates.
- Jet candidates within $\Delta R' = 0.2$ of an electron candidate are removed unless the jet candidate is a b-jet with $p_{\mathrm{T}} < 100$ GeV. Jets with fewer than three tracks that lie within $\Delta R' = 0.4$ of a muon candidate are removed.
- Subsequently, electrons and muons within $\Delta R' = \min\{0.4, 0.1 + 9.6\,\mathrm{GeV}/p_{\mathrm{T}}(\ell)\}$ of a jet candidate are removed to reject non-prompt or fake leptons originating from hadron decays.

The $\mathbf{p}_{\mathrm{T}}^{\mathrm{miss}}$ is defined as the negative vector sum of the transverse momenta of all identified objects (baseline electrons, photons [177], muons and jets) and an additional soft term. The soft term is constructed from all tracks associated with the primary vertex but not with leptons or jets. In this way, the magnitude of the $\mathbf{p}_{\mathrm{T}}^{\mathrm{miss}}$, $E_{\mathrm{T}}^{\mathrm{miss}}$, is adjusted for the best calibration of the identified objects listed above, while maintaining approximate pile-up independence in the soft term [185, 186]. Overlaps between objects in the $E_{\mathrm{T}}^{\mathrm{miss}}$ calculation are resolved as described in Ref. [185].

6 Analysis strategy and event selection

After a basic event-cleaning procedure is applied, events are required to have a primary vertex with at least two associated tracks with $p_{\mathrm{T}} > 500$ MeV. Jets likely to have been produced by beam-induced backgrounds, cosmic rays or detector noise are removed and other jet quality criteria are imposed [187]. Events with at least one muon with low momentum resolution are rejected.

Events with at least two signal leptons, with the leading lepton satisfying $p_{\mathrm{T}} > 20$ GeV, are selected. In addition, there must be either at least one pair of leptons with identical electric charges among the ensemble of signal leptons or exactly three leptons. The presence of at least one jet is also required in most signal regions (SRs) in order to improve the selection of signal events and to specifically target compressed-spectra

[4] The quantity $y = (1/2)[(E + p_z)/(E - p_z)]$ denotes the rapidity of an object.

Table 1: Signal region definitions designed for the Wh model. The variables are defined in the text.

	$\text{SR}^{Wh}_{\text{high-}m_{\text{T2}}}$			$\text{SR}^{Wh}_{\text{low-}m_{\text{T2}}}$		
	$e^{\pm}e^{\pm}$	$e^{\pm}\mu^{\pm}$	$\mu^{\pm}\mu^{\pm}$	$e^{\pm}e^{\pm}$	$e^{\pm}\mu^{\pm}$	$\mu^{\pm}\mu^{\pm}$
$N_{\text{BL}}(\ell)$	$= 2$					
$N_{\text{Sig}}(\ell)$	$= 2$					
Charge(ℓ)	same-sign					
$p_{\text{T}}(\ell)$	≥ 25 GeV					
n_{jets} ($p_{\text{T}} > 25$ GeV)	≥ 1					
$n_{b\text{-jets}}$	$= 0$					
m_{jj}	< 350 GeV					
m_{T2}	≥ 80 GeV			< 80 GeV		
$m_{\text{T}}^{\text{min}}$	–			≥ 100 GeV		
$\mathcal{S}(E_{\text{T}}^{\text{miss}})$	≥ 7			≥ 6		
$E_{\text{T}}^{\text{miss}}$	≥ 75 GeV			≥ 50 GeV		
$E_{\text{T}}^{\text{miss}}$ binning [GeV][a]	$\text{SR}^{Wh}_{\text{high-}m_{\text{T2}}}$-1: $\in [75, 125)$ $\text{SR}^{Wh}_{\text{high-}m_{\text{T2}}}$-2: $\in [125, 175)$ $\text{SR}^{Wh}_{\text{high-}m_{\text{T2}}}$-3: $\in [175, +\infty)$			–		

[a] The $E_{\text{T}}^{\text{miss}}$ binning applies separately to each flavour channel of $\text{SR}^{Wh}_{\text{high-}m_{\text{T2}}}$.

regions. To distinguish between hypothetical SUSY signal processes and SM backgrounds, sets of SRs are optimised for the SUSY models defined in Section 2. Each of these SRs, described in Tables 1 to 3, is kept orthogonal to those in other ATLAS analyses [56] to facilitate future statistical combinations. Several kinematic variables are deployed to maximise the sensitivities to the targeted signals.

The 'stransverse mass', m_{T2}, is an event variable used to bound the masses of an unseen pair of particles which are presumed to have decayed semi-invisibly into particles which were seen [188, 189]. Therefore, it is defined as a function of the momenta of two visible particles and the $\mathbf{p}_{\text{T}}^{\text{miss}}$ of the event:

$$m_{\text{T2}} = \min_{\mathbf{q}_{\text{T}}} \left[\max \left(m_{\text{T},\ell_1}(\mathbf{p}_{\text{T},\ell_1}, \mathbf{q}_{\text{T}}), m_{\text{T},\ell_2}(\mathbf{p}_{\text{T},\ell_2}, \mathbf{p}_{\text{T}}^{\text{miss}} - \mathbf{q}_{\text{T}}) \right) \right],$$

where $\mathbf{p}_{\text{T},\ell_1}$ and $\mathbf{p}_{\text{T},\ell_2}$ are the transverse momenta of the two leading leptons, and $\mathbf{q}_{\text{T}}$ is the transverse momentum vector that minimises the larger of the two transverse masses m_{T,ℓ_1} and m_{T,ℓ_2}. These two transverse masses are defined as

$$m_{\text{T}}(\mathbf{p}_{\text{T}}, \mathbf{q}_{\text{T}}) = \sqrt{2(p_{\text{T}} q_{\text{T}} - \mathbf{p}_{\text{T}} \cdot \mathbf{q}_{\text{T}})}.$$

In this analysis, the invisible particle mass is always set to zero when calculating the event m_{T2}.

For the Wh and WZ models, m_{T2} was used to define two orthogonal sets of signal regions, 'high-m_{T2}' and 'low-m_{T2}', to target models with different kinematics. Exactly two baseline leptons, $N_{\text{BL}}(\ell) = 2$, were required for these two models to further suppress the background. Requiring the invariant mass of the two leading jets, m_{jj},[5] to be less than 350 GeV proved to be efficient in reducing the $W^{\pm}W^{\pm}$ background. The

[5] If the event has only one jet, m_{jj} was set to zero.

Table 2: Signal region definitions designed for the WZ model. The variables are defined in the text.

	$\mathrm{SR}^{WZ}_{\text{high-}m_{\mathrm{T2}}}$	$\mathrm{SR}^{WZ}_{\text{low-}m_{\mathrm{T2}}}$
$N_{\mathrm{BL}}(\ell)$	$= 2$	
$N_{\mathrm{Sig}}(\ell)$	$= 2$	
Charge(ℓ)	same-sign	
$p_{\mathrm{T}}(\ell)$	≥ 25 GeV	
n_{jets} $(p_{\mathrm{T}} > 25$ GeV$)$	≥ 1	
$n_{b\text{-jets}}$	$= 0$	
m_{jj}	≤ 350 GeV	
m_{T2}	≥ 100 GeV	≤ 100 GeV
$m_{\mathrm{T}}^{\mathrm{min}}$	≥ 100 GeV	≥ 130 GeV
$E_{\mathrm{T}}^{\mathrm{miss}}$	≥ 100 GeV	≥ 140 GeV
m_{eff}	–	≤ 600 GeV
$\Delta R(\ell^{\pm}, \ell^{\pm})$	–	≤ 3
Bins	$\mathcal{S}(E_{\mathrm{T}}^{\mathrm{miss}})$: $\in [0, 10)$ Spread$(\Phi) \geq 2.2$	–
	$\mathcal{S}(E_{\mathrm{T}}^{\mathrm{miss}})$: $\in [10, 13)$	
	$\mathcal{S}(E_{\mathrm{T}}^{\mathrm{miss}})$: $\in [13, +\infty]$ $\Delta R(\ell^{\pm}, \ell^{\pm}) \geq 1$	

Table 3: Signal region definitions designed for the bRPV model. The variables are defined in the text.

	$\mathrm{SR}^{\mathrm{bRPV}}_{2\ell\text{-SS}}$	$\mathrm{SR}^{\mathrm{bRPV}}_{3\ell}$
$N_{\mathrm{BL}}(\ell)$	–	
p_{T} (ℓ)	≥ 20 GeV for (sub)leading leptons	
n_{jets} $(p_{\mathrm{T}} > 25$ GeV$)$	≥ 1	
$N_{\mathrm{Sig}}(\ell)$	$= 2$	$= 3$
Charge(ℓ)	same-sign	–
m_{T2}	≥ 60 GeV	≥ 80 GeV
$E_{\mathrm{T}}^{\mathrm{miss}}$	≥ 100 GeV	≥ 120 GeV
m_{eff}	–	≥ 350 GeV
$n_{b\text{-jets}}$	$= 0$	–
n_{jets} $(p_{\mathrm{T}} > 40$ GeV$)$	≥ 4	–
$m_{e^{\pm}e^{\mp}}$, $m_{\mu^{\pm}\mu^{\mp}}$	–	$\notin [81, 101]$ GeV

transverse mass of the $\mathbf{p}_{\mathrm{T}}^{\mathrm{miss}}$ and each of the two leading leptons was calculated, and the smaller of the two values, $m_{\mathrm{T}}^{\mathrm{min}}$, is used to recover the sensitivity which would otherwise be lost if only high m_{T2} were considered. The $E_{\mathrm{T}}^{\mathrm{miss}}$ and its significance, $\mathcal{S}(E_{\mathrm{T}}^{\mathrm{miss}})$ [190],[6] which quantifies the robustness of the $E_{\mathrm{T}}^{\mathrm{miss}}$

[6] $\mathcal{S}(E_{\mathrm{T}}^{\mathrm{miss}}) = \frac{|E_{\mathrm{T}}^{\mathrm{miss}}|^2}{\sigma_{\mathrm{L}}^2(1-\rho_{\mathrm{LT}}^2)}$, with σ_{L}^2 the total variance in the longitudinal direction along $\mathbf{p}_{\mathrm{T}}^{\mathrm{miss}}$ and ρ_{LT}^2 the correlation between the

values against object mismeasurements in events without a genuine source of $E_{\mathrm{T}}^{\mathrm{miss}}$, are also used to target the large $E_{\mathrm{T}}^{\mathrm{miss}}$ induced by the (invisible) LSP in RPC scenarios. The angular distance between the two SS leptons, $\Delta R(\ell^{\pm}, \ell^{\pm})$, is used only for the WZ model since the SS leptons come from two separate decay legs and should not be too far apart when the masses of the SUSY particles are similar.

A multi-bin strategy is applied in the 'high-m_{T2}' SRs, using $E_{\mathrm{T}}^{\mathrm{miss}}$ and flavour for the Wh model and $\mathcal{S}(E_{\mathrm{T}}^{\mathrm{miss}})$ for the WZ model, to maximise the sensitivity across the model's phase space. No similar binning is employed in the 'low-m_{T2}' SRs for the WZ model, due to the limited number of surviving events. For the bins defined for $\mathrm{SR}^{WZ}_{\text{high-}m_{\mathrm{T2}}}$, requirements on the Spread(Φ)[7] or $\Delta R(\ell^{\pm}, \ell^{\pm})$ are applied to further improve the sensitivities to the benchmark model. The Wh SRs are divided into different flavour channels to maximise the power of the analysis.

For the bRPV model, large $E_{\mathrm{T}}^{\mathrm{miss}}$ is expected due to the presence of a neutrino in the leptonic decay of the W boson. High jet multiplicity is required in the two-SS-lepton SR to improve the sensitivity to possible hadronic decays of the higgsinos and the W boson. An m_{T2} threshold at 60 GeV or 80 GeV is found to be helpful because the $E_{\mathrm{T}}^{\mathrm{miss}}$ composition differs between the signal and the background sources. For the two-SS-lepton SR, a b-jet veto is applied to further reduce the $t\bar{t}$ backgrounds. For the three-lepton SR, a lower bound on the effective mass m_{eff}, defined as the scalar sum of the $E_{\mathrm{T}}^{\mathrm{miss}}$ and the objects' p_{T} values, is placed at 350 GeV and has proven useful in reducing the remaining background after applying the Z-boson veto ($m_{e^{\pm}e^{\mp}},\ m_{\mu^{\pm}\mu^{\mp}} \notin [81, 101]$ GeV).

Within each signal model, the SRs are designed to be orthogonal to allow their statistical combination in the interpretation of the results. In the wino–bino models, this is achieved with the m_{T2} variable, while the number of signal leptons, $N_{\mathrm{Sig}}(\ell)$, ensures orthogonality in the bRPV model.

While these SRs are designed to maximise the sensitivity to specific benchmark models, a different set of *discovery SRs* were defined to enhance the discovery potential for a variety of BSM scenarios, such as simplified models with electroweak SUSY production which span the compressed to high mass-splitting scenarios. The inclusive $\mathrm{SR}^{Wh}_{\text{high-}m_{\mathrm{T2}}}$ and $\mathrm{SR}^{Wh}_{\text{low-}m_{\mathrm{T2}}}$ for the Wh model and the $\mathrm{SR}^{WZ}_{\text{high-}m_{\mathrm{T2}}}$ and $\mathrm{SR}^{WZ}_{\text{low-}m_{\mathrm{T2}}}$ for the WZ model, defined without any $E_{\mathrm{T}}^{\mathrm{miss}}$ or $\mathcal{S}(E_{\mathrm{T}}^{\mathrm{miss}})$ binning or flavour splitting, act as such discovery regions.

The product $A \times \epsilon$ of the acceptance A of the selection criteria and the efficiency ϵ that accounts for the detector effects, ranges from 0.01% to a few percent for the SRs defined in Tables 1 to 3. For example, $\mathrm{SR}^{Wh}_{\text{high-}m_{\mathrm{T2}}}$ ($\mathrm{SR}^{WZ}_{\text{low-}m_{\mathrm{T2}}}$) yields an $A \times \epsilon$ of ~0.02% (~2%) in the Wh (WZ) model for $m(\tilde{\chi}_1^{\pm}/\tilde{\chi}_2^0) = 200$ GeV and a massless LSP.

7 Background estimation

The treatment of the SM backgrounds is based on their classification as either irreducible backgrounds, from processes with genuine same-sign prompt leptons, or reducible backgrounds, with events entering the SRs because of misidentification of the lepton ('fake/non-prompt') or the lepton charge ('charge-flip'). The

longitudinal and transverse resolutions of the objects.

[7] The spread of the Φ angles of the leptons, $E_{\mathrm{T}}^{\mathrm{miss}}$, and jets is used to describe the event topology in the transverse plane. It was defined and used in Ref. [191]. It is defined as: $\mathrm{Spread}(\Phi) = \frac{\mathcal{R}(\phi_{\ell 1},\ \phi_{\ell 2},\ \phi_{E_{\mathrm{T}}^{\mathrm{miss}}}) \cdot \mathcal{R}(\phi_{j1},\ \phi_{j2},\dots)}{\mathcal{R}(\phi_{\ell 1},\ \phi_{\ell 2},\ \phi_{E_{\mathrm{T}}^{\mathrm{miss}}},\ \phi_{j1},\ \phi_{j2},\dots)}$, where $\mathcal{R}$ means the root-mean-square of the inputs.

'charge-flip' events (referred to in the following as CF events) are caused by the emission of a bremsstrahlung photon which, through interaction with detector material, converts into a pair of secondary electron tracks. One of those tracks happens to match the position of the calorimeter energy cluster better than the original electron track does, and has a charge opposite to that of the prompt electron. The CF contribution coming from muons is negligible due to the small cross section for interactions with matter. The 'fake/non-prompt' events (referred to in the following as FNP events) are mainly due to heavy-flavour meson decays, converted photons of various origin, light hadrons faking the electron shower, and in-flight decays of kaons or pions to muons. Lepton candidates reconstructed from these different sources share the properties of being generally not well-isolated and being mostly rejected by the lepton identification and isolation criteria and impact parameter requirements.

The dominant irreducible background processes in the SRs defined in this analysis are WZ, $W^{\pm}W^{\pm}$ for SRs with a b-jet veto ($\mathrm{SR}^{Wh}_{\text{high-}m_{\mathrm{T2}}}$, $\mathrm{SR}^{Wh}_{\text{low-}m_{\mathrm{T2}}}$, $\mathrm{SR}^{WZ}_{\text{high-}m_{\mathrm{T2}}}$, $\mathrm{SR}^{WZ}_{\text{low-}m_{\mathrm{T2}}}$ and $\mathrm{SR}^{\mathrm{bRPV}}_{2\ell\text{-SS}}$) and $t\bar{t}$+V for the b-jet-agnostic SR ($\mathrm{SR}^{\mathrm{bRPV}}_{3\ell}$). The WZ and $W^{\pm}W^{\pm}$ contributions to the respective SRs are evaluated by normalising the MC prediction in dedicated control regions (CRs). All other irreducible backgrounds, discussed in Section 4, are estimated from MC simulation. The reducible backgrounds are estimated through data-driven estimation techniques.

The background estimates are obtained by performing a profile log-likelihood fit [192], implemented in the HistFitter [193] software framework, considering only the CRs and assuming no signal presence. The statistical and systematic uncertainties are implemented as nuisance parameters in the likelihood; Poisson constraints are used to estimate the uncertainties arising from limited numbers of events in the MC samples, whilst Gaussian constraints are used for experimental and theoretical systematic uncertainties. The normalisation factors and nuisance parameters are adjusted by maximising the likelihood. The significance of the difference between the observed and expected yields is calculated with the profile likelihood method [194].

The validation regions (VRs), which serve solely to validate the background estimation in the SRs, are defined to be orthogonal to, but close to, both the SRs and the CRs. The background prediction as obtained from this background-only fit is compared with data in the VRs to assess the quality of the background modelling.

For the dominant backgrounds in SRs optimised for the Wh model ($\mathrm{SR}^{Wh}_{\text{high-}m_{\mathrm{T2}}}$ and $\mathrm{SR}^{Wh}_{\text{low-}m_{\mathrm{T2}}}$), dedicated CRs are designed for the WZ ($\mathrm{CR}WZ^{Wh}$) process and the $W^{\pm}W^{\pm}$ process ($\mathrm{CR}WW^{Wh}$). The correction factor for each targeted background process is obtained via a simultaneous fit in the specific control region. VRs with enriched contributions from WZ ($\mathrm{VR}WZ^{Wh}$) or $W^{\pm}W^{\pm}$ ($\mathrm{VR}WW^{Wh}$) are also defined in order to validate the estimates. The CR and VR definitions for the Wh model are listed in Table 4.

The requirements on the numbers of leptons, $N_{\mathrm{Sig}}(\ell)$ and $N_{\mathrm{BL}}(\ell)$, number of jets, n_{jets}, and $E_{\mathrm{T}}^{\mathrm{miss}}$ applied in the CRs and VRs are similar to those applied in $\mathrm{SR}^{Wh}_{\text{high-}m_{\mathrm{T2}}}$ and $\mathrm{SR}^{Wh}_{\text{low-}m_{\mathrm{T2}}}$, and are listed in Table 4. Values of the $E_{\mathrm{T}}^{\mathrm{miss}}$ significance ($\mathcal{S}(E_{\mathrm{T}}^{\mathrm{miss}})$) larger or smaller than six are used to distinguish the CRs from the VRs while keeping the VRs close to the SRs. For WZ-enriched regions, the third lepton satisfies the baseline lepton criteria *without* fulfilling the signal lepton definition in order to maintain the orthogonality between CRs, VRs and SRs. In addition, the invariant mass of a pair of same-flavour opposite-sign leptons (SFOS), m_{SFOS}, is required to be within a window of ±15 GeV around m_Z, and the invariant mass of the three leptons, $m_{\ell\ell\ell}$, is required to be away from the Z mass peak. Such criteria further improve the purity and suppress other backgrounds. The purity of the WZ process in $\mathrm{CR}WZ^{Wh}$ and $\mathrm{VR}WZ^{Wh}$ is about 90% with negligible contamination from signal.

Table 4: Control region and validation region definitions for evaluating and validating the dominant irreducible backgrounds in SRs defined for the Wh model. Requirements guaranteeing orthogonality to SRs are in boldface.

	CRWZ^{Wh}	VRWZ^{Wh}	CRWW^{Wh}	VRWW^{Wh}
$N_{\text{BL}}(\ell)$	$= 3$		$= 2$	
$N_{\text{Sig}}(\ell)$			$= 2$	
Charge(ℓ)			same-sign	
$p_{\text{T}}(\ell)$			≥ 25 GeV	
$n_{b\text{-jets}}$			$= 0$	
$E_{\text{T}}^{\text{miss}}$			≥ 50 GeV	
n_{jets}	≥ 1		≥ 2	
$\mathcal{S}(E_{\text{T}}^{\text{miss}})$	$< \mathbf{6}$	≥ 6	$< \mathbf{6}$	≥ 6
Other cuts	$75 < m_{\text{SFOS}} < 105$ GeV		–	
	$m_{\ell\ell\ell} \notin [80, 100]$GeV		–	
	–		$\boldsymbol{m_{jj} \geq 350}$ GeV	
	–		p_{T}(jets) ≥ 75 GeV for (sub)leading jets	
	–		$\lvert m_{e^\pm e^\pm} - m_Z \rvert \geq 15$ GeV	
Purity	90%	90%	45%	55%

To target the $W^\pm W^\pm$ process for the $W^\pm W^\pm$-enriched regions CRWW^{Wh} and VRWW^{Wh}, two boosted jets with $p_{\text{T}} \geq 75$ GeV are required, while requiring $m_{jj} \geq 350$ GeV ensures orthogonality with respect to the SRs. To suppress the CF contribution, events are rejected if $|m_{e^\pm e^\pm} - m_Z| < 15$ GeV. The final purity of CRWW^{Wh} (VRWW^{Wh}) is about 45% (55%) with a signal contamination of less than 3% in both the CR and the VR. The correction factors are $1.06^{+0.14}_{-0.08}$ and $1.00^{+0.25}_{-0.28}$ for the WZ and $W^\pm W^\pm$ backgrounds, respectively, and are applied to these background events in the regions designed for the Wh model. Both the statistical and systematic uncertainties, described in Section 8, are considered in the corrections factors. In Figure 3, good agreement between the observed data and the estimated backgrounds can be seen for VRWZ^{Wh} and VRWW^{Wh}.

For SRs designed for the WZ model and models of higgsino-like electroweakinos in RPV SUSY considered in this analysis, a general control region CR$WZ_{2j}^{WZ,\text{(b)RPV}}$ for the WZ process is defined in order to correct the cross section in a region of phase space with at least two jets, where imprecise modelling was observed in previous analyses [35]. The validation regions for the WZ process (VR$WZ_{4j}^{WZ,\text{(b)RPV}}$ and VR$WZ_{5j}^{WZ,\text{(b)RPV}}$) and the $t\bar{t}+V$ process (VR$t\bar{t}V^{WZ,\text{(b)RPV}}$), defined in Table 5, are designed to validate the estimates from the MC simulation of these processes. Large jet multiplicities are required in those validation regions in order to validate the modelling of those processes in the phase space where previous analyses observed the largest disagreements [35].

To define WZ and bRPV CRs, requirements are placed on the number of signal leptons, $N_{\text{Sig}}(\ell)$, the number of baseline leptons, $N_{\text{BL}}(\ell)$, the number of jets, n_{jets}, and the number of b-jets, $n_{b\text{-jets}}$. Additional requirements are set on $E_{\text{T}}^{\text{miss}}$, m_{eff}, m_{SFOS} and the presence of SS leptons. A minimum angular separation between the leading lepton and the jets, $\Delta R(\ell_1, j)_{\text{min}}$, is required in the validation regions targeting $t\bar{t}+V$ events, as well as requirements on $\sum p_{\text{T}}^{b\text{-jet}} / \sum p_{\text{T}}^{\text{jet}}$. The leading and subleading lepton p_{T} are required to be above 20 GeV. The events belonging to the SRs of the WZ model and the bRPV model defined in Section 6

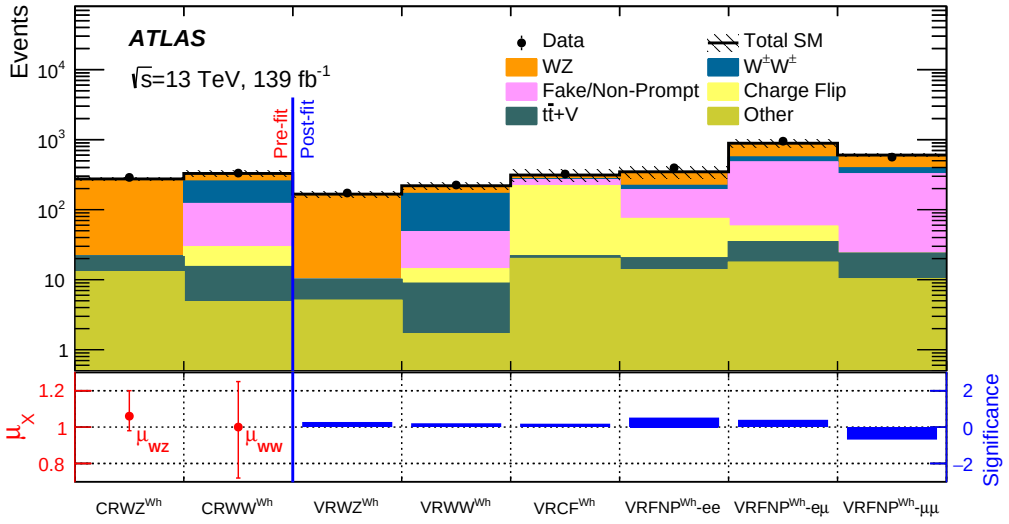

Figure 3: Expected SM backgrounds and data yields in the CRWZ^{Wh}, CRWW^{Wh}, VRWZ^{Wh}, VRWW^{Wh}, VRCF^{Wh} and VRFNP^{Wh} designed for the Wh model. The 'Other' category contains the $t\bar{t}$+H, rare top, triboson, and other diboson processes with the SS final state. The error band includes the statistical, theoretical and experimental uncertainties. The bottom panel shows the obtained scale factors (μ_{WZ}, μ_{WW}) in the CRs and the statistical significance [194] of the discrepancy between the observed number of events and the SM expectation.

are vetoed. In addition, the selections given in Table 5 are applied to ensure a more stringent rejection of possible bRPV and *UDD* RPV signal events, as well as other SUSY signals with several (b-)jets and moderate $E_{\mathrm{T}}^{\mathrm{miss}}$ in the final state. These vetoes help to reduce the expected signal contamination to a few percent. The purity of the target background process varies from a minimum of 62% (VR$t\bar{t}V^{WZ,(\mathrm{b})\mathrm{RPV}}$) to a maximum of 85% (CR$WZ_{2j}^{WZ,(\mathrm{b})\mathrm{RPV}}$).

The correction factor and its uncertainty are extracted from CR$WZ_{2j}^{WZ,(\mathrm{b})\mathrm{RPV}}$ and are found to be 0.88 ± 0.30. The estimated backgrounds and the observed data in CR$WZ_{2j}^{WZ,(\mathrm{b})\mathrm{RPV}}$, VR$WZ_{4j}^{WZ,(\mathrm{b})\mathrm{RPV}}$, VR$WZ_{5j}^{WZ,(\mathrm{b})\mathrm{RPV}}$ and VR$t\bar{t}V^{WZ,(\mathrm{b})\mathrm{RPV}}$ are shown in Figure 4, where good agreement is observed.

The contributions of CF events are evaluated from reweighted data events with two opposite-sign leptons ($e^{\pm}e^{\mp}$, $e^{\pm}\mu^{\mp}$). The weight expresses the probability of one electron charge to be mismeasured and is a function of the electron CF rates. This method largely improves the statistical accuracy by relying entirely on data to obtain the reweighting factors, thus eliminating uncertainties associated with MC simulations. An additional 25% uncertainty stems from the choice of lepton selections, and was derived by comparing the nominal CF predictions with those obtained using BL leptons.

The CF rates are measured as a function of lepton p_{T} and $|\eta|$ for simulated SM processes that contribute to the SRs due to CF. They are multiplied by the scale factors obtained from a 'tag and probe' method [177] to match the rates observed in data. The nominal CF rates are no more than $O(10^{-6})$ in the low-p_{T} region, but reach $O(1\%)$ in the higher p_{T} and $|\eta|$ regions. Systematic uncertainties are estimated from the statistical uncertainties of the measured CF rates and the uncertainties from the scale factors, leading to a 10% to 40% uncertainty in the predicted SR yields for the CF background.

Table 5: Control region and validation region definitions for evaluating and validating the dominant irreducible backgrounds in SRs defined for the WZ model and models of higgsino-like electroweakinos in (b)RPV SUSY. Requirements guaranteeing orthogonality with SRs are in boldface.

	$\mathrm{CR}WZ_{2j}^{WZ,\text{(b)RPV}}$	$\mathrm{VR}WZ_{4j}^{WZ,\text{(b)RPV}}$	$\mathrm{VR}WZ_{5j}^{WZ,\text{(b)RPV}}$	$\mathrm{VR}t\bar{t}V^{WZ,\text{(b)RPV}}$
$N_{\mathrm{BL}}(\ell)$		$= 3$		≥ 2
$N_{\mathrm{Sig}}(\ell)$		$= 3$		≥ 2
Charge(ℓ)		–		same-sign
$p_{\mathrm{T}}(\ell)$		$p_{\mathrm{T}} > 20\,\mathrm{GeV}$ for (sub)leading leptons		$p_{\mathrm{T}} > 30\,\mathrm{GeV}$ for SS pair leptons
$n_{b\text{-jets}}$		$= 0$		≥ 1
n_{jets} ($p_{\mathrm{T}} \geq 25\,\mathrm{GeV}$)	≥ 2	≥ 4	≥ 5	≥ 3 with $p_{\mathrm{T}} > 40\,\mathrm{GeV}$
Other selections	$50 < E_{\mathrm{T}}^{\mathrm{miss}} < 150\,\mathrm{GeV}$	$50 < E_{\mathrm{T}}^{\mathrm{miss}} < 250\,\mathrm{GeV}$		–
	$m_{\mathrm{eff}} < 1\,\mathrm{TeV}$	$m_{\mathrm{eff}} < 1.5\,\mathrm{TeV}$		–
	$81 < m_{\mathrm{SFOS}} < 101\,\mathrm{GeV}$	$81 < m_{\mathrm{SFOS}} < 101\,\mathrm{GeV}$		–
		–		$\Delta R(\ell_1, \mathrm{jet})_{\mathrm{min}} > 1.1$
		–		$\sum p_{\mathrm{T}}^{b\text{-jet}} / \sum p_{\mathrm{T}}^{\mathrm{jet}} > 0.4$
		–		$E_{\mathrm{T}}^{\mathrm{miss}} / m_{\mathrm{eff}} > 0.1$
	explicit veto on $\mathrm{SR}^{WZ}_{\text{high-}m_{\mathrm{T2}}}$ & $\mathrm{SR}^{WZ}_{\text{low-}m_{\mathrm{T2}}}$ & $\mathrm{SR}^{\text{bRPV}}_{2\ell\text{-SS}}$ & $\mathrm{SR}^{\text{bRPV}}_{3\ell}$ events			
Vetoing other possible BSM events	$n_{b\text{-jets}} \geq 3$ $n_{b\text{-jets}} \geq 1$, $n_{\mathrm{jets}} \geq 4$ ($p_{\mathrm{T}} > 50\,\mathrm{GeV}$), $E_{\mathrm{T}}^{\mathrm{miss}} > 130\,\mathrm{GeV}$ $n_{b\text{-jets}} = 0$, $n_{\mathrm{jets}} \geq 3$ ($p_{\mathrm{T}} > 50\,\mathrm{GeV}$), $E_{\mathrm{T}}^{\mathrm{miss}} > 130\,\mathrm{GeV}$ $n_{b\text{-jets}} = 0$, $n_{\mathrm{jets}} \geq 5$ ($p_{\mathrm{T}} > 50\,\mathrm{GeV}$)			
Purity	85%	84%	77%	62%

The fake-factor method, the matrix method and the MC template method are used in this analysis to estimate the contributions of FNP events in the SRs. Both the fake-factor method and the matrix method are purely data-driven methods, which are commonly employed in the ATLAS Collaboration [195–197] to estimate the FNP background in dedicated regions. In this analysis, the fake-factor method is used to estimate the contribution of FNP events in the Wh regions. Hence, the measurements of the values of the fake-factors are specifically tailored to reflect the FNP composition of the two-SS-lepton SRs of the Wh model. The implementation of the matrix method in this analysis is instead designed to be more universal, which enables it to estimate the FNP contribution in more complex regions. Therefore, it is used to evaluate the FNP events in SRs defined for the WZ model and models of higgsino-like electroweakinos in RPV SUSY which have two SS leptons or three leptons, and b-vetoed or b-favoured channels. Finally, the (semi-data-driven) MC template method [39] is used to validate specific matrix-method estimates to ensure that the more universal matrix method is functioning well for the specific cases in this analysis.

The fake-factor method estimates the FNP events in a specific region by reweighting events passing the same selection except for inverted lepton identification and/or isolation requirements. The reweighting factors, called 'fake factors' (FFs), are measured separately for electrons and muons from data in FNP-enriched CRs ($\mathrm{CR}FF_e$ and $\mathrm{CR}FF_\mu$) as functions of the lepton p_{T} and $|\eta|$. The CRs listed in Table 6 are designed to be as close as possible to $\mathrm{SR}^{Wh}_{\text{high-}m_{\mathrm{T2}}}$ and $\mathrm{SR}^{Wh}_{\text{low-}m_{\mathrm{T2}}}$ in order to share the same sources of FNP contributions as the target SRs. The measured FFs are around 0.1 for both electrons and muons in most bins, but reach 0.3 for some p_{T} and $|\eta|$ bins. The uncertainties of this method come principally from the measurement of the FFs which are propagated to the final estimate via the reweighting. In this analysis, the FF uncertainties coming from statistics, possible FNP contribution differences between the CRs and the targeted SRs, and prompt-lepton and CF background subtraction, amount to around 20% of the final estimate in total.

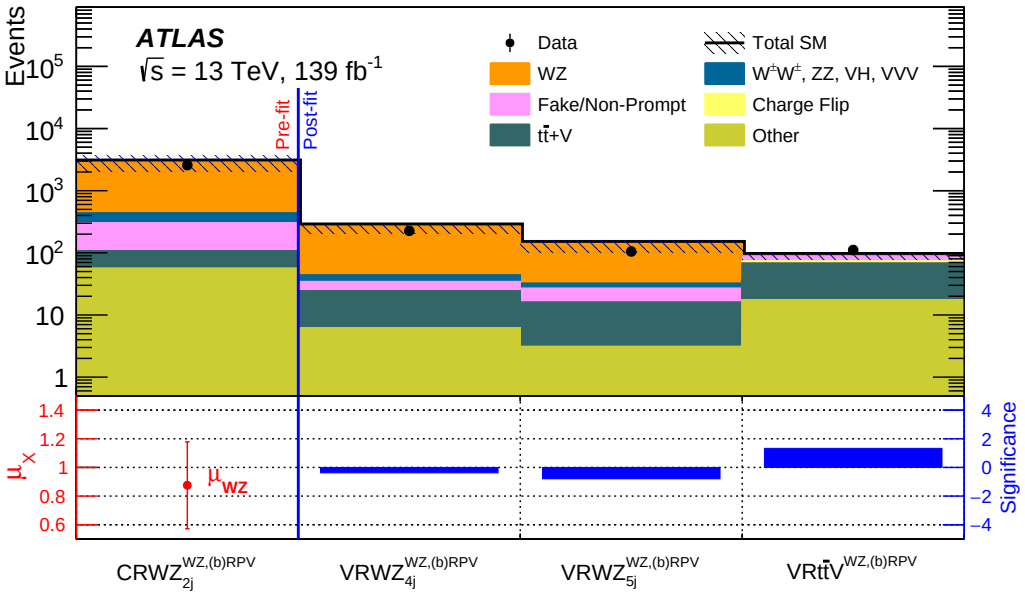

Figure 4: Expected SM backgrounds and data yields in CR$WZ_{2j}^{WZ,(b)\text{RPV}}$, VR$WZ_{4j}^{WZ,(b)\text{RPV}}$, VR$WZ_{5j}^{WZ,(b)\text{RPV}}$ and VR$t\bar{t}V^{WZ,(b)\text{RPV}}$ designed for the WZ model and models of higgsino-like electroweakinos in RPV SUSY. The 'Other' category contains the $t\bar{t}$+H and rare top processes with the SS final state. The error band includes the statistical, theoretical and experimental uncertainties. The bottom panel shows the scale factor obtained from CR$WZ_{2j}^{WZ,(b)\text{RPV}}$ (μ_{WZ}) and the statistical significance [194] of the discrepancy between the observed number of events and the SM expectation.

Two validation regions VRFNP^{Wh} and VRCF^{Wh}, listed in Table 6, are defined in order to validate the data-driven methods applied to estimate the FNP and CF events in $\text{SR}^{Wh}_{\text{high-}m_{\text{T2}}}$ and $\text{SR}^{Wh}_{\text{low-}m_{\text{T2}}}$. Good agreement between data and expectation is observed in the VRs, as shown in Figure 3, thus validating the application of the above methods.

The matrix method involves the inversion of the matrix relating the numbers of observed baseline and signal leptons to the estimated numbers of real and FNP leptons via measured real (ε) and FNP (ζ) lepton efficiencies; the implementation used in Ref. [35] is applied here. The value of ε is around 50%–60% (70%) for electrons (muons) in the region of lepton p_{T} around 15 GeV, increasing to 98% (99%) for lepton $p_{\text{T}} > 100$ GeV (60 GeV). The total uncertainty in ε is 0.33%–7% (0.1%–3%) for electrons (muons) depending on the (p_{T}, η) region. The ζ probabilities are ~10%–20% for both electrons and muons up to $p_{\text{T}} \sim 45$ GeV, and increase to 30%–40% for $p_{\text{T}} > 60$ GeV. They can be up to twice as large in events with two b-tagged jets. The effects of variations in the relative contributions of different sources of FNP leptons or in the overall event activity are considered as uncertainties of ζ. For electrons (muons), the latter is 30%–50% (30%–80%), increasing with p_{T}. The level of agreement between the data and the estimated background in a loose event preselection region requiring two SS leptons, $E_{\text{T}}^{\text{miss}} > 50$ GeV and at least one jet with $p_{\text{T}} > 25$ GeV, in different lepton-flavour and b-jet-multiplicity combinations, as shown in Figure 5, indicates the universality of the matrix method in estimating the FNP lepton background in general cases. Together with the level of agreement observed seen in Figure 4, this validates the estimation of the FNP background using the matrix method.

To further validate the estimation of the FNP and CF backgrounds, the MC template method is introduced

Table 6: Definitions of the FNP-enriched control regions used to measure the FFs, and definitions of the validation regions used to validate the estimates of the FNP and CF events in SRs defined for the Wh model. Requirements guaranteeing orthogonality to SRs are in boldface.

	$\mathrm{CR}FF_e$	$\mathrm{CR}FF_\mu$	$\mathrm{VR}FNP^{Wh}$			$\mathrm{VR}CF^{Wh}$
	$e^\pm e^\pm$	$\mu^\pm\mu^\pm$	$e^\pm e^\pm$	$e^\pm\mu^\pm$	$\mu^\pm\mu^\pm$	$e^\pm e^\pm$
$N_{\mathrm{BL}}(\ell)$	= 2					
Charge(ℓ)	same-sign					
$N_{\mathrm{Sig}}(\ell)$	= 1		= 2			
$p_{\mathrm{T}}(\ell)$	≥ 25 GeV					
n_{jets}	≥ 1					
$n_{b\text{-jets}}$	–	= 1	= 0			
$E_{\mathrm{T}}^{\mathrm{miss}}$	∈ **[30, 50) GeV**	< **50 GeV**	≥ 50 GeV			
$\lvert m_{\ell^\pm\ell^\pm} - m_Z\rvert$	≥ 15 GeV	–	≥ 15 GeV	–	–	< 15 GeV
m_{jj}	–		< 350 GeV			
m_{T2}	–		< 80 GeV			
$m_{\mathrm{T}}^{\mathrm{min}}$	–		< 100 GeV			
$\mathcal{S}(E_{\mathrm{T}}^{\mathrm{miss}})$	–		< **5**			

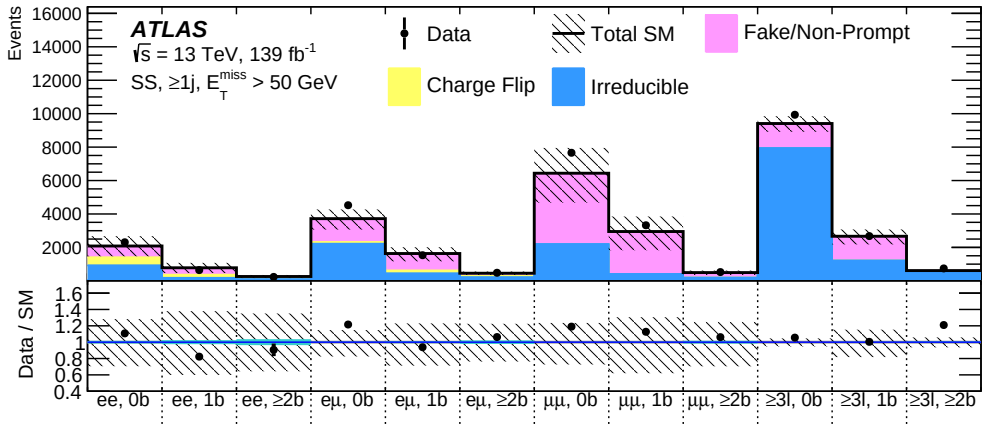

Figure 5: Data event yields compared with the expected contributions from the irreducible and the reducible backgrounds after a loose preselection requiring SS leptons, $E_{\mathrm{T}}^{\mathrm{miss}} > 50$ GeV and at least one jet with $p_{\mathrm{T}} > 25$ GeV. The observed and predicted event yields are classified as a function of the number of leptons and their flavour, as well as the number of b-jets. The error bars only include the statistical uncertainty and the full uncertainties for the data-driven background estimates, in order to validate the matrix method itself. The bottom panel shows the ratio of the observed data to the predicted yields.

to this analysis. It relies on data-corrected CRs enriched in various sources of fake leptons and electron CF backgrounds to extrapolate the background predictions to the SRs. In this analysis, the correction factors are obtained for seven templates representing different types of backgrounds from six control regions, using discriminating variables such as m_{eff} and lepton p_{T}. The uncertainties due to limited statistical precision and from the effects of the used discriminating variables are considered. The similarity of the

m_{T2} distributions obtained using the matrix method and the MC template method for SRs defined for the WZ and bRPV models proves the validity of the background estimation.

8 Systematic uncertainties

Several sources of systematic uncertainty, besides the various statistical uncertainties, are considered in this analysis. They are grouped into experimental uncertainties, theoretical uncertainties, uncertainties from the data-driven methods applied in this analysis, and normalisation and MC statistical uncertainties.

The experimental uncertainties encompass all possible differences between data and simulations in all analysis elements including the trigger, pile-up, and reconstructed objects. A 1.7% relative uncertainty in the luminosity [105] is applied. For leptons, uncertainties in the reconstruction efficiencies [177], identification efficiencies [179], isolation efficiencies, energy scales [177] and resolutions, and trigger efficiencies are considered. For jets, uncertainties in the jet vertex tagger [198] performance which affect the residual contamination from pile-up jets, uncertainties in the jet energy scale [181] and jet energy resolution [199], and uncertainties in flavour tagging [183, 200, 201] are also considered. The uncertainties associated with the objects used to compute the $E_{\mathrm{T}}^{\mathrm{miss}}$ are propagated through the computation, and additional uncertainties in the scale and resolution of the contribution from low-momentum tracks not associated with the primary objects are also included [186]. These experimental uncertainties are correlated between the processes and regions that enter the simultaneous fit, including the signal models.

The theoretical uncertainties account for the uncertainties in modelling of the relevant SM and SUSY processes, including uncertainties in cross sections and due to the choice of scales, the PDF and the value of α_{s}. Modelling uncertainties for backgrounds making subdominant contributions in the SRs are neglected except for cross-section uncertainties. If the background process is normalised to data, the associated uncertainties are applied instead of the total cross-section uncertainty. The uncertainties that affect the acceptance, such as the choice of scales and the PDF, are applied everywhere. The theoretical uncertainties vary from 10% to 50% in all regions defined in this analysis.

The total uncertainty and the contributions from different sources are shown in Figures 6 and 7 for all the signal regions. For regions designed for the Wh model, the total uncertainties vary from 8% to 25%. In some Wh-model-specific SRs, the total uncertainty is less than the largest uncertainty contribution because of the large anti-correlation between the FNP-related uncertainties and the normalisation-related uncertainties. The largest contribution comes from the estimation of the FNP background.

For SRs designed for the WZ and bRPV models, total uncertainties vary from 30% to 50%, with the uncertainties from the estimations of FNP and CF events accounting for the largest contribution in most of the regions. They are larger than those of the Wh model, as the correlations between the relevant systematic uncertainties were not constrained by the CRs during the fit.

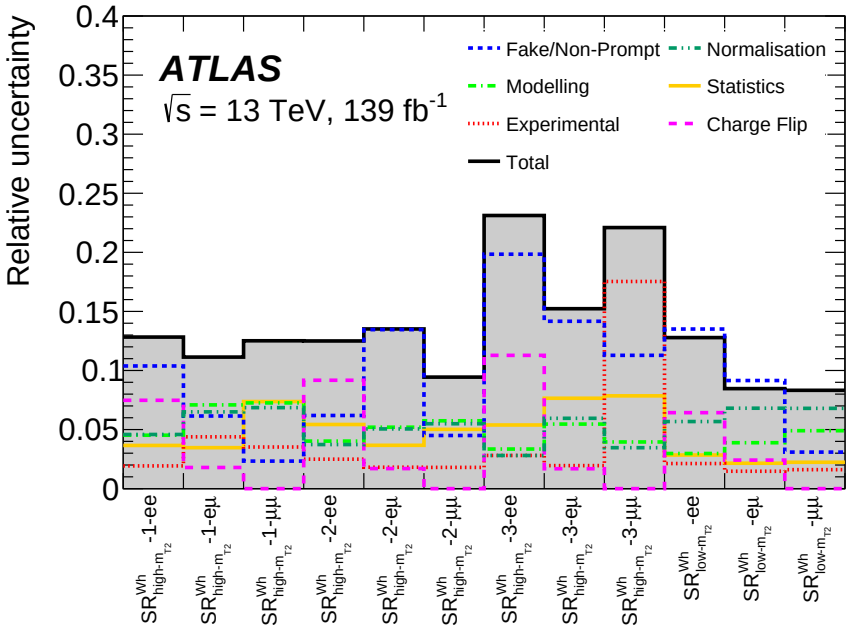

Figure 6: Breakdown of the total systematic uncertainty in the background prediction for each of the SRs of the Wh model. Total and individual uncertainties for different source categories are shown. The individual components can be correlated and therefore do not necessarily add up in quadrature to the total systematic uncertainty.

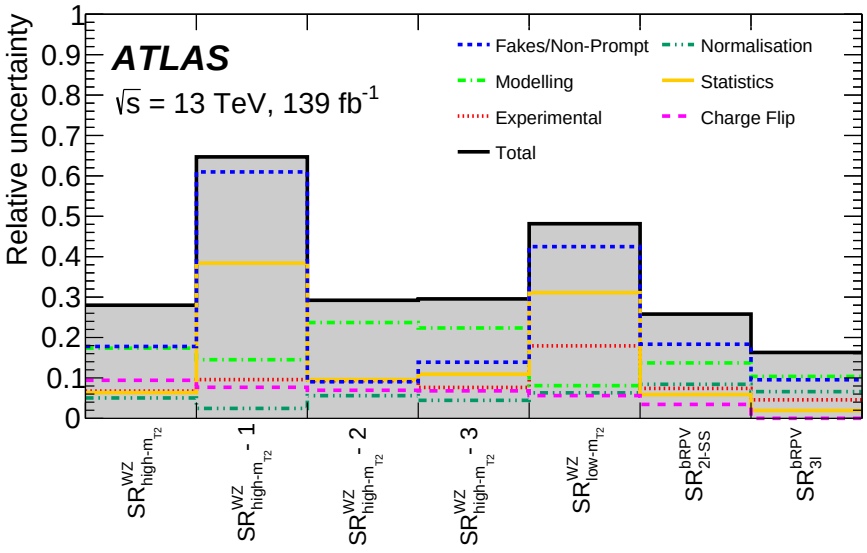

Figure 7: Breakdown of the total systematic uncertainty in the background prediction for the each of the SRs of the WZ and bRPV models. Total and individual uncertainties for different source categories are shown. The individual components can be correlated and therefore do not necessarily add up in quadrature to the total systematic uncertainty.

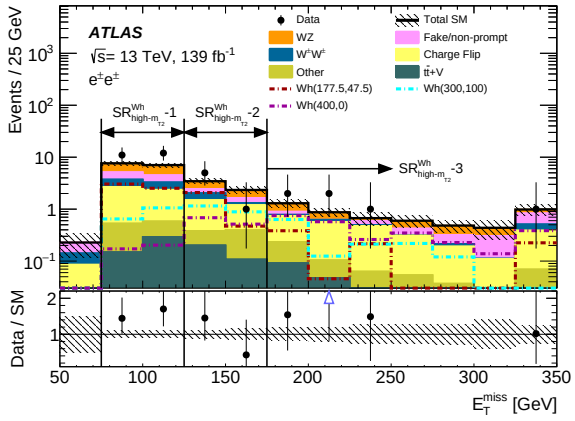

(a)

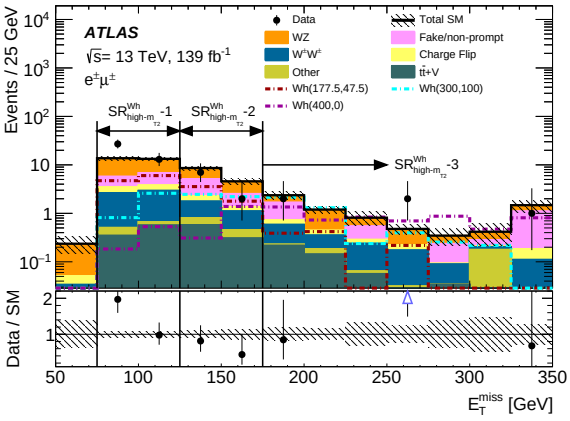

(b)

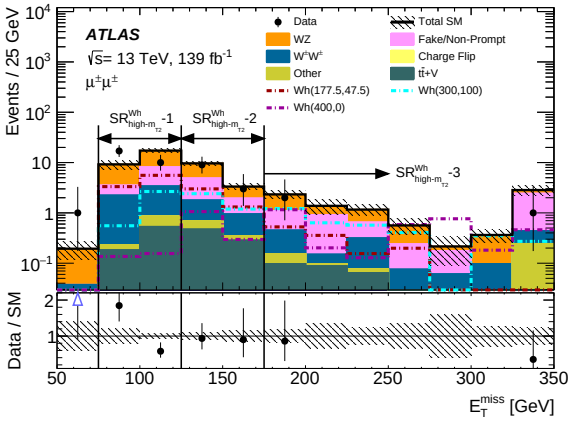

(c)

Figure 8: $E_{\mathrm{T}}^{\mathrm{miss}}$ distributions after the background-only fit, showing the data and the post-fit expected background in all the flavour and $E_{\mathrm{T}}^{\mathrm{miss}}$ bins of the $\mathrm{SR}^{Wh}_{\text{high-}m_{\mathrm{T2}}}$ region. The vertical black lines and the corresponding arrows indicate the cuts defining the three $E_{\mathrm{T}}^{\mathrm{miss}}$ bins of the $\mathrm{SR}^{Wh}_{\text{high-}m_{\mathrm{T2}}}$ region: $\mathrm{SR}^{Wh}_{\text{high-}m_{\mathrm{T2}}}$-1, $\mathrm{SR}^{Wh}_{\text{high-}m_{\mathrm{T2}}}$-2, and $\mathrm{SR}^{Wh}_{\text{high-}m_{\mathrm{T2}}}$-3. The last bin includes overflow. The 'Other' category contains the $t\bar{t}+H$, rare top, triboson, and other diboson processes with the SS final state. Distributions for three representative signal mass points of the Wh model are overlaid. The bottom panel shows the ratio of the observed data to the predicted yields. The hatched bands indicate the combined theoretical, experimental, data-driven and MC statistical uncertainties.

9 Results

The $E_{\mathrm{T}}^{\mathrm{miss}}$ and $\mathcal{S}(E_{\mathrm{T}}^{\mathrm{miss}})$ distributions for all events passing the Wh SR requirements, except for the $E_{\mathrm{T}}^{\mathrm{miss}}$ and $\mathcal{S}(E_{\mathrm{T}}^{\mathrm{miss}})$ requirements themselves, are shown in Figure 8 and Figure 9, respectively. Data are compared with the expected SM background; each source is estimated as described in Section 7. Separate distributions are provided for each SS-dilepton flavour: $e^{\pm}e^{\pm}$, $e^{\pm}\mu^{\pm}$ and $\mu^{\pm}\mu^{\pm}$. Fake and non-prompt leptons as well as the WZ irreducible background dominate the events mimicking signal events, while the CF events are an important source of background in the $e^{\pm}e^{\pm}$ SRs, as observed in Figure 8(a) and Figure 9(a). The expected distributions for three representative signal mass points are also overlaid as indicated. Good agreement between the data and total expected SM background is observed.

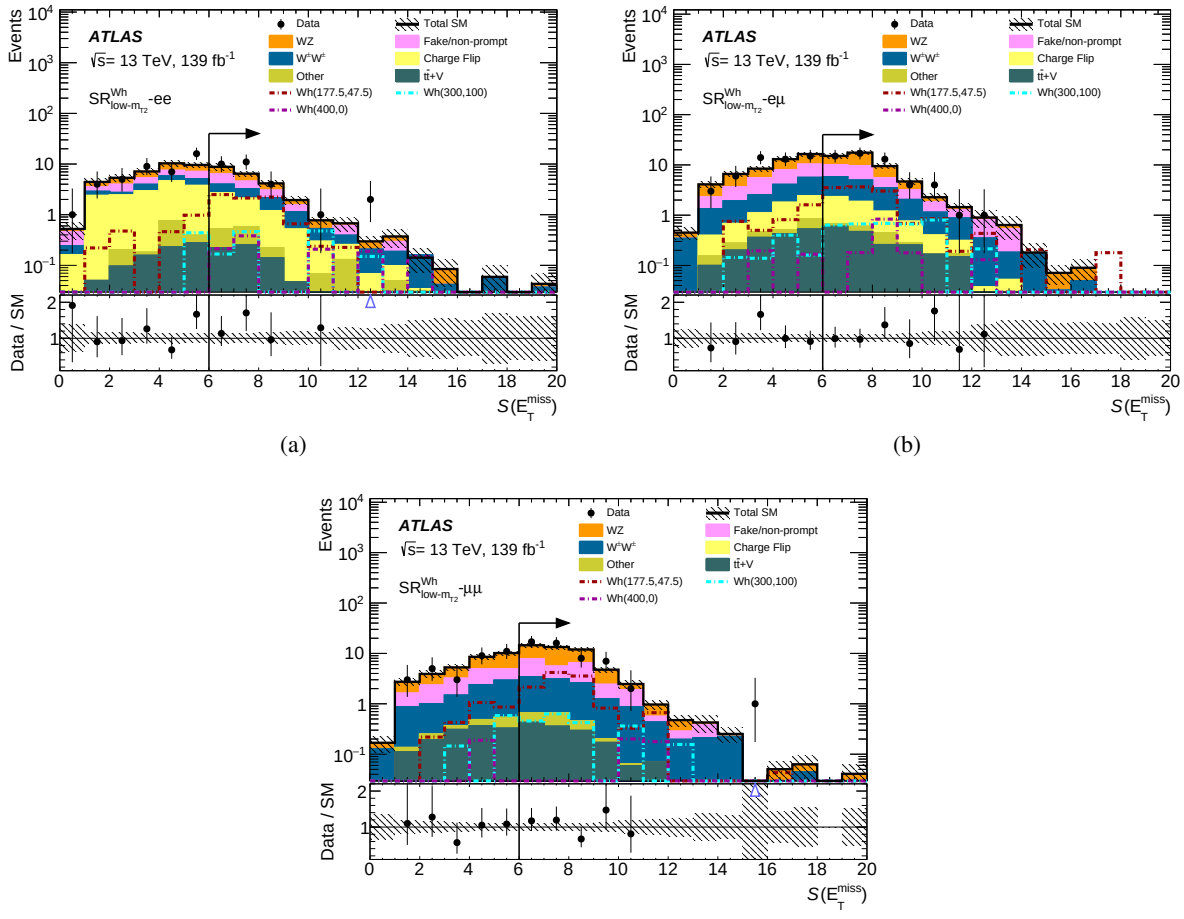

(a) (b)

(c)

Figure 9: $\mathcal{S}(E_{\mathrm{T}}^{\mathrm{miss}})$ distributions after the background-only fit, showing the data and the post-fit expected background in all the flavour bins of the $\mathrm{SR}^{Wh}_{\text{low-}m_{\mathrm{T2}}}$ region. The vertical black line and the corresponding arrow indicates the cut defining the $\mathrm{SR}^{Wh}_{\text{low-}m_{\mathrm{T2}}}$ region. The last bin includes overflow. The 'Other' category contains the $t\bar{t}$+H, rare top, triboson, and other diboson processes with the SS final state. Distributions for three representative signal mass points of the Wh model are overlaid. The bottom panel shows the ratio of the observed data to the predicted yields. The hatched bands indicate the combined theoretical, experimental, data-driven and MC statistical uncertainties.

The observed number of events in each SR defined in Section 6 for the Wh model along with the background expectations and uncertainties are reported in Figure 10. The observed data are compatible with the SM prediction, with a -2.0σ data deficit observed in $\mathrm{SR}^{Wh}_{\text{high-}m_{\mathrm{T2}}}$-3-$\mu\mu$. The largest excess of events is observed in $\mathrm{SR}^{Wh}_{\text{high-}m_{\mathrm{T2}}}$-1-$ee$, with a significance of less than 2.0σ.

The distributions of m_{T2} in the SRs defined for the WZ model and the bRPV models after applying all selection criteria apart from the m_{T2} cut are shown in Figures 11(a) to 11(b) and in Figures 11(c) to 11(d), respectively. All considered sources of background are also plotted, estimated with the data-driven techniques detailed in Section 7. The background is dominated by the SM WZ process and the reducible background due to fake and non-prompt leptons. For comparison, representative signal mass points for winos/binos and higgsinos ($\tilde{H}$) are overlaid. The data distributions are in agreement with the background expectations.

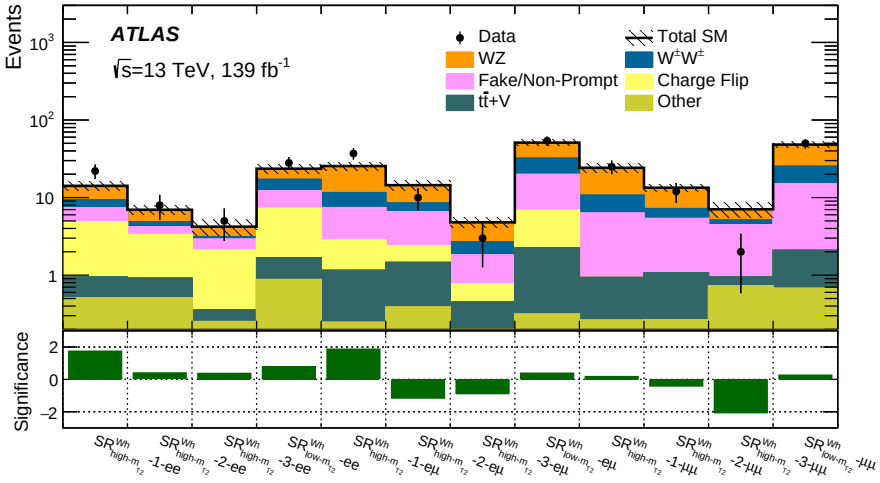

Figure 10: Expected SM background and data yields in the SRs optimised for the Wh model. The total uncertainties in the expected event yields are shown as the hashed bands. The SM prediction is taken from the background-only fit. The 'Other' category contains the $t\bar{t}+H$, rare top, triboson, and other diboson processes with the SS final state. The bottom panel shows the statistical significance [194] of the discrepancy between the observed number of events and the SM expectation.

In Figure 12, the observed yields in each signal region defined in Section 6 along with the background expectations and uncertainties are presented for the WZ and bRPV models. The observed data are compatible with the SM prediction.

The results from the UDD RPV model SRs are discussed in Appendix A.3. The data agree within uncertainties with the SM expectation in the SRs designed for this model.

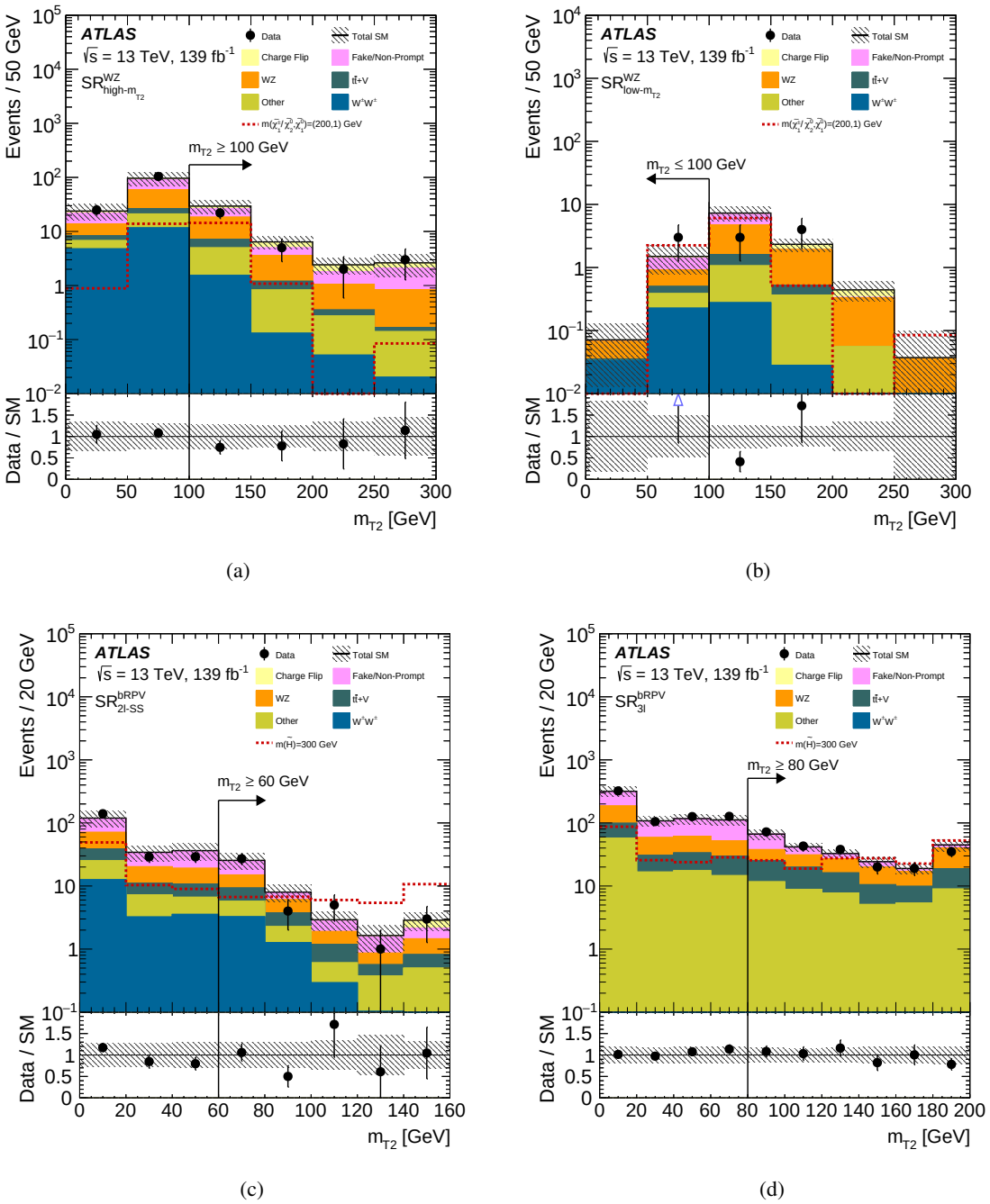

Figure 11: m_{T2} distributions in SRs defined for the WZ model ((a) and (b)) and the bRPV model ((c) and (d)). All SR selection criteria are satisfied except for that on m_{T2}. The vertical black lines and the corresponding arrows indicate the cuts defining those regions. The matrix method is used for background estimation and the CF events are estimated via a data-driven method. The 'Other' category contains the $t\bar{t}$+H, rare top, triboson, and other diboson processes with the SS final state. Uncertainties from theoretical, experimental, data-driven and MC statistical sources are all considered. The last bin includes overflow. Distributions for representative signal mass points are overlaid. The bottom panel shows the ratio of the observed data to the predicted yields.

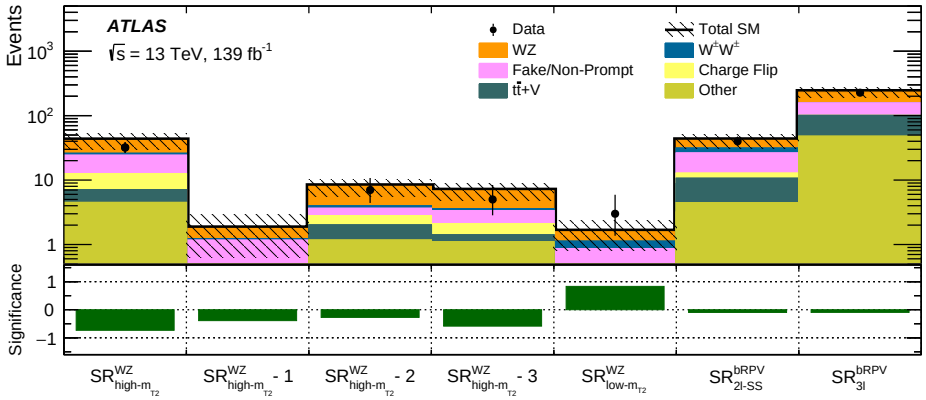

Figure 12: Expected SM background and data yields in the SRs optimised for the WZ and bRPV models. The SM prediction is taken from the background-only fit. The 'Other' category contains the $t\bar{t}+H$, rare top, triboson, and other diboson processes with the SS final state. The total uncertainties in the expected event yields are shown as the hashed bands. The bottom panel shows the statistical significance [194] of the discrepancy between the observed number of events and the SM expectation.

10 Interpretation

Model-independent upper limits on the number of BSM events in each SR are derived using the CL_s prescription [202, 203] and neglecting any possible signal contamination in the control regions. The HistFitter [193] framework is used for the statistical interpretation of the results. In order to quantify the probability for the background-only hypothesis to fluctuate to at least the observed number of events, a one-sided p_0-value is calculated using pseudo-experiments, where the profile likelihood ratio is used as a test statistic [192] to exclude the signal-plus-background hypothesis. Normalisation to the integrated luminosity of the data sample allows an interpretation in terms of upper limits on the visible BSM cross section, defined as the product of the acceptance, reconstruction efficiency and production cross section.

The number of observed events and the background expectation in each SR are used to set an upper limit on the number of events from any BSM physics scenario. The model-independent upper limits at 95% confidence level (CL) on the visible cross section, $\langle \epsilon\sigma \rangle^{95}_{\text{obs}}$, for the Wh, WZ and bRPV signal regions are presented in Table 7. Also listed are the 95% CL upper limits on the number of signal events S^{95}_{obs}, as well as the expected 95% CL upper limit on the number of signal events, S^{95}_{exp}. The last two columns indicate the CL_b value and the discovery p-value, p_0 ($p(s) = 0$), with the corresponding Gaussian significance Z. The CL_b value provides a measure of compatibility of the observed data with the 95% CL signal strength hypothesis relative to fluctuations of the background, and p_0 measures the compatibility of the observed data with the background-only (zero signal strength) hypothesis relative to fluctuations of the background. Larger values indicate greater relative compatibility.

For $\text{SR}^{WZ}_{\text{high-}m_{\text{T2}}}$, $\text{SR}^{\text{bRPV}}_{2\ell\text{-SS}}$ and $\text{SR}^{\text{bRPV}}_{3\ell}$, p_0 is capped at 0.5 since the predictions exceed the data. In all other SRs the significances are low, with no appreciable excess observed over the expected background. The most stringent observed limit is from $\text{SR}^{WZ}_{\text{low-}m_{\text{T2}}}$, where visible cross sections larger than 0.04 fb are excluded. Model-independent limits are also provided in Appendix A (Table 9) for the UDD RPV SRs.

Table 7: Model-independent statistical analysis for SRs (binned and inclusively) optimised for the Wh, WZ and bRPV models: 95% CL upper limits on the visible cross section, $\langle\epsilon\sigma\rangle^{95}_{\text{obs}}$, and on the number of signal events S^{95}_{obs}. The S^{95}_{exp} is the expected 95% CL upper limit on the number of signal events, given the expected number (and $\pm1\sigma$ variations) of background events. The last two columns report the CL_b value for the background-only hypothesis, the one-sided p_0-value and the local significance Z (the number of equivalent Gaussian standard deviations).

Signal region	$\langle\epsilon\sigma\rangle^{95}_{\text{obs}}$ [fb]	S^{95}_{obs}	S^{95}_{exp}	CL_b	p_0 (Z)
$\text{SR}^{Wh}_{\text{high-}m_{\text{T2}}}$	0.28	39.3	$33.9^{+14.3}_{-10.0}$	0.66	0.34 (0.41)
$\text{SR}^{Wh}_{\text{high-}m_{\text{T2}}}$-1-$ee$	0.13	17.4	$9.9^{+4.4}_{-2.8}$	0.94	0.04 (1.72)
$\text{SR}^{Wh}_{\text{high-}m_{\text{T2}}}$-1-$e\mu$	0.17	23.6	$12.9^{+5.6}_{-3.6}$	0.96	0.03 (1.85)
$\text{SR}^{Wh}_{\text{high-}m_{\text{T2}}}$-1-$\mu\mu$	0.09	13.0	$12.6^{+5.4}_{-3.6}$	0.55	0.45 (0.14)
$\text{SR}^{Wh}_{\text{high-}m_{\text{T2}}}$-2-$ee$	0.06	7.8	$7.2^{+3.1}_{-2.2}$	0.63	0.36 (0.36)
$\text{SR}^{Wh}_{\text{high-}m_{\text{T2}}}$-2-$e\mu$	0.05	6.8	$9.5^{+4.0}_{-2.7}$	0.16	0.50 (0.00)
$\text{SR}^{Wh}_{\text{high-}m_{\text{T2}}}$-2-$\mu\mu$	0.07	9.6	$7.7^{+0.6}_{-0.2}$	0.64	0.50 (0.00)
$\text{SR}^{Wh}_{\text{high-}m_{\text{T2}}}$-3-$ee$	0.05	6.9	$6.1^{+3.0}_{-1.6}$	0.61	0.37 (0.33)
$\text{SR}^{Wh}_{\text{high-}m_{\text{T2}}}$-3-$e\mu$	0.03	4.8	$6.1^{+3.0}_{-1.6}$	0.24	0.50 (0.00)
$\text{SR}^{Wh}_{\text{high-}m_{\text{T2}}}$-3-$\mu\mu$	0.03	4.3	$6.9^{+3.0}_{-2.0}$	0.06	0.50 (0.00)
$\text{SR}^{Wh}_{\text{low-}m_{\text{T2}}}$	0.24	33.0	$29.5^{+11.7}_{-8.8}$	0.63	0.33 (0.43)
$\text{SR}^{Wh}_{\text{low-}m_{\text{T2}}}$-$ee$	0.12	16.2	$12.6^{+5.4}_{-3.6}$	0.76	0.23 (0.76)
$\text{SR}^{Wh}_{\text{low-}m_{\text{T2}}}$-$e\mu$	0.14	19.9	$17.6^{+7.4}_{-5.1}$	0.63	0.36 (0.35)
$\text{SR}^{Wh}_{\text{low-}m_{\text{T2}}}$-$\mu\mu$	0.13	18.2	$17.0^{+7.0}_{-4.9}$	0.59	0.41 (0.22)
$\text{SR}^{WZ}_{\text{high-}m_{\text{T2}}}$	0.13	18.7	$24.4^{+6.8}_{-5.0}$	0.12	0.50 (0.00)
$\text{SR}^{WZ}_{\text{high-}m_{\text{T2}}}$-1	0.01	1.7	$3.6^{+1.3}_{-0.6}$	0.02	0.45 (0.12)
$\text{SR}^{WZ}_{\text{high-}m_{\text{T2}}}$-2	0.05	7.4	$8.3^{+3.2}_{-2.2}$	0.34	0.50 (0.00)
$\text{SR}^{WZ}_{\text{high-}m_{\text{T2}}}$-3	0.04	5.2	$7.3^{+2.7}_{-1.8}$	0.11	0.50 (0.00)
$\text{SR}^{WZ}_{\text{low-}m_{\text{T2}}}$	0.04	5.9	$4.4^{+1.8}_{-0.8}$	0.81	0.22 (0.76)
$\text{SR}^{\text{bRPV}}_{2\ell\text{-SS}}$	0.16	22.6	$25.8^{+7.9}_{-5.8}$	0.29	0.50 (0.00)
$\text{SR}^{\text{bRPV}}_{3\ell}$	0.44	61.4	$93.0^{+56.0}_{-20.3}$	0.02	0.50 (0.00)

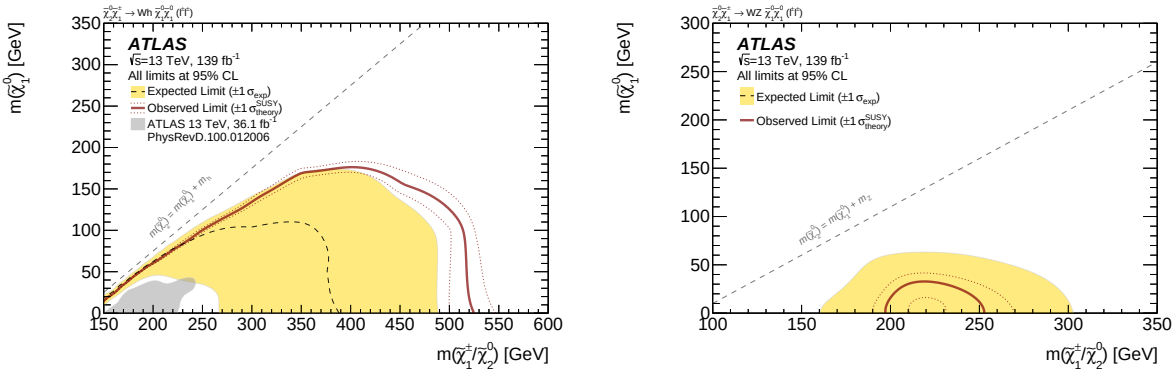

(a) (b)

Figure 13: Exclusion limits at 95% CL for the (a) Wh-mediated and the (b) WZ-mediated simplified model of wino $\tilde{\chi}_1^{\pm}\tilde{\chi}_2^0$ production. Observed (solid) and expected (dashed) limits on $\tilde{\chi}_1^{\pm}/\tilde{\chi}_2^0$ and $\tilde{\chi}_1^0$ masses are indicated. The red dotted lines around the observed limit reflect the theoretical variation due to the signal cross-section uncertainty. The band around the expected limits expresses the $\pm 1\sigma$ variation due to all uncertainties except theoretical uncertainties in the signal cross section. The grey region in (a) denotes the observed limits obtained in a previous search in the same channel with 36.1 fb^{-1} of data [43].

Model-dependent exclusion limits were extracted by performing hypothesis tests on the background-only hypothesis and the signal-plus-background hypothesis using the HistFitter package. Both fits were carried out simultaneously in all SRs of each model and for each benchmark point together with its uncertainty. All SRs corresponding to a model are statistically combined. Following the CL_s prescription, the p-values of the signal-plus-background hypothesis are tested against those of the background-only hypothesis to extract the corresponding CL_s values for each point. A signal point is considered excluded at 95% CL when such values fall below a 5% threshold.

The resulting expected and observed exclusion limits for the Wh model are shown in Figure 13(a). The large $\pm 1\sigma$ uncertainty band around the expected limit is almost entirely dominated by the statistical uncertainty of the MC simulated signals. The observed bounds are stronger than the expected ones due to the deficit of data compared to the SM background expectation seen in $\mathrm{SR}^{Wh}_{\text{high-}m_{\mathrm{T2}}}$-3-$\mu\mu$, as shown in Figure 10. This SR features the strongest sensitivity in the region with high chargino–LSP mass splittings, as it combines the highest $E_{\mathrm{T}}^{\mathrm{miss}}$ threshold and the greatest expected number of events and purity that characterises the dimuon channel. However, this discrepancy falls within a 2σ fluctuation of the expected limit.

In the Wh model, $\tilde{\chi}_1^{\pm}/\tilde{\chi}_2^0$ masses are excluded up to about 525 GeV for a massless $\tilde{\chi}_1^0$. On the other hand, the exclusion for $\tilde{\chi}_1^0$ masses reaches about 180 GeV for $m(\tilde{\chi}_1^{\pm}/\tilde{\chi}_2^0) \simeq 400$ GeV. The comparison with the observed exclusion limits from the previous 36.1 fb^{-1} search [43] in the same channel demonstrates that the current analysis has a greatly improved reach.

The observed and expected exclusion limits for the WZ model are shown in Figure 13(b), where two orthogonal SRs, $\mathrm{SR}^{WZ}_{\text{high-}m_{\mathrm{T2}}}$ and $\mathrm{SR}^{WZ}_{\text{low-}m_{\mathrm{T2}}}$, are statistically combined. The deficit of data events compared to the SM expectation in $\mathrm{SR}^{WZ}_{\text{high-}m_{\mathrm{T2}}}$, seen in Figure 12, leads to the observed limits being more stringent than the expected ones, yet within the 1σ band around the latter. The uncertainty in the expected exclusion limit is dominated by the FNP background determination, as observed in Figure 7. For a massless $m(\tilde{\chi}_1^0)$, $\tilde{\chi}_1^{\pm}/\tilde{\chi}_2^0$ masses in the interval 200–250 GeV are excluded. This is the first analysis in ATLAS with sensitivity to the WZ model in the two-SS-lepton channel. Previous analyses, assuming a nearly

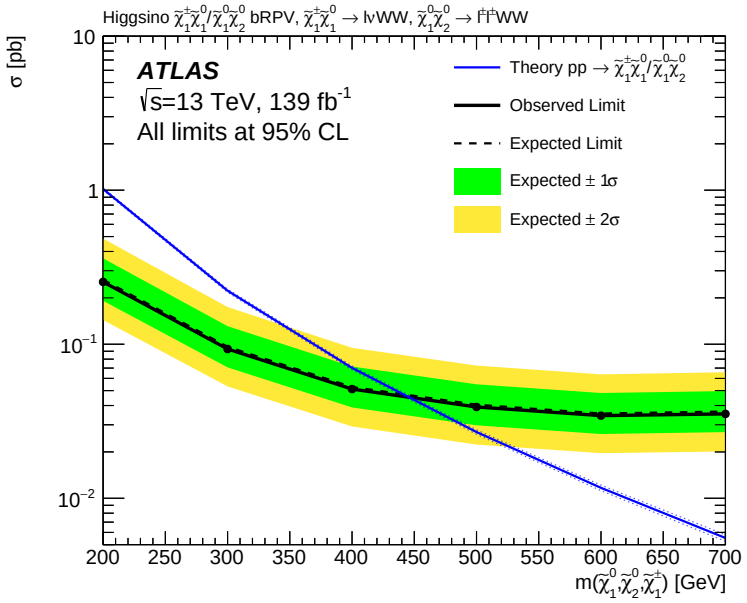

Figure 14: Observed (black solid line) and expected (black dashed line) 95% CL exclusion limits as a function of higgsino $\tilde{\chi}_1^0/\tilde{\chi}_2^0/\tilde{\chi}_1^{\pm}$ mass in the bilinear RPV model. The green (yellow) contours of the band around the expected limit are the $\pm 1\sigma$ ($\pm 2\sigma$) variations including all uncertainties. The prediction for the theoretical production cross section is also shown (blue solid line) with its uncertainty (blue dotted lines).

massless $\tilde{\chi}_1^0$, excluded $\tilde{\chi}_1^{\pm}/\tilde{\chi}_2^0$ masses of up to 640 GeV by selecting three-lepton events [56], while the search with boosted hadronically decaying bosons was sensitive to higher masses, excluding a mass range of 440–960 GeV [58].

The expected and observed production cross-section upper limits for light higgsinos in the bRPV model can be seen in Figure 14 with the statistical combination of two orthogonal SRs, namely $\text{SR}_{2\ell\text{-SS}}^{\text{bRPV}}$ and $\text{SR}_{3\ell}^{\text{bRPV}}$. By comparing the observed upper limits on the cross section with the theoretical expected cross section, higgsino $\tilde{\chi}_1^0/\tilde{\chi}_2^0/\tilde{\chi}_1^{\pm}$ masses smaller than 440 GeV are excluded when assuming inclusive higgsino production and allowing all predicted sparticle decay modes. These are the first experimental constraints on bRPV models with degenerate higgsino masses.

11 Conclusion

This paper presents a search for directly produced electroweak gauginos and higgsinos in events with two electrons or muons of the same charge or three leptons based on a 139 fb^{-1} sample of $\sqrt{s} = 13$ TeV proton–proton collisions collected by the ATLAS experiment at the LHC from 2015 to 2018. Events are categorised according to the number of jets, the number of b-jets, the missing transverse momentum, the effective mass and other relevant observables, substantially improving the sensitivity to specific R-parity-conserving and R-parity-violating scenarios. No significant excess over the expected background is observed. Observed 95% CL limits are placed on the visible cross section in the defined signal regions and constraints are set on the parameters of the simplified topologies and complete models considered. In a wino–bino Wh-mediated model, NLSP masses of up to 525 GeV are excluded for a massless lightest neutralino, a considerable improvement on previous limits of 240 GeV and 300 GeV set by ATLAS [43]

with a 36.1 fb^{-1} data set and CMS [46] with a 137 fb^{-1} sample, respectively. The analogous excluded $\tilde{\chi}_1^{\pm}/\tilde{\chi}_2^0$ mass range for the WZ topology is between 200 GeV and 250 GeV in a channel probed for the first time by ATLAS in the two-same-sign-lepton final state. In a natural RPV model with bilinear terms, never explored before in electroweak SUSY production, mass-degenerate higgsinos $\tilde{\chi}_1^0/\tilde{\chi}_2^0/\tilde{\chi}_1^{\pm}$ lighter than 440 GeV are excluded. Model-independent production cross-section upper bounds as low as 40 ab are set in signal regions inspired by an R-parity-violating scenario with a baryon-number-violating term. Search regions orthogonal to those in other ATLAS analyses were deployed in all considered models, allowing better future statistical combinations with other channels.

Acknowledgements

We thank CERN for the very successful operation of the LHC, as well as the support staff from our institutions without whom ATLAS could not be operated efficiently.

We acknowledge the support of ANPCyT, Argentina; YerPhI, Armenia; ARC, Australia; BMWFW and FWF, Austria; ANAS, Azerbaijan; CNPq and FAPESP, Brazil; NSERC, NRC and CFI, Canada; CERN; ANID, Chile; CAS, MOST and NSFC, China; Minciencias, Colombia; MEYS CR, Czech Republic; DNRF and DNSRC, Denmark; IN2P3-CNRS and CEA-DRF/IRFU, France; SRNSFG, Georgia; BMBF, HGF and MPG, Germany; GSRI, Greece; RGC and Hong Kong SAR, China; ISF and Benoziyo Center, Israel; INFN, Italy; MEXT and JSPS, Japan; CNRST, Morocco; NWO, Netherlands; RCN, Norway; MEiN, Poland; FCT, Portugal; MNE/IFA, Romania; MESTD, Serbia; MSSR, Slovakia; ARRS and MIZŠ, Slovenia; DSI/NRF, South Africa; MICINN, Spain; SRC and Wallenberg Foundation, Sweden; SERI, SNSF and Cantons of Bern and Geneva, Switzerland; MOST, Taiwan; TENMAK, Türkiye; STFC, United Kingdom; DOE and NSF, United States of America. In addition, individual groups and members have received support from BCKDF, CANARIE, Compute Canada and CRC, Canada; PRIMUS 21/SCI/017 and UNCE SCI/013, Czech Republic; COST, ERC, ERDF, Horizon 2020 and Marie Skłodowska-Curie Actions, European Union; Investissements d'Avenir Labex, Investissements d'Avenir Idex and ANR, France; DFG and AvH Foundation, Germany; Herakleitos, Thales and Aristeia programmes co-financed by EU-ESF and the Greek NSRF, Greece; BSF-NSF and MINERVA, Israel; Norwegian Financial Mechanism 2014-2021, Norway; NCN and NAWA, Poland; La Caixa Banking Foundation, CERCA Programme Generalitat de Catalunya and PROMETEO and GenT Programmes Generalitat Valenciana, Spain; Göran Gustafssons Stiftelse, Sweden; The Royal Society and Leverhulme Trust, United Kingdom.

The crucial computing support from all WLCG partners is acknowledged gratefully, in particular from CERN, the ATLAS Tier-1 facilities at TRIUMF (Canada), NDGF (Denmark, Norway, Sweden), CC-IN2P3 (France), KIT/GridKA (Germany), INFN-CNAF (Italy), NL-T1 (Netherlands), PIC (Spain), ASGC (Taiwan), RAL (UK) and BNL (USA), the Tier-2 facilities worldwide and large non-WLCG resource providers. Major contributors of computing resources are listed in Ref. [204].

Appendix

A RPV analysis with *UDD* terms

A.1 Signal regions

The signal regions designed to maximise the sensitivity to signals in this model are listed in Table 8. Orthogonal signal regions are defined with the number of b-jets. In each case, the signal regions are split according to the jet multiplicity targeting different higgsino mass ranges.

Within each SR, variables such as the sum of the jets' p_{T} ($\sum p_{\mathrm{T}}^{\mathrm{jet}}$), the sum of the b-jets' p_{T} divided by the sum of the jets' p_{T} ($\sum p_{\mathrm{T}}^{b\text{-jet}} / \sum p_{\mathrm{T}}^{\mathrm{jet}}$), the minimum angular distance between the leading lepton and jets ($\Delta R(\ell_1, \mathrm{jet})_{\mathrm{min}}$) and the angular distance between the two SS leptons are used to maximise the sensitivity to the target signal, based on a series of dedicated optimisation studies.

Table 8: Signal region definitions designed for the *UDD* RPV model. The variables are defined in the text.

	$\mathrm{SR}^{\mathrm{RPV}}_{2\ell 1b}$		$\mathrm{SR}^{\mathrm{RPV}}_{2\ell 2b}$			$\mathrm{SR}^{\mathrm{RPV}}_{2\ell 3b}$		
	L	M	L	M	H	L	M	H
$N_{\mathrm{BL}}(\ell)$	= 2							
$N_{\mathrm{Sig}}(\ell)$	= 2							
Charge(ℓ)	same-sign							
$p_{\mathrm{T}}(\ell)$	> 25 GeV							
n_{jets} (p_{T} > 25 GeV)	≥ 1							
$n_{b\text{-jets}}$	= 1		= 2			≥ 3		
$\sum p_{\mathrm{T}}(\ell)$	≥ 100 GeV		–			–		
$E_{\mathrm{T}}^{\mathrm{miss}}$	≥ 100 GeV	≥ 50 GeV	≥ 80 GeV			≥ 20 GeV		
n_{jets} (p_{T} > 25 GeV)	≤ 2	= 2 or = 3	≤ 3	=3 or = 4	≥ 5 and ≤ 6	≤ 3	≤ 3	≤ 6
$\sum p_{\mathrm{T}}^{b\text{-jet}} / \sum p_{\mathrm{T}}^{\mathrm{jet}}$	≥ 0.7	≥ 0.45	≥ 0.9	≥ 0.75	–	≥ 0.8	≥ 0.8	≥ 0.5
$\sum p_{\mathrm{T}}^{\mathrm{jet}}$	≥ 120 GeV	≥ 400 GeV	≥ 300 GeV	≥ 420 GeV	≥ 420 GeV	–	–	≥ 350 GeV
$\Delta R(\ell_1, \mathrm{jet})_{\mathrm{min}}$	≤ 1.2	≤ 1.0	≤ 1.0	≤ 1.0	≤ 1.0	≤ 1.5	–	≤ 1.0
$\Delta R(\ell^{\pm}, \ell^{\pm})$	≥ 2.0	≥ 2.5	≥ 2.5	≥ 2.5	≥ 2.0	≥ 2.0	–	≥ 2.0

A.2 Background estimation and systematic uncertainties

The background composition is similar to that in the SRs described in Section 6, but with $t\bar{t}$+V as the dominant irreducible background in the above SRs because of the b-jet requirement.

The background estimation strategy is the same as that used for the regions designed for the WZ and bRPV models, described in detail in Section 7. The irreducible backgrounds are estimated through MC simulation, after applying data-driven correction factors for the WZ background events with at least two jets obtained from $\mathrm{CR}WZ_{2j}^{WZ,(\mathrm{b})\mathrm{RPV}}$. The CF events are estimated via the data-driven method described in Section 7. The FNP events are estimated from the data by applying the matrix method, after it was validated by comparing its estimates with those of the MC template method.

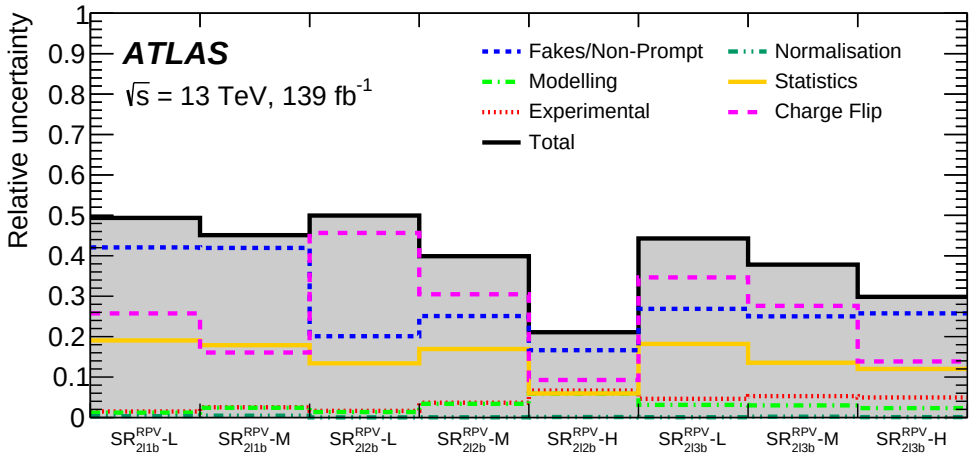

Figure 15: Relative contributions from experimental and theoretical uncertainties in SRs defined for the *UDD* RPV model. The individual components can be correlated and therefore do not necessarily add up in quadrature to the total systematic uncertainty.

Figure 15 shows the uncertainties' contributions in the signal regions designed for this model. The uncertainties vary from 20% to 50% depending on the regions. The largest contribution comes from the data-driven methods applied.

A.3 Results

The $\sum p_{\mathrm{T}}^{b\text{-jet}}/\sum p_{\mathrm{T}}^{\mathrm{jet}}$ distributions for the data and background sources are presented for a subset of the SRs in Figure 16. All selection criteria defined in Table 8 are applied apart from the one on $\sum p_{\mathrm{T}}^{b\text{-jet}}/\sum p_{\mathrm{T}}^{\mathrm{jet}}$, which is indicated in the graphs by a vertical line and an arrow. The data and total background expectation are in agreement, considering the involved uncertainties.

A comparison between the data and background yields for all the SRs defined for the *UDD* RPV model is shown in Figure 17. The observed and expected numbers of events are compatible in all SRs, with the largest excess being $\sim 1\sigma$, observed in $\mathrm{SR}^{\mathrm{RPV}}_{2\ell 3b}$-H. Following the procedure described in Section 10, these results are used to set model-independent upper limits as low as 40 ab on BSM production cross sections, as listed in Table 9.

Figure 18 shows the expected upper limits for the higgsino *UDD* RPV model. All combinations of orthogonal SRs which target the same mass point are considered, including $\mathrm{SR}^{\mathrm{RPV}}$-L (the statistical combination of $\mathrm{SR}^{\mathrm{RPV}}_{2\ell 1b}$-L, $\mathrm{SR}^{\mathrm{RPV}}_{2\ell 2b}$-L, $\mathrm{SR}^{\mathrm{RPV}}_{2\ell 3b}$-L), $\mathrm{SR}^{\mathrm{RPV}}$-M (the statistical combination of $\mathrm{SR}^{\mathrm{RPV}}_{2\ell 1b}$-M, $\mathrm{SR}^{\mathrm{RPV}}_{2\ell 2b}$-M, $\mathrm{SR}^{\mathrm{RPV}}_{2\ell 3b}$-M) and $\mathrm{SR}^{\mathrm{RPV}}$-H (the statistical combination of $\mathrm{SR}^{\mathrm{RPV}}_{2\ell 2b}$-H, $\mathrm{SR}^{\mathrm{RPV}}_{2\ell 3b}$-H). Among these combinations, the one providing the strongest expected limit is chosen for each $\tilde{\chi}^0_{1,2}$ mass point.

A higgsino-like $\tilde{\chi}^0_1/\tilde{\chi}^0_2$ mass of 200 GeV is excluded in this analysis, considering $\tilde{\chi}^0_1\tilde{\chi}^0_2$ production only. This value was excluded by a previous ATLAS search [84] based on the selection of events with one lepton, but also using $\tilde{\chi}^\pm_1\tilde{\chi}^0_1$ and $\tilde{\chi}^\pm_1\tilde{\chi}^0_2$ production with $\tilde{\chi}^\pm_1 \to bbs$.

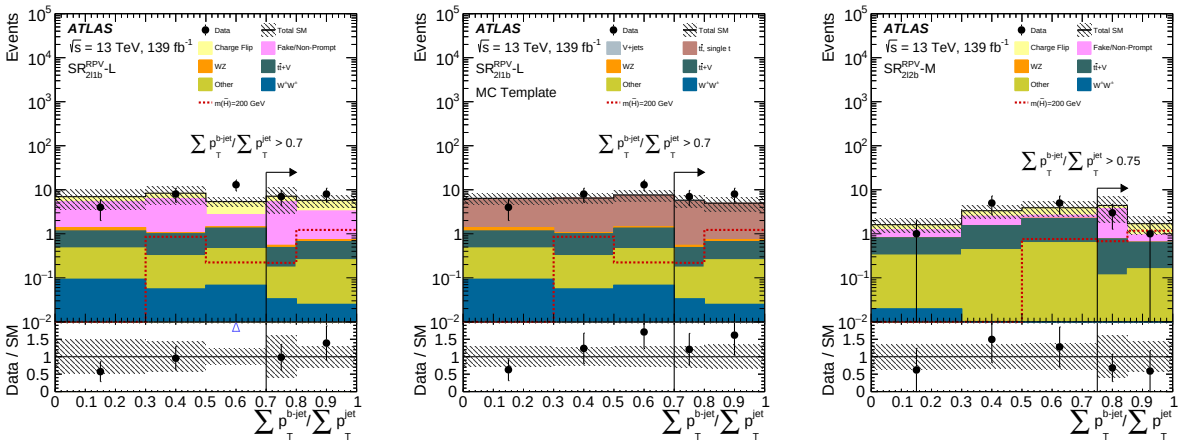

Figure 16: $\sum p_{\mathrm{T}}^{b\text{-jet}} / \sum p_{\mathrm{T}}^{\mathrm{jet}}$ distributions of the data and the expected background in some SRs defined for the *UDD* RPV model with data-driven methods applied. All uncertainties are considered. The vertical black lines and the corresponding arrows indicate the cuts defining those regions. The last bin includes overflow. The 'Other' category contains the $t\bar{t}+H$, rare top, triboson, and other diboson processes with the SS final state. Distributions for a representative signal mass point are overlaid. The bottom panel shows the ratio of the observed data to the predicted yields.

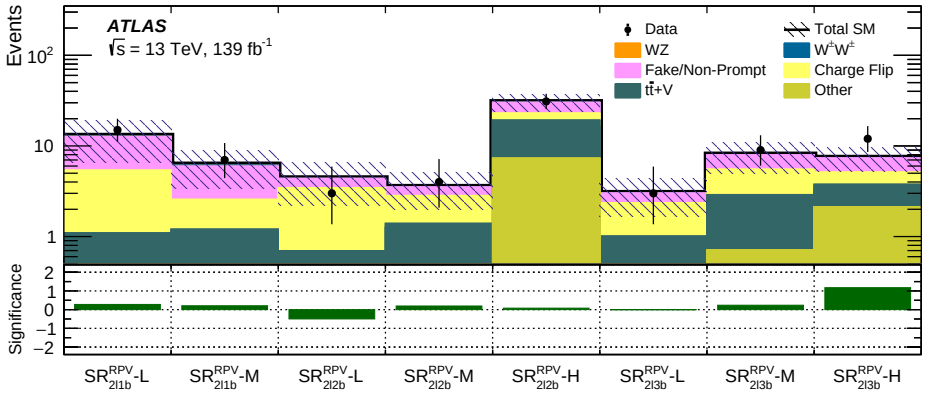

Figure 17: Expected SM background and data yields in the SRs optimised for the *UDD* RPV model. The SM prediction is taken from the background-only fit. The 'Other' category contains the $t\bar{t}+H$, rare top, triboson, and other diboson processes with the SS final state. The total uncertainties in the expected event yields are shown as the hashed bands. The bottom panel shows the statistical significance [194] of the discrepancy between the observed number of events and the SM expectation.

Table 9: Model-independent statistical analysis for SRs optimised for the *UDD* RPV models: the 95% CL upper limit on the visible cross section times efficiency ($\langle\epsilon\sigma\rangle^{95}_{\text{obs}}$), the observed number of signal events (S^{95}_{obs}), and the signal events given the expected number of background events (S^{95}_{exp}, $\pm1\sigma$ variations of the expected number). The last two columns report the CL_b value for the background-only hypothesis, the one-sided p_0-value and the local significance Z (the number of equivalent Gaussian standard deviations).

Signal channel	$\langle\epsilon\sigma\rangle^{95}_{\text{obs}}$ [fb]	S^{95}_{obs}	S^{95}_{exp}	CL_b	p_0 (Z)
$\text{SR}^{\text{RPV}}_{2\ell 1b}$-L	0.13	17.5	$15.1^{+4.8}_{-3.7}$	0.69	0.38 (0.32)
$\text{SR}^{\text{RPV}}_{2\ell 1b}$-M	0.07	10.1	$8.9^{+3.1}_{-1.7}$	0.66	0.46 (0.11)
$\text{SR}^{\text{RPV}}_{2\ell 2b}$-L	0.04	6.1	$6.2^{+2.4}_{-1.1}$	0.48	0.50 (0.00)
$\text{SR}^{\text{RPV}}_{2\ell 2b}$-M	0.05	6.8	$6.0^{+2.3}_{-1.2}$	0.65	0.38 (0.30)
$\text{SR}^{\text{RPV}}_{2\ell 2b}$-H	0.15	20.7	$18.6^{+6.0}_{-4.3}$	0.64	0.41 (0.22)
$\text{SR}^{\text{RPV}}_{2\ell 3b}$-L	0.04	6.1	$5.7^{+1.9}_{-1.0}$	0.61	0.50 (0.00)
$\text{SR}^{\text{RPV}}_{2\ell 3b}$-M	0.08	11.5	$9.7^{+3.2}_{-1.8}$	0.70	0.35 (0.37)
$\text{SR}^{\text{RPV}}_{2\ell 3b}$-H	0.10	13.5	$8.6^{+3.2}_{-2.5}$	0.92	0.10 (1.31)

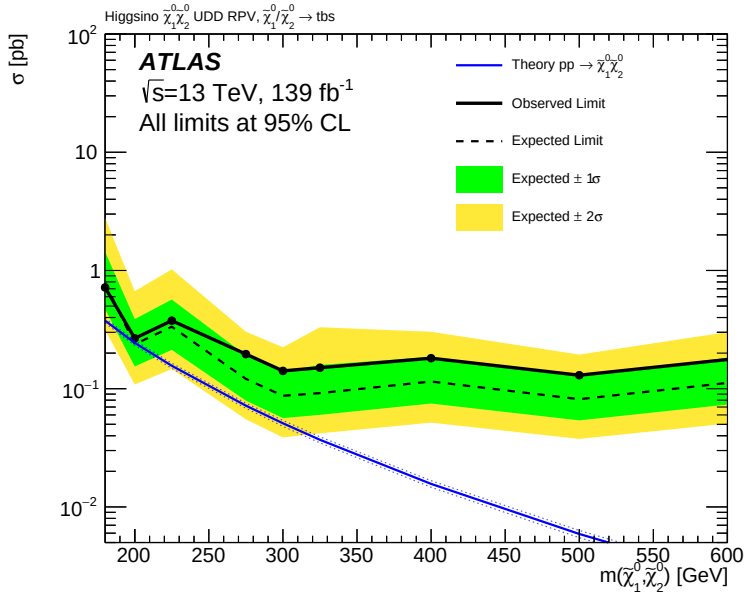

Figure 18: Observed (black solid line) and expected (black dashed line) 95% CL exclusion limits as a function of higgsino $\tilde{\chi}_1^0/\tilde{\chi}_2^0$ mass in the *UDD* RPV model. The green (yellow) contours of the band around the expected limit are the $\pm1\sigma$ ($\pm2\sigma$) variations including all uncertainties. The prediction for the theoretical production cross section is also shown (blue solid line) with its uncertainty (blue dotted lines).

References

[1] J. Alwall et al., *The automated computation of tree-level and next-to-leading order differential cross sections, and their matching to parton shower simulations*, JHEP **07** (2014) 079, arXiv: 1405.0301 [hep-ph].

[2] P. A. Zyla et al., *Review of Particle Physics*, PTEP **2020** (2020) 083C01.

[3] R. M. Barnett, J. F. Gunion and H. E. Haber, *Discovering supersymmetry with like-sign dileptons*, Phys. Lett. B **315** (1993) 349, arXiv: hep-ph/9306204.

[4] M. Guchait and D. P. Roy, *Like-sign dilepton signature for gluino production at CERN LHC including top quark and Higgs boson effects*, Phys. Rev. D **52** (1995) 133, arXiv: hep-ph/9412329.

[5] Y. Bai and Z. Han, *Top-antitop and Top-top Resonances in the Dilepton Channel at the CERN LHC*, JHEP **04** (2009) 056, arXiv: 0809.4487 [hep-ph].

[6] E. L. Berger, Q.-H. Cao, C.-R. Chen, C. S. Li and H. Zhang, *Top Quark Forward-Backward Asymmetry and Same-Sign Top Quark Pairs*, Phys. Rev. Lett. **106** (2011) 201801, arXiv: 1101.5625 [hep-ph].

[7] T. Plehn and T. M. P. Tait, *Seeking Sgluons*, J. Phys. G **36** (2009) 075001, arXiv: 0810.3919 [hep-ph].

[8] S. Calvet, B. Fuks, P. Gris and L. Valery, *Searching for sgluons in multitop events at a center-of-mass energy of 8 TeV*, JHEP **04** (2013) 043, arXiv: 1212.3360 [hep-ph].

[9] K. J. F. Gaemers and F. Hoogeveen, *Higgs production and decay into heavy flavors with the gluon fusion mechanism*, Phys. Lett. B **146** (1984) 347.

[10] G. C. Branco et al., *Theory and phenomenology of two-Higgs-doublet models*, Phys. Rept. **516** (2012) 1, arXiv: 1106.0034 [hep-ph].

[11] F. M. L. Almeida Jr., Y. do Amaral Coutinho, J. A. Martins Simoes, P. P. Queiroz Filho and C. M. Porto, *Same-sign dileptons as a signature for heavy Majorana neutrinos in hadron hadron collisions*, Phys. Lett. B **400** (1997) 331, arXiv: hep-ph/9703441.

[12] A. Atre, T. Han, S. Pascoli and B. Zhang, *The Search for Heavy Majorana Neutrinos*, JHEP **05** (2009) 030, arXiv: 0901.3589 [hep-ph].

[13] R. Contino and G. Servant, *Discovering the top partners at the LHC using same-sign dilepton final states*, JHEP **06** (2008) 026, arXiv: 0801.1679 [hep-ph].

[14] L. Evans and P. Bryant, *LHC Machine*, JINST **3** (2008) S08001.

[15] ATLAS Collaboration, *The ATLAS Experiment at the CERN Large Hadron Collider*, JINST **3** (2008) S08003.

[16] CMS Collaboration, *The CMS Experiment at the CERN LHC*, JINST **3** (2008) S08004.

[17] Y. Golfand and E. Likhtman, *Extension of the Algebra of Poincare Group Generators and Violation of P Invariance*, JETP Lett. **13** (1971) 323, [Pisma Zh. Eksp. Teor. Fiz. **13** (1971) 452].

[18] D. Volkov and V. Akulov, *Is the neutrino a goldstone particle?*, Phys. Lett. B **46** (1973) 109.

[19] J. Wess and B. Zumino, *Supergauge transformations in four dimensions*, Nucl. Phys. B **70** (1974) 39.

[20] J. Wess and B. Zumino, *Supergauge invariant extension of quantum electrodynamics*, Nucl. Phys. B **78** (1974) 1.

[21] S. Ferrara and B. Zumino, *Supergauge invariant Yang-Mills theories*, Nucl. Phys. B **79** (1974) 413.

[22] A. Salam and J. Strathdee, *Super-symmetry and non-Abelian gauges*, Phys. Lett. B **51** (1974) 353.

[23] S. P. Martin, *A Supersymmetry Primer*, Adv. Ser. Direct. High Energy Phys. **18** (1998) 1, arXiv: hep-ph/9709356.

[24] N. Sakai, *Naturalness in supersymmetric GUTS*, Z. Phys. C **11** (1981) 153.

[25] S. Dimopoulos, S. Raby and F. Wilczek, *Supersymmetry and the scale of unification*, Phys. Rev. D **24** (1981) 1681.

[26] L. E. Ibáñez and G. G. Ross, *Low-energy predictions in supersymmetric grand unified theories*, Phys. Lett. B **105** (1981) 439.

[27] S. Dimopoulos and H. Georgi, *Softly broken supersymmetry and SU(5)*, Nucl. Phys. B **193** (1981) 150.

[28] R. Barbieri and G. Giudice, *Upper bounds on supersymmetric particle masses*, Nucl. Phys. B **306** (1988) 63.

[29] B. de Carlos and J. Casas, *One-loop analysis of the electroweak breaking in supersymmetric models and the fine-tuning problem*, Phys. Lett. B **309** (1993) 320, arXiv: hep-ph/9303291.

[30] H. Goldberg, *Constraint on the Photino Mass from Cosmology*, Phys. Rev. Lett. **50** (1983) 1419, Erratum: Phys. Rev. Lett. **103** (2009) 099905.

[31] J. Ellis, J. Hagelin, D. V. Nanopoulos, K. A. Olive and M. Srednicki, *Supersymmetric relics from the big bang*, Nucl. Phys. B **238** (1984) 453.

[32] G. R. Farrar and P. Fayet, *Phenomenology of the production, decay, and detection of new hadronic states associated with supersymmetry*, Phys. Lett. B **76** (1978) 575.

[33] D. Hooper and T. Plehn, *Supersymmetric dark matter: How light can the LSP be?*, Phys. Lett. B **562** (2003) 18, arXiv: hep-ph/0212226.

[34] H. K. Dreiner, *An Introduction to Explicit R-Parity Violation*, Adv. Ser. Direct. High Energy Phys. **21** (2010) 565, ed. by G. L. Kane, arXiv: hep-ph/9707435.

[35] ATLAS Collaboration, *Search for squarks and gluinos in final states with same-sign leptons and jets using* $139\,fb^{-1}$ *of data collected with the ATLAS detector*, JHEP **06** (2020) 046, arXiv: 1909.08457 [hep-ex].

[36] ATLAS Collaboration, *Search for electroweak production of supersymmetric states in scenarios with compressed mass spectra at* $\sqrt{s} = 13\,TeV$ *with the ATLAS detector*, Phys. Rev. D **97** (2018) 052010, arXiv: 1712.08119 [hep-ex].

[37] CMS Collaboration, *Search for supersymmetry with a compressed mass spectrum in the vector boson fusion topology with 1-lepton and 0-lepton final states in proton–proton collisions at* $\sqrt{s} = 13\,TeV$, JHEP **08** (2019) 150, arXiv: 1905.13059 [hep-ex].

[38] ATLAS Collaboration, *Searches for electroweak production of supersymmetric particles with compressed mass spectra in* $\sqrt{s} = 13$ *TeV* pp *collisions with the ATLAS detector*, Phys. Rev. D **101** (2020) 052005, arXiv: 1911.12606 [hep-ex].

[39] ATLAS Collaboration, *Search for supersymmetry at* $\sqrt{s} = 8$ *TeV in final states with jets and two same-sign leptons or three leptons with the ATLAS detector*, JHEP **06** (2014) 035, arXiv: 1404.2500 [hep-ex].

[40] ATLAS Collaboration, *Search for direct pair production of a chargino and a neutralino decaying to the* 125 *GeV Higgs boson in* $\sqrt{s} = 8$ *TeV* pp *collisions with the ATLAS detector*, Eur. Phys. J. C **75** (2015) 208, arXiv: 1501.07110 [hep-ex].

[41] ATLAS Collaboration, *Search for supersymmetry at* $\sqrt{s} = 13$ *TeV in final states with jets and two same-sign leptons or three leptons with the ATLAS detector*, Eur. Phys. J. C **76** (2016) 259, arXiv: 1602.09058 [hep-ex].

[42] ATLAS Collaboration, *Search for supersymmetry in final states with two same-sign or three leptons and jets using* $36\,fb^{-1}$ *of* $\sqrt{s} = 13$ *TeV* pp *collision data with the ATLAS detector*, JHEP **09** (2017) 084, arXiv: 1706.03731 [hep-ex], Erratum: JHEP **08** (2019) 121.

[43] ATLAS Collaboration, *Search for chargino and neutralino production in final states with a Higgs boson and missing transverse momentum at* $\sqrt{s} = 13$ *TeV with the ATLAS detector*, Phys. Rev. D **100** (2019) 012006, arXiv: 1812.09432 [hep-ex].

[44] CMS Collaboration, *Search for physics beyond the standard model in events with two leptons of same sign, missing transverse momentum, and jets in proton–proton collisions at* $\sqrt{s} = 13$ *TeV*, Eur. Phys. J. C **77** (2017) 578, arXiv: 1704.07323 [hep-ex].

[45] CMS Collaboration, *Search for physics beyond the standard model in events with jets and two same-sign or at least three charged leptons in proton–proton collisions at* $\sqrt{s} = 13$ *TeV*, Eur. Phys. J. C **80** (2020) 752, arXiv: 2001.10086 [hep-ex].

[46] CMS Collaboration, *Search for electroweak production of charginos and neutralinos in proton–proton collisions at* $\sqrt{s} = 13$ *TeV*, JHEP **04** (2021) 147, arXiv: 2106.14246 [hep-ex].

[47] CMS Collaboration, *Search for resonant production of second-generation sleptons with same-sign dimuon events in proton–proton collisions at* $\sqrt{s} = 13$ *TeV*, Eur. Phys. J. C **79** (2019) 305, arXiv: 1811.09760 [hep-ex].

[48] CMS Collaboration, *Search for anomalous production of events with three or more leptons in* pp *collisions at* $\sqrt{s} = 8$ *TeV*, Phys. Rev. D **90** (2014) 032006, arXiv: 1404.5801 [hep-ex].

[49] ATLAS Collaboration, *Search for direct production of charginos and neutralinos in events with three leptons and missing transverse momentum in* $\sqrt{s} = 8$ *TeV* pp *collisions with the ATLAS detector*, JHEP **04** (2014) 169, arXiv: 1402.7029 [hep-ex].

[50] CMS Collaboration, *Search for Top Squarks in R-Parity-Violating Supersymmetry Using Three or More Leptons and b-Tagged Jets*, Phys. Rev. Lett. **111** (2013) 221801, arXiv: 1306.6643 [hep-ex].

[51] ATLAS Collaboration, *Search for electroweak production of supersymmetric particles in final states with two or three leptons at* $\sqrt{s} = 13$ *TeV with the ATLAS detector*, Eur. Phys. J. C **78** (2018) 995, arXiv: 1803.02762 [hep-ex].

[52] CMS Collaboration, *Search for new phenomena with multiple charged leptons in proton—proton collisions at* $\sqrt{s} = 13$ *TeV*, Eur. Phys. J. C **77** (2017) 635, arXiv: 1701.06940 [hep-ex].

[53] CMS Collaboration, *Search for supersymmetry in events with at least three electrons or muons, jets, and missing transverse momentum in proton–proton collisions at* $\sqrt{s} = 13$ *TeV*, JHEP **02** (2018) 067, arXiv: 1710.09154 [hep-ex].

[54] ATLAS Collaboration, *Search for chargino–neutralino production using recursive jigsaw reconstruction in final states with two or three charged leptons in proton–proton collisions at* $\sqrt{s} = 13$ *TeV with the ATLAS detector*, Phys. Rev. D **98** (2018) 092012, arXiv: 1806.02293 [hep-ex].

[55] ATLAS Collaboration, *Search for chargino–neutralino production with mass splittings near the electroweak scale in three-lepton final states in* $\sqrt{s} = 13$ *TeV pp collisions with the ATLAS detector*, Phys. Rev. D **101** (2020) 072001, arXiv: 1912.08479 [hep-ex].

[56] ATLAS Collaboration, *Search for chargino–neutralino pair production in final states with three leptons and missing transverse momentum in* $\sqrt{s} = 13$ *TeV pp collisions with the ATLAS detector*, Eur. Phys. J. C **81** (2021) 1118, arXiv: 2106.01676 [hep-ex].

[57] ATLAS Collaboration, *Search for trilepton resonances from chargino and neutralino pair production in* $\sqrt{s} = 13$ *TeV pp collisions with the ATLAS detector*, Phys. Rev. D **103** (2020) 112003, arXiv: 2011.10543 [hep-ex].

[58] ATLAS Collaboration, *Search for charginos and neutralinos in final states with two boosted hadronically decaying bosons and missing transverse momentum in pp collisions at* $\sqrt{s} = 13$ *TeV with the ATLAS detector*, Phys. Rev. D **104** (2021) 112010, arXiv: 2108.07586 [hep-ex].

[59] ATLAS Collaboration, *Search for direct production of electroweakinos in final states with missing transverse momentum and a Higgs boson decaying into photons in pp collisions at* $\sqrt{s} = 13$ *TeV with the ATLAS detector*, JHEP **10** (2020) 005, arXiv: 2004.10894 [hep-ex].

[60] CMS Collaboration, *Search for electroweak production of charginos and neutralinos in multilepton final states in proton–proton collisions at* $\sqrt{s} = 13$ *TeV*, JHEP **03** (2018) 166, arXiv: 1709.05406 [hep-ex].

[61] ATLAS Collaboration, *Searches for new phenomena in events with two leptons, jets, and missing transverse momentum in* $139\,fb^{-1}$ *of* $\sqrt{s} = 13$ *TeV pp collisions with the ATLAS detector*, (2022), arXiv: 2204.13072 [hep-ex].

[62] V. A. Mitsou, *R-parity violating supersymmetry and neutrino physics: experimental signatures*, PoS **PLANCK2015** (2015) 085, ed. by I. Antoniadis, G. K. Leontaris and K. Tamvakis, arXiv: 1510.02660 [hep-ph].

[63] A. H. Chamseddine, R. L. Arnowitt and P. Nath, *Locally Supersymmetric Grand Unification*, Phys. Rev. Lett. **49** (1982) 970.

[64] R. Barbieri, S. Ferrara and C. A. Savoy, *Gauge Models with Spontaneously Broken Local Supersymmetry*, Phys. Lett. B **119** (1982) 343.

[65] G. L. Kane, C. F. Kolda, L. Roszkowski and J. D. Wells, *Study of constrained minimal supersymmetry*, Phys. Rev. D **49** (1994) 6173, arXiv: hep-ph/9312272.

[66] ATLAS Collaboration, *Search for supersymmetry in final states with jets, missing transverse momentum and one isolated lepton in $\sqrt{s} = 7$ TeV pp collisions using $1\,fb^{-1}$ of ATLAS data*, Phys. Rev. D **85** (2012) 012006, arXiv: 1109.6606 [hep-ex].

[67] ATLAS Collaboration, *Search for squarks and gluinos in events with isolated leptons, jets and missing transverse momentum at $\sqrt{s} = 8$ TeV with the ATLAS detector*, JHEP **04** (2015) 116, arXiv: 1501.03555 [hep-ex].

[68] ATLAS Collaboration, *Search for supersymmetry in events with large missing transverse momentum, jets, and at least one tau lepton in $20\,fb^{-1}$ of $\sqrt{s} = 8$ TeV proton–proton collision data with the ATLAS detector*, JHEP **09** (2014) 103, arXiv: 1407.0603 [hep-ex].

[69] ATLAS Collaboration, *Summary of the searches for squarks and gluinos using $\sqrt{s} = 8$ TeV pp collisions with the ATLAS experiment at the LHC*, JHEP **10** (2015) 054, arXiv: 1507.05525 [hep-ex].

[70] ATLAS Collaboration, *Constraints on promptly decaying supersymmetric particles with lepton-number- and R-parity-violating interactions using Run-1 ATLAS data*, ATLAS-CONF-2015-018, 2015, URL: https://cds.cern.ch/record/2017303.

[71] A. Djouadi et al., *The Minimal supersymmetric standard model: Group summary report*, 1998, arXiv: hep-ph/9901246.

[72] C. F. Berger, J. S. Gainer, J. L. Hewett and T. G. Rizzo, *Supersymmetry Without Prejudice*, JHEP **02** (2009) 023, arXiv: 0812.0980 [hep-ph].

[73] ATLAS Collaboration, *Search for massive supersymmetric particles decaying to many jets using the ATLAS detector in pp collisions at $\sqrt{s} = 8$ TeV*, Phys. Rev. D **91** (2015) 112016, arXiv: 1502.05686 [hep-ex], Erratum: Phys. Rev. D **93** (2016) 039901.

[74] ATLAS Collaboration, *A search for top squarks with R-parity-violating decays to all-hadronic final states with the ATLAS detector in $\sqrt{s} = 8$ TeV proton–proton collisions*, JHEP **06** (2016) 067, arXiv: 1601.07453 [hep-ex].

[75] ATLAS Collaboration, *Search for new phenomena in a lepton plus high jet multiplicity final state with the ATLAS experiment using $\sqrt{s} = 13$ TeV proton–proton collision data*, JHEP **09** (2017) 088, arXiv: 1704.08493 [hep-ex].

[76] ATLAS Collaboration, *A search for pair-produced resonances in four-jet final states at $\sqrt{s} = 13$ TeV with the ATLAS detector*, Eur. Phys. J. C **78** (2018) 250, arXiv: 1710.07171 [hep-ex].

[77] ATLAS Collaboration, *Search for R-parity-violating supersymmetric particles in multi-jet final states produced in pp collisions at $\sqrt{s} = 13$ TeV using the ATLAS detector at the LHC*, Phys. Lett. B **785** (2018) 136, arXiv: 1804.03568 [hep-ex].

[78] ATLAS Collaboration, *Search for phenomena beyond the Standard Model in events with large b-jet multiplicity using the ATLAS detector at the LHC*, Eur. Phys. J. C **81** (2021) 11, arXiv: 2010.01015 [hep-ex].

[79] CMS Collaboration, *Search for anomalous production of multilepton events in pp collisions at $\sqrt{s} = 7$ TeV*, JHEP **06** (2012) 169, arXiv: 1204.5341 [hep-ex].

[80] CMS Collaboration, *Searches for R-parity-violating supersymmetry in pp collisions at $\sqrt{s} = 8$ TeV in final states with 0–4 leptons*, Phys. Rev. D **94** (2016) 112009, arXiv: 1606.08076 [hep-ex].

[81] CMS Collaboration, *Search for R-parity violating supersymmetry with displaced vertices in proton–proton collisions at* $\sqrt{s} = 8$ *TeV*, Phys. Rev. D **95** (2017) 012009, arXiv: 1610.05133 [hep-ex].

[82] CMS Collaboration, *Search for R-parity violating supersymmetry in* pp *collisions at* $\sqrt{s} = 13$ *TeV using b jets in a final state with a single lepton, many jets, and high sum of large-radius jet masses*, Phys. Lett. B **783** (2018) 114, arXiv: 1712.08920 [hep-ex].

[83] CMS Collaboration, *Search for top squarks in final states with two top quarks and several light-flavor jets in proton–proton collisions at* $\sqrt{s} = 13$ *TeV*, Phys. Rev. D **104** (2021) 032006, arXiv: 2102.06976 [hep-ex].

[84] ATLAS Collaboration, *Search for R-parity-violating supersymmetry in a final state containing leptons and many jets with the ATLAS experiment using* $\sqrt{s} = 13$ *TeV proton–proton collision data*, Eur. Phys. J. C **81** (2021) 1023, arXiv: 2106.09609 [hep-ex].

[85] ATLAS Collaboration, *Reinterpretation of searches for supersymmetry in models with variable R-parity-violating coupling strength and long-lived R-hadrons*, ATLAS-CONF-2018-003, 2018, URL: https://cds.cern.ch/record/2308391.

[86] J. Alwall, M.-P. Le, M. Lisanti and J. G. Wacker, *Searching for directly decaying gluinos at the Tevatron*, Phys. Lett. B **666** (2008) 34, arXiv: 0803.0019 [hep-ph].

[87] J. Alwall, P. Schuster and N. Toro, *Simplified models for a first characterization of new physics at the LHC*, Phys. Rev. D **79** (2009) 075020, arXiv: 0810.3921 [hep-ph].

[88] D. Alves et al., *Simplified models for LHC new physics searches*, J. Phys. G **39** (2012) 105005, arXiv: 1105.2838 [hep-ph].

[89] W. Porod, M. Hirsch, J. Romao and J. W. F. Valle, *Testing neutrino mixing at future collider experiments*, Phys. Rev. D **63** (2001) 115004, arXiv: hep-ph/0011248.

[90] S. Roy and B. Mukhopadhyaya, *Some implications of a supersymmetric model with R-parity breaking bilinear interactions*, Phys. Rev. D **55** (1997) 7020, arXiv: hep-ph/9612447.

[91] J. C. Romao, M. A. Diaz, M. Hirsch, W. Porod and J. W. F. Valle, *Supersymmetric solution to the solar and atmospheric neutrino problems*, Phys. Rev. D **61** (2000) 071703, arXiv: hep-ph/9907499.

[92] M. Hirsch, M. A. Diaz, W. Porod, J. C. Romao and J. W. F. Valle, *Neutrino masses and mixings from supersymmetry with bilinear R parity violation: A theory for solar and atmospheric neutrino oscillations*, Phys. Rev. D **62** (2000) 113008, arXiv: hep-ph/0004115, Erratum: Phys. Rev. D **65** (2002) 119901.

[93] M. A. Diaz, M. Hirsch, W. Porod, J. C. Romao and J. W. F. Valle, *Solar neutrino masses and mixing from bilinear R parity broken supersymmetry: Analytical versus numerical results*, Phys. Rev. D **68** (2003) 013009, arXiv: hep-ph/0302021, Erratum: Phys. Rev. D **71** (2005) 059904.

[94] S. Biswas, E. J. Chun and P. Sharma, *Di-Higgs signatures from R-parity violating supersymmetry as the origin of neutrino mass*, JHEP **12** (2016) 062, arXiv: 1604.02821 [hep-ph].

[95] F. Thomas and W. Porod, *Determining R-parity violating parameters from neutrino and LHC data*, JHEP **10** (2011) 089, arXiv: 1106.4658 [hep-ph].

[96] R. Barbier et al., *R-Parity-violating supersymmetry*, Phys. Rept. **420** (2005) 1, arXiv: hep-ph/0406039.

[97] C. Csaki, Y. Grossman and B. Heidenreich, *MFV SUSY: A Natural Theory for R-Parity Violation*, Phys. Rev. D **85** (2012) 095009, arXiv: 1111.1239 [hep-ph].

[98] H. Georgi and S. L. Glashow, *Unity of All Elementary-Particle Forces*, Phys. Rev. Lett. **32** (1974) 438.

[99] J. D. Bekenstein, *Nonexistence of baryon number for static black holes*, Phys. Rev. D **5** (1972) 1239.

[100] A. D. Sakharov, *Violation of CP Invariance, C asymmetry, and baryon asymmetry of the universe*, Pisma Zh. Eksp. Teor. Fiz. **5** (1967) 32.

[101] ATLAS Collaboration, *ATLAS Insertable B-Layer: Technical Design Report*, ATLAS-TDR-19; CERN-LHCC-2010-013, 2010, URL: https://cds.cern.ch/record/1291633, Addendum: ATLAS-TDR-19-ADD-1; CERN-LHCC-2012-009, 2012, URL: https://cds.cern.ch/record/1451888.

[102] B. Abbott et al., *Production and integration of the ATLAS Insertable B-Layer*, JINST **13** (2018) T05008, arXiv: 1803.00844 [physics.ins-det].

[103] ATLAS Collaboration, *The ATLAS Collaboration Software and Firmware*, ATL-SOFT-PUB-2021-001, 2021, URL: https://cds.cern.ch/record/2767187.

[104] ATLAS Collaboration, *ATLAS data quality operations and performance for 2015–2018 data-taking*, JINST **15** (2020) P04003, arXiv: 1911.04632 [physics.ins-det].

[105] ATLAS Collaboration, *Luminosity determination in pp collisions at $\sqrt{s} = 13$ TeV using the ATLAS detector at the LHC*, ATLAS-CONF-2019-021, 2019, URL: https://cds.cern.ch/record/2677054.

[106] G. Avoni et al., *The new LUCID-2 detector for luminosity measurement and monitoring in ATLAS*, JINST **13** (2018) P07017.

[107] ATLAS Collaboration, *Performance of electron and photon triggers in ATLAS during LHC Run 2*, Eur. Phys. J. C **80** (2020) 47, arXiv: 1909.00761 [hep-ex].

[108] ATLAS Collaboration, *Performance of the ATLAS muon triggers in Run 2*, JINST **15** (2020) P09015, arXiv: 2004.13447 [hep-ex].

[109] ATLAS Collaboration, *Performance of the missing transverse momentum triggers for the ATLAS detector during Run-2 data taking*, JHEP **08** (2020) 080, arXiv: 2005.09554 [hep-ex].

[110] T. Sjöstrand, S. Mrenna and P. Skands, *A brief introduction to PYTHIA 8.1*, Comput. Phys. Commun. **178** (2008) 852, arXiv: 0710.3820 [hep-ph].

[111] T. Sjöstrand et al., *An introduction to PYTHIA 8.2*, Comput. Phys. Commun. **191** (2015) 159, arXiv: 1410.3012 [hep-ph].

[112] R. D. Ball et al., *Parton distributions with LHC data*, Nucl. Phys. B **867** (2013) 244, arXiv: 1207.1303 [hep-ph].

[113] ATLAS Collaboration, *The Pythia 8 A3 tune description of ATLAS minimum bias and inelastic measurements incorporating the Donnachie–Landshoff diffractive model*, ATL-PHYS-PUB-2016-017, 2016, URL: https://cds.cern.ch/record/2206965.

[114] D. J. Lange, *The EvtGen particle decay simulation package*, Nucl. Instrum. Meth. A **462** (2001) 152.

[115] ATLAS Collaboration, *The ATLAS Simulation Infrastructure*, Eur. Phys. J. C **70** (2010) 823, arXiv: 1005.4568 [physics.ins-det].

[116] GEANT4 Collaboration, S. Agostinelli et al., *GEANT4 – a simulation toolkit*, Nucl. Instrum. Meth. A **506** (2003) 250.

[117] ATLAS Collaboration, *The simulation principle and performance of the ATLAS fast calorimeter simulation FastCaloSim*, ATL-PHYS-PUB-2010-013, 2010, URL: https://cds.cern.ch/record/1300517.

[118] R. Frederix and S. Frixione, *Merging meets matching in MC@NLO*, JHEP **12** (2012) 061, arXiv: 1209.6215 [hep-ph].

[119] ATLAS Collaboration, *ATLAS Pythia 8 tunes to 7 TeV data*, ATL-PHYS-PUB-2014-021, 2014, URL: https://cds.cern.ch/record/1966419.

[120] S. Mrenna and P. Skands, *Automated parton-shower variations in PYTHIA 8*, Phys. Rev. D **94** (2016) 074005, arXiv: 1605.08352 [hep-ph].

[121] L. Lönnblad, *Correcting the Colour-Dipole Cascade Model with Fixed Order Matrix Elements*, JHEP **05** (2002) 046, arXiv: hep-ph/0112284.

[122] L. Lönnblad and S. Prestel, *Matching tree-level matrix elements with interleaved showers*, JHEP **03** (2012) 019, arXiv: 1109.4829 [hep-ph].

[123] W. Porod, *SPheno, a program for calculating supersymmetric spectra, SUSY particle decays and SUSY particle production at e+ e- colliders*, Comput. Phys. Commun. **153** (2003) 275, arXiv: hep-ph/0301101.

[124] W. Porod and F. Staub, *SPheno 3.1: Extensions including flavour, CP-phases and models beyond the MSSM*, Comput. Phys. Commun. **183** (2012) 2458, arXiv: 1104.1573 [hep-ph].

[125] F. Staub, *Exploring New Models in All Detail with SARAH*, Adv. High Energy Phys. **2015** (2015) 840780, arXiv: 1503.04200 [hep-ph].

[126] A. Vicente, *Computer tools in particle physics*, (2015), arXiv: 1507.06349 [hep-ph].

[127] W. Beenakker et al., *Production of Charginos, Neutralinos, and Sleptons at Hadron Colliders*, Phys. Rev. Lett. **83** (1999) 3780, arXiv: hep-ph/9906298, Erratum: Phys. Rev. Lett. **100** (2008) 029901.

[128] J. Debove, B. Fuks and M. Klasen, *Threshold resummation for gaugino pair production at hadron colliders*, Nucl. Phys. B **842** (2011) 51, arXiv: 1005.2909 [hep-ph].

[129] B. Fuks, M. Klasen, D. R. Lamprea and M. Rothering, *Gaugino production in proton-proton collisions at a center-of-mass energy of 8 TeV*, JHEP **10** (2012) 081, arXiv: 1207.2159 [hep-ph].

[130] B. Fuks, M. Klasen, D. R. Lamprea and M. Rothering,
Precision predictions for electroweak superpartner production at hadron colliders with RESUMMINO,
Eur. Phys. J. C **73** (2013) 2480, arXiv: 1304.0790 [hep-ph].

[131] J. Fiaschi and M. Klasen, *Neutralino-chargino pair production at NLO+NLL with resummation-improved parton density functions for LHC Run II*, Phys. Rev. D **98** (2018) 055014, arXiv: 1805.11322 [hep-ph].

[132] C. Borschensky et al.,
Squark and gluino production cross sections in pp collisions at $\sqrt{s} = 13, 14, 33$ *and* 100 *TeV*,
Eur. Phys. J. C **74** (2014) 3174, arXiv: 1407.5066 [hep-ph].

[133] J. Butterworth et al., *PDF4LHC recommendations for LHC Run II*, J. Phys. G **43** (2016) 023001, arXiv: 1510.03865 [hep-ph].

[134] E. Bothmann et al., *Event generation with Sherpa 2.2*, SciPost Phys. **7** (2019) 034, arXiv: 1905.09127 [hep-ph].

[135] T. Gleisberg and S. Höche, *Comix, a new matrix element generator*, JHEP **12** (2008) 039, arXiv: 0808.3674 [hep-ph].

[136] S. Schumann and F. Krauss,
A parton shower algorithm based on Catani–Seymour dipole factorisation, JHEP **03** (2008) 038, arXiv: 0709.1027 [hep-ph].

[137] S. Höche, F. Krauss, M. Schönherr and F. Siegert,
A critical appraisal of NLO+PS matching methods, JHEP **09** (2012) 049, arXiv: 1111.1220 [hep-ph].

[138] S. Höche, F. Krauss, M. Schönherr and F. Siegert,
QCD matrix elements + parton showers. The NLO case, JHEP **04** (2013) 027, arXiv: 1207.5030 [hep-ph].

[139] S. Catani, F. Krauss, B. R. Webber and R. Kuhn, *QCD Matrix Elements + Parton Showers*, JHEP **11** (2001) 063, arXiv: hep-ph/0109231.

[140] S. Höche, F. Krauss, S. Schumann and F. Siegert, *QCD matrix elements and truncated showers*, JHEP **05** (2009) 053, arXiv: 0903.1219 [hep-ph].

[141] F. Buccioni et al., *OpenLoops 2*, Eur. Phys. J. C **79** (2019) 866, arXiv: 1907.13071 [hep-ph].

[142] F. Cascioli, P. Maierhöfer and S. Pozzorini, *Scattering Amplitudes with Open Loops*, Phys. Rev. Lett. **108** (2012) 111601, arXiv: 1111.5206 [hep-ph].

[143] A. Denner, S. Dittmaier and L. Hofer,
COLLIER: A fortran-based complex one-loop library in extended regularizations,
Comput. Phys. Commun. **212** (2017) 220, arXiv: 1604.06792 [hep-ph].

[144] R. D. Ball et al., *Parton distributions for the LHC run II*, JHEP **04** (2015) 040, arXiv: 1410.8849 [hep-ph].

[145] S. Frixione, G. Ridolfi and P. Nason,
A positive-weight next-to-leading-order Monte Carlo for heavy flavour hadroproduction,
JHEP **09** (2007) 126, arXiv: 0707.3088 [hep-ph].

[146] P. Nason, *A new method for combining NLO QCD with shower Monte Carlo algorithms*, JHEP **11** (2004) 040, arXiv: hep-ph/0409146.

[147] S. Frixione, P. Nason and C. Oleari,
Matching NLO QCD computations with parton shower simulations: the POWHEG method,
JHEP **11** (2007) 070, arXiv: 0709.2092 [hep-ph].

[148] S. Alioli, P. Nason, C. Oleari and E. Re, *A general framework for implementing NLO calculations in shower Monte Carlo programs: the POWHEG BOX*, JHEP **06** (2010) 043,
arXiv: 1002.2581 [hep-ph].

[149] H. B. Hartanto, B. Jäger, L. Reina and D. Wackeroth,
Higgs boson production in association with top quarks in the POWHEG BOX,
Phys. Rev. D **91** (2015) 094003, arXiv: 1501.04498 [hep-ph].

[150] R. Frederix, D. Pagani and M. Zaro, *Large NLO corrections in $t\bar{t}W^{\pm}$ and $t\bar{t}t\bar{t}$ hadroproduction from supposedly subleading EW contributions*, JHEP **02** (2018) 031,
arXiv: 1711.02116 [hep-ph].

[151] S. Frixione, E. Laenen, P. Motylinski and B. R. Webber, *Angular correlations of lepton pairs from vector boson and top quark decays in Monte Carlo simulations*, JHEP **04** (2007) 081,
arXiv: hep-ph/0702198.

[152] P. Artoisenet, R. Frederix, O. Mattelaer and R. Rietkerk,
Automatic spin-entangled decays of heavy resonances in Monte Carlo simulations,
JHEP **03** (2013) 015, arXiv: 1212.3460 [hep-ph].

[153] P. Nason and C. Oleari,
NLO Higgs boson production via vector-boson fusion matched with shower in POWHEG,
JHEP **02** (2010) 037, arXiv: 0911.5299 [hep-ph].

[154] ATLAS Collaboration, *Measurement of the Z/γ^* boson transverse momentum distribution in pp collisions at $\sqrt{s} = 7$ TeV with the ATLAS detector*, JHEP **09** (2014) 145,
arXiv: 1406.3660 [hep-ex].

[155] M. L. Ciccolini, S. Dittmaier and M. Krämer,
Electroweak radiative corrections to associated WH and ZH production at hadron colliders,
Phys. Rev. D **68** (2003) 073003, arXiv: hep-ph/0306234 [hep-ph].

[156] O. Brein, A. Djouadi and R. Harlander,
NNLO QCD corrections to the Higgs-strahlung processes at hadron colliders,
Phys. Lett. B **579** (2004) 149, arXiv: hep-ph/0307206.

[157] O. Brein, R. V. Harlander, M. Wiesemann and T. Zirke,
Top-quark mediated effects in hadronic Higgs-Strahlung, Eur. Phys. J. C **72** (2012) 1868,
arXiv: 1111.0761 [hep-ph].

[158] L. Altenkamp, S. Dittmaier, R. V. Harlander, H. Rzehak and T. J. E. Zirke,
Gluon-induced Higgs-strahlung at next-to-leading order QCD, JHEP **02** (2013) 078,
arXiv: 1211.5015 [hep-ph].

[159] A. Denner, S. Dittmaier, S. Kallweit and A. Mück, *HAWK 2.0: A Monte Carlo program for Higgs production in vector-boson fusion and Higgs strahlung at hadron colliders*,
Comput. Phys. Commun. **195** (2015) 161, arXiv: 1412.5390 [hep-ph].

[160] O. Brein, R. V. Harlander and T. J. E. Zirke, *vh@nnlo – Higgs Strahlung at hadron colliders*,
Comput. Phys. Commun. **184** (2013) 998, arXiv: 1210.5347 [hep-ph].

[161] R. V. Harlander, A. Kulesza, V. Theeuwes and T. Zirke,
Soft gluon resummation for gluon-induced Higgs Strahlung, JHEP **11** (2014) 082,
arXiv: 1410.0217 [hep-ph].

[162] M. Ciccolini, A. Denner and S. Dittmaier, *Strong and Electroweak Corrections to the Production of a Higgs Boson + 2 Jets via Weak Interactions at the Large Hadron Collider*,
Phys. Rev. Lett. **99** (2007) 161803, arXiv: 0707.0381 [hep-ph].

[163] M. Ciccolini, A. Denner and S. Dittmaier,
Electroweak and QCD corrections to Higgs production via vector-boson fusion at the CERN LHC,
Phys. Rev. D **77** (2008) 013002, arXiv: 0710.4749 [hep-ph].

[164] P. Bolzoni, F. Maltoni, S.-O. Moch and M. Zaro,
Higgs Boson Production via Vector-Boson Fusion at Next-to-Next-to-Leading Order in QCD,
Phys. Rev. Lett. **105** (2010) 011801, arXiv: 1003.4451 [hep-ph].

[165] A. Djouadi, J. Kalinowski and M. Spira, *HDECAY: A program for Higgs boson decays in the Standard Model and its supersymmetric extension*, Comput. Phys. Commun. **108** (1998) 56,
arXiv: hep-ph/9704448.

[166] M. Spira, *QCD Effects in Higgs Physics*, Fortsch. Phys. **46** (1998) 203, arXiv: hep-ph/9705337.

[167] A. Djouadi, M. M. Mühlleitner and M. Spira,
Decays of Supersymmetric particles: The Program SUSY-HIT (SUspect-SdecaY-Hdecay-InTerface),
Acta Phys. Polon. B **38** (2007) 635, arXiv: hep-ph/0609292.

[168] A. Bredenstein, A. Denner, S. Dittmaier and M. M. Weber, *Radiative corrections to the semileptonic and hadronic Higgs-boson decays $H \to WW/ZZ \to 4$ fermions*,
JHEP **02** (2007) 080, arXiv: hep-ph/0611234.

[169] A. Bredenstein, A. Denner, S. Dittmaier and M. M. Weber,
Precise predictions for the Higgs-boson decay $H \to WW/ZZ \to 4$ leptons,
Phys. Rev. D **74** (2006) 013004, arXiv: hep-ph/0604011 [hep-ph].

[170] A. Bredenstein, A. Denner, S. Dittmaier and M. M. Weber,
Precision calculations for the Higgs decays $H \to ZZ/WW \to 4$ leptons,
Nucl. Phys. Proc. Suppl. **160** (2006) 131, arXiv: hep-ph/0607060 [hep-ph].

[171] C. Anastasiou, L. Dixon, K. Melnikov and F. Petriello, *High-precision QCD at hadron colliders: Electroweak gauge boson rapidity distributions at next-to-next-to leading order*,
Phys. Rev. D **69** (2004) 094008, arXiv: hep-ph/0312266.

[172] A. Buckley et al., *A comparative study of Higgs boson production from vector-boson fusion*,
JHEP **11** (2021) 108, arXiv: 2105.11399 [hep-ph].

[173] ATLAS Collaboration, *Studies on top-quark Monte Carlo modelling for Top2016*,
ATL-PHYS-PUB-2016-020, 2016, URL: https://cds.cern.ch/record/2216168.

[174] S. Alioli, P. Nason, C. Oleari and E. Re,
NLO single-top production matched with shower in POWHEG: s- and t-channel contributions,
JHEP **09** (2009) 111, arXiv: 0907.4076 [hep-ph], Erratum: JHEP **02** (2010) 011.

[175] R. Frederix, E. Re and P. Torrielli,
Single-top t-channel hadroproduction in the four-flavour scheme with POWHEG and aMC@NLO,
JHEP **09** (2012) 130, arXiv: 1207.5391 [hep-ph].

[176] S. Frixione, E. Laenen, P. Motylinski, C. White and B. R. Webber, *Single-top hadroproduction in association with a W boson*, JHEP **07** (2008) 029, arXiv: 0805.3067 [hep-ph].

[177] ATLAS Collaboration, *Electron and photon performance measurements with the ATLAS detector using the 2015–2017 LHC proton–proton collision data*, JINST **14** (2019) P12006, arXiv: 1908.00005 [hep-ex].

[178] ATLAS Collaboration, *Muon reconstruction performance of the ATLAS detector in proton–proton collision data at* $\sqrt{s} = 13$ *TeV*, Eur. Phys. J. C **76** (2016) 292, arXiv: 1603.05598 [hep-ex].

[179] ATLAS Collaboration, *Muon reconstruction and identification efficiency in ATLAS using the full Run 2 pp collision data set at* $\sqrt{s} = 13$ *TeV*, Eur. Phys. J. C **81** (2021) 578, arXiv: 2012.00578 [hep-ex].

[180] M. Cacciari, G. P. Salam and G. Soyez, *The anti-*k_t *jet clustering algorithm*, JHEP **04** (2008) 063, arXiv: 0802.1189 [hep-ph].

[181] ATLAS Collaboration, *Jet energy scale measurements and their systematic uncertainties in proton–proton collisions at* $\sqrt{s} = 13$ *TeV with the ATLAS detector*, Phys. Rev. D **96** (2017) 072002, arXiv: 1703.09665 [hep-ex].

[182] ATLAS Collaboration, *Performance of pile-up mitigation techniques for jets in pp collisions at* $\sqrt{s} = 8$ *TeV using the ATLAS detector*, Eur. Phys. J. C **76** (2016) 581, arXiv: 1510.03823 [hep-ex].

[183] ATLAS Collaboration, *ATLAS b-jet identification performance and efficiency measurement with* $t\bar{t}$ *events in pp collisions at* $\sqrt{s} = 13$ *TeV*, Eur. Phys. J. C **79** (2019) 970, arXiv: 1907.05120 [hep-ex].

[184] ATLAS Collaboration, *Optimisation and performance studies of the ATLAS b-tagging algorithms for the 2017-18 LHC run*, ATL-PHYS-PUB-2017-013, 2017, URL: https://cds.cern.ch/record/2273281.

[185] ATLAS Collaboration, *Performance of missing transverse momentum reconstruction with the ATLAS detector using proton–proton collisions at* $\sqrt{s} = 13$ *TeV*, Eur. Phys. J. C **78** (2018) 903, arXiv: 1802.08168 [hep-ex].

[186] ATLAS Collaboration, E_T^{miss} *performance in the ATLAS detector using 2015–2016 LHC pp collisions*, ATLAS-CONF-2018-023, 2018, URL: https://cds.cern.ch/record/2625233.

[187] ATLAS Collaboration, *Selection of jets produced in* 13 *TeV proton–proton collisions with the ATLAS detector*, ATLAS-CONF-2015-029, 2015, URL: https://cds.cern.ch/record/2037702.

[188] C. G. Lester and D. J. Summers, *Measuring masses of semiinvisibly decaying particles pair produced at hadron colliders*, Phys. Lett. B **463** (1999) 99, arXiv: hep-ph/9906349.

[189] A. Barr, C. Lester and P. Stephens, *m(T2): The Truth behind the glamour*, J. Phys. G **29** (2003) 2343, arXiv: hep-ph/0304226.

[190] ATLAS Collaboration, *Object-based missing transverse momentum significance in the ATLAS Detector*, ATLAS-CONF-2018-038, 2018, URL: https://cds.cern.ch/record/2630948.

[191] ATLAS Collaboration,
Search for doubly and singly charged Higgs bosons decaying into vector bosons in multi-lepton final states with the ATLAS detector using proton–proton collisions at $\sqrt{s} = 13$ *TeV*,
JHEP **06** (2021) 146, arXiv: 2101.11961 [hep-ex].

[192] G. Cowan, K. Cranmer, E. Gross and O. Vitells,
Asymptotic formulae for likelihood-based tests of new physics, Eur. Phys. J. C **71** (2011) 1554, arXiv: 1007.1727 [physics.data-an], Erratum: Eur. Phys. J. C **73** (2013) 2501.

[193] M. Baak et al., *HistFitter software framework for statistical data analysis*,
Eur. Phys. J. C **75** (2015) 153, arXiv: 1410.1280 [hep-ex].

[194] R. D. Cousins, J. T. Linnemann and J. Tucker,
Evaluation of three methods for calculating statistical significance when incorporating a systematic uncertainty into a test of the background-only hypothesis for a Poisson process,
Nucl. Instrum. Meth. A **595** (2008) 480, arXiv: physics/0702156 [physics.data-an].

[195] ATLAS Collaboration, *Measurement of the WW cross section in* $\sqrt{s} = 7$ *TeV* pp *collisions with the ATLAS detector and limits on anomalous gauge couplings*, Phys. Lett. B **712** (2012) 289,
arXiv: 1203.6232 [hep-ex].

[196] ATLAS Collaboration, *Prospects for Higgs boson searches using the* $H \to WW^{(*)} \to \ell\nu\ell\nu$ *decay mode with the ATLAS detector at* 10 *TeV*, ATL-PHYS-PUB-2010-005, 2010,
URL: https://cds.cern.ch/record/1270568.

[197] ATLAS Collaboration, *Measurement of the top quark-pair production cross section with ATLAS in* pp *collisions at* $\sqrt{s} = 7$ *TeV*, Eur. Phys. J. C **71** (2011) 1577, arXiv: 1012.1792 [hep-ex].

[198] ATLAS Collaboration, *Forward jet vertex tagging using the particle flow algorithm*,
ATL-PHYS-PUB-2019-026, 2019, URL: https://cds.cern.ch/record/2683100.

[199] ATLAS Collaboration, *Jet energy scale and resolution measured in proton–proton collisions at* $\sqrt{s} = 13$ *TeV with the ATLAS detector*, Eur. Phys. J. C **81** (2020) 689,
arXiv: 2007.02645 [hep-ex].

[200] ATLAS Collaboration, *Measurement of the c-jet mistagging efficiency in* $t\bar{t}$ *events using* pp *collision data at* $\sqrt{s} = 13$ *TeV collected with the ATLAS detector*, Eur. Phys. J. C **82** (2021) 95,
arXiv: 2109.10627 [hep-ex].

[201] ATLAS Collaboration, *Calibration of light-flavour b-jet mistagging rates using ATLAS proton–proton collision data at* $\sqrt{s} = 13$ *TeV*, ATLAS-CONF-2018-006, 2018,
URL: https://cds.cern.ch/record/2314418.

[202] T. Junk, *Confidence level computation for combining searches with small statistics*,
Nucl. Instrum. Meth. A **434** (1999) 435, arXiv: hep-ex/9902006.

[203] A. L. Read, *Presentation of search results: the* CL_S *technique*, J. Phys. G **28** (2002) 2693.

[204] ATLAS Collaboration, *ATLAS Computing Acknowledgements*, ATL-SOFT-PUB-2021-003, 2021,
URL: https://cds.cern.ch/record/2776662.

The ATLAS Collaboration

G. Aad [102], B. Abbott [120], D.C. Abbott [103], K. Abeling [55], S.H. Abidi [29], A. Aboulhorma [35e], H. Abramowicz [151], H. Abreu [150], Y. Abulaiti [117], A.C. Abusleme Hoffman [137a], B.S. Acharya [69a,69b,o], C. Adam Bourdarios [4], L. Adamczyk [85a], L. Adamek [155], S.V. Addepalli [26], J. Adelman [115], A. Adiguzel [21c], S. Adorni [56], T. Adye [134], A.A. Affolder [136], Y. Afik [36], M.N. Agaras [13], J. Agarwala [73a,73b], A. Aggarwal [100], C. Agheorghiesei [27c], J.A. Aguilar-Saavedra [130f], A. Ahmad [36], F. Ahmadov [38,y], W.S. Ahmed [104], S. Ahuja [95], X. Ai [48], G. Aielli [76a,76b], M. Ait Tamlihat [35e], B. Aitbenchikh [35a], I. Aizenberg [169], M. Akbiyik [100], T.P.A. Åkesson [98], A.V. Akimov [37], K. Al Khoury [41], G.L. Alberghi [23b], J. Albert [165], P. Albicocco [53], S. Alderweireldt [52], M. Aleksa [36], I.N. Aleksandrov [38], C. Alexa [27b], T. Alexopoulos [10], A. Alfonsi [114], F. Alfonsi [23b], M. Alhroob [120], B. Ali [132], S. Ali [148], M. Aliev [37], G. Alimonti [71a], W. Alkakhi [55], C. Allaire [66], B.M.M. Allbrooke [146], C.A. Allendes Flores [137f], P.P. Allport [20], A. Aloisio [72a,72b], F. Alonso [90], C. Alpigiani [138], M. Alvarez Estevez [99], A. Alvarez Fernandez [100], M.G. Alviggi [72a,72b], M. Aly [101], Y. Amaral Coutinho [82b], A. Ambler [104], C. Amelung[36], M. Amerl [1], C.G. Ames [109], D. Amidei [106], S.P. Amor Dos Santos [130a], K.R. Amos [163], V. Ananiev [125], C. Anastopoulos [139], T. Andeen [11], J.K. Anders [36], S.Y. Andrean [47a,47b], A. Andreazza [71a,71b], S. Angelidakis [9], A. Angerami [41,aa], A.V. Anisenkov [37], A. Annovi [74a], C. Antel [56], M.T. Anthony [139], E. Antipov [121], M. Antonelli [53], D.J.A. Antrim [17a], F. Anulli [75a], M. Aoki [83], T. Aoki [153], J.A. Aparisi Pozo [163], M.A. Aparo [146], L. Aperio Bella [48], C. Appelt [18], N. Aranzabal [36], V. Araujo Ferraz [82a], C. Arcangeletti [53], A.T.H. Arce [51], E. Arena [92], J-F. Arguin [108], S. Argyropoulos [54], J.-H. Arling [48], A.J. Armbruster [36], O. Arnaez [155], H. Arnold [114], Z.P. Arrubarrena Tame[109], G. Artoni [75a,75b], H. Asada [111], K. Asai [118], S. Asai [153], N.A. Asbah [61], J. Assahsah [35d], K. Assamagan [29], R. Astalos [28a], R.J. Atkin [33a], M. Atkinson[162], N.B. Atlay [18], H. Atmani[62b], P.A. Atmasiddha [106], K. Augsten [132], S. Auricchio [72a,72b], A.D. Auriol [20], V.A. Austrup [171], G. Avner [150], G. Avolio [36], K. Axiotis [56], G. Azuelos [108,ac], D. Babal [28a], H. Bachacou [135], K. Bachas [152,q], A. Bachiu [34], F. Backman [47a,47b], A. Badea [61], P. Bagnaia [75a,75b], M. Bahmani [18], A.J. Bailey [163], V.R. Bailey [162], J.T. Baines [134], C. Bakalis [10], O.K. Baker [172], P.J. Bakker [114], E. Bakos [15], D. Bakshi Gupta [8], S. Balaji [147], R. Balasubramanian [114], E.M. Baldin [37], P. Balek [133], E. Ballabene [71a,71b], F. Balli [135], L.M. Baltes [63a], W.K. Balunas [32], J. Balz [100], E. Banas [86], M. Bandieramonte [129], A. Bandyopadhyay [24], S. Bansal [24], L. Barak [151], E.L. Barberio [105], D. Barberis [57b,57a], M. Barbero [102], G. Barbour[96], K.N. Barends [33a], T. Barillari [110], M-S. Barisits [36], T. Barklow [143], R.M. Barnett [17a], P. Baron [122], D.A. Baron Moreno [101], A. Baroncelli [62a], G. Barone [29], A.J. Barr [126], L. Barranco Navarro [47a,47b], F. Barreiro [99], J. Barreiro Guimarães da Costa [14a], U. Barron [151], M.G. Barros Teixeira [130a], S. Barsov [37], F. Bartels [63a], R. Bartoldus [143], A.E. Barton [91], P. Bartos [28a], A. Basalaev [48], A. Basan [100], M. Baselga [49], I. Bashta [77a,77b], A. Bassalat [66], M.J. Basso [155], C.R. Basson [101], R.L. Bates [59], S. Batlamous[35e], J.R. Batley [32], B. Batool [141], M. Battaglia [136], D. Battulga [18], M. Bauce [75a,75b], P. Bauer [24], J.B. Beacham [51], T. Beau [127], P.H. Beauchemin [158], F. Becherer [54], P. Bechtle [24], H.P. Beck [19,p], K. Becker [167], A.J. Beddall [21d], V.A. Bednyakov [38], C.P. Bee [145], L.J. Beemster[15], T.A. Beermann [36], M. Begalli [82d,82d], M. Begel [29], A. Behera [145], J.K. Behr [48], C. Beirao Da Cruz E Silva [36], J.F. Beirer [55,36], F. Beisiegel [24], M. Belfkir [159], G. Bella [151], L. Bellagamba [23b], A. Bellerive [34], P. Bellos [20], K. Beloborodov [37], K. Belotskiy [37], N.L. Belyaev [37], D. Benchekroun [35a], F. Bendebba [35a], Y. Benhammou [151], D.P. Benjamin [29], M. Benoit [29], J.R. Bensinger [26],

S. Bentvelsen[114], L. Beresford[36], M. Beretta[53], E. Bergeaas Kuutmann[161], N. Berger[4], B. Bergmann[132], J. Beringer[17a], S. Berlendis[7], G. Bernardi[5], C. Bernius[143], F.U. Bernlochner[24], T. Berry[95], P. Berta[133], A. Berthold[50], I.A. Bertram[91], S. Bethke[110], A. Betti[75a,75b], A.J. Bevan[94], M. Bhamjee[33c], S. Bhatta[145], D.S. Bhattacharya[166], P. Bhattarai[26], V.S. Bhopatkar[121], R. Bi[29,af], R.M. Bianchi[129], O. Biebel[109], R. Bielski[123], M. Biglietti[77a], T.R.V. Billoud[132], M. Bindi[55], A. Bingul[21b], C. Bini[75a,75b], A. Biondini[92], C.J. Birch-sykes[101], G.A. Bird[20,134], M. Birman[169], M. Biros[133], T. Bisanz[36], E. Bisceglie[43b,43a], D. Biswas[170], A. Bitadze[101], K. Bjørke[125], I. Bloch[48], C. Blocker[26], A. Blue[59], U. Blumenschein[94], J. Blumenthal[100], G.J. Bobbink[114], V.S. Bobrovnikov[37], M. Boehler[54], D. Bogavac[36], A.G. Bogdanchikov[37], C. Bohm[47a], V. Boisvert[95], P. Bokan[48], T. Bold[85a], M. Bomben[5], M. Bona[94], M. Boonekamp[135], C.D. Booth[95], A.G. Borbély[59], H.M. Borecka-Bielska[108], L.S. Borgna[96], G. Borissov[91], D. Bortoletto[126], D. Boscherini[23b], M. Bosman[13], J.D. Bossio Sola[36], K. Bouaouda[35a], N. Bouchhar[163], J. Boudreau[129], E.V. Bouhova-Thacker[91], D. Boumediene[40], R. Bouquet[5], A. Boveia[119], J. Boyd[36], D. Boye[29], I.R. Boyko[38], J. Bracinik[20], N. Brahimi[62d], G. Brandt[171], O. Brandt[32], F. Braren[48], B. Brau[103], J.E. Brau[123], K. Brendlinger[48], R. Brener[169], L. Brenner[114], R. Brenner[161], S. Bressler[169], D. Britton[59], D. Britzger[110], I. Brock[24], G. Brooijmans[41], W.K. Brooks[137f], E. Brost[29], L.M. Brown[165], T.L. Bruckler[126], P.A. Bruckman de Renstrom[86], B. Brüers[48], D. Bruncko[28b,*], A. Bruni[23b], G. Bruni[23b], M. Bruschi[23b], N. Bruscino[75a,75b], T. Buanes[16], Q. Buat[138], P. Buchholz[141], A.G. Buckley[59], I.A. Budagov[38,*], M.K. Bugge[125], O. Bulekov[37], B.A. Bullard[143], S. Burdin[92], C.D. Burgard[49], A.M. Burger[40], B. Burghgrave[8], J.T.P. Burr[32], C.D. Burton[11], J.C. Burzynski[142], E.L. Busch[41], V. Büscher[100], P.J. Bussey[59], J.M. Butler[25], C.M. Buttar[59], J.M. Butterworth[96], W. Buttinger[134], C.J. Buxo Vazquez[107], A.R. Buzykaev[37], G. Cabras[23b], S. Cabrera Urbán[163], D. Caforio[58], H. Cai[129], Y. Cai[14a,14d], V.M.M. Cairo[36], O. Cakir[3a], N. Calace[36], P. Calafiura[17a], G. Calderini[127], P. Calfayan[68], G. Callea[59], L.P. Caloba[82b], D. Calvet[40], S. Calvet[40], T.P. Calvet[102], M. Calvetti[74a,74b], R. Camacho Toro[127], S. Camarda[36], D. Camarero Munoz[26], P. Camarri[76a,76b], M.T. Camerlingo[72a,72b], D. Cameron[125], C. Camincher[165], M. Campanelli[96], A. Camplani[42], V. Canale[72a,72b], A. Canesse[104], M. Cano Bret[80], J. Cantero[163], Y. Cao[162], F. Capocasa[26], M. Capua[43b,43a], A. Carbone[71a,71b], R. Cardarelli[76a], J.C.J. Cardenas[8], F. Cardillo[163], T. Carli[36], G. Carlino[72a], J.I. Carlotto[13], B.T. Carlson[129,r], E.M. Carlson[165,156a], L. Carminati[71a,71b], M. Carnesale[75a,75b], S. Caron[113], E. Carquin[137f], S. Carrá[71a,71b], G. Carratta[23b,23a], F. Carrio Argos[33g], J.W.S. Carter[155], T.M. Carter[52], M.P. Casado[13,i], A.F. Casha[155], E.G. Castiglia[172], F.L. Castillo[63a], L. Castillo Garcia[13], V. Castillo Gimenez[163], N.F. Castro[130a,130e], A. Catinaccio[36], J.R. Catmore[125], V. Cavaliere[29], N. Cavalli[23b,23a], V. Cavasinni[74a,74b], E. Celebi[21a], F. Celli[126], M.S. Centonze[70a,70b], K. Cerny[122], A.S. Cerqueira[82a], A. Cerri[146], L. Cerrito[76a,76b], F. Cerutti[17a], A. Cervelli[23b], S.A. Cetin[21d], Z. Chadi[35a], D. Chakraborty[115], M. Chala[130f], J. Chan[170], W.Y. Chan[153], J.D. Chapman[32], B. Chargeishvili[149b], D.G. Charlton[20], T.P. Charman[94], M. Chatterjee[19], S. Chekanov[6], S.V. Chekulaev[156a], G.A. Chelkov[38,a], A. Chen[106], B. Chen[151], B. Chen[165], H. Chen[14c], H. Chen[29], J. Chen[62c], J. Chen[142], S. Chen[153], S.J. Chen[14c], X. Chen[62c], X. Chen[14b,ab], Y. Chen[62a], C.L. Cheng[170], H.C. Cheng[64a], S. Cheong[143], A. Cheplakov[38], E. Cheremushkina[48], E. Cherepanova[114], R. Cherkaoui El Moursli[35e], E. Cheu[7], K. Cheung[65], L. Chevalier[135], V. Chiarella[53], G. Chiarelli[74a], N. Chiedde[102], G. Chiodini[70a], A.S. Chisholm[20], A. Chitan[27b], M. Chitishvili[163], Y.H. Chiu[165], M.V. Chizhov[38], K. Choi[11], A.R. Chomont[75a,75b], Y. Chou[103], E.Y.S. Chow[114], T. Chowdhury[33g], L.D. Christopher[33g],

K.L. Chu[64a], M.C. Chu [64a], X. Chu [14a,14d], J. Chudoba [131], J.J. Chwastowski [86], D. Cieri [110], K.M. Ciesla [85a], V. Cindro [93], A. Ciocio [17a], F. Cirotto [72a,72b], Z.H. Citron [169,l], M. Citterio [71a], D.A. Ciubotaru[27b], B.M. Ciungu [155], A. Clark [56], P.J. Clark [52], J.M. Clavijo Columbie [48], S.E. Clawson [101], C. Clement [47a,47b], J. Clercx [48], L. Clissa [23b,23a], Y. Coadou [102], M. Cobal [69a,69c], A. Coccaro [57b], R.F. Coelho Barrue [130a], R. Coelho Lopes De Sa [103], S. Coelli [71a], H. Cohen [151], A.E.C. Coimbra [71a,71b], B. Cole [41], J. Collot [60], P. Conde Muiño [130a,130g], M.P. Connell [33c], S.H. Connell [33c], I.A. Connelly [59], E.I. Conroy [126], F. Conventi [72a,ad], H.G. Cooke [20], A.M. Cooper-Sarkar [126], F. Cormier [164], L.D. Corpe [36], M. Corradi [75a,75b], E.E. Corrigan [98], F. Corriveau [104,w], A. Cortes-Gonzalez [18], M.J. Costa [163], F. Costanza [4], D. Costanzo [139], B.M. Cote [119], G. Cowan [95], J.W. Cowley [32], K. Cranmer [117], S. Crépé-Renaudin [60], F. Crescioli [127], M. Cristinziani [141], M. Cristoforetti [78a,78b,c], V. Croft [158], G. Crosetti [43b,43a], A. Cueto [36], T. Cuhadar Donszelmann [160], H. Cui [14a,14d], Z. Cui [7], W.R. Cunningham [59], F. Curcio [43b,43a], P. Czodrowski [36], M.M. Czurylo [63b], M.J. Da Cunha Sargedas De Sousa [62a], J.V. Da Fonseca Pinto [82b], C. Da Via [101], W. Dabrowski [85a], T. Dado [49], S. Dahbi [33g], T. Dai [106], C. Dallapiccola [103], M. Dam [42], G. D'amen [29], V. D'Amico [109], J. Damp [100], J.R. Dandoy [128], M.F. Daneri [30], M. Danninger [142], V. Dao [36], G. Darbo [57b], S. Darmora [6], S.J. Das [29], S. D'Auria [71a,71b], C. David [156b], T. Davidek [133], D.R. Davis [51], B. Davis-Purcell [34], I. Dawson [94], K. De [8], R. De Asmundis [72a], M. De Beurs [114], N. De Biase [48], S. De Castro [23b,23a], N. De Groot [113], P. de Jong [114], H. De la Torre [107], A. De Maria [14c], A. De Salvo [75a], U. De Sanctis [76a,76b], A. De Santo [146], J.B. De Vivie De Regie [60], D.V. Dedovich[38], J. Degens [114], A.M. Deiana [44], F. Del Corso [23b,23a], J. Del Peso [99], F. Del Rio [63a], F. Deliot [135], C.M. Delitzsch [49], M. Della Pietra [72a,72b], D. Della Volpe [56], A. Dell'Acqua [36], L. Dell'Asta [71a,71b], M. Delmastro [4], P.A. Delsart [60], S. Demers [172], M. Demichev [38], S.P. Denisov [37], L. D'Eramo [115], D. Derendarz [86], F. Derue [127], P. Dervan [92], K. Desch [24], K. Dette [155], C. Deutsch [24], F.A. Di Bello [57b,57a], A. Di Ciaccio [76a,76b], L. Di Ciaccio [4], A. Di Domenico [75a,75b], C. Di Donato [72a,72b], A. Di Girolamo [36], G. Di Gregorio [5], A. Di Luca [78a,78b], B. Di Micco [77a,77b], R. Di Nardo [77a,77b], C. Diaconu [102], F.A. Dias [114], T. Dias Do Vale [142], M.A. Diaz [137a,137b], F.G. Diaz Capriles [24], M. Didenko [163], E.B. Diehl [106], L. Diehl [54], S. Díez Cornell [48], C. Diez Pardos [141], C. Dimitriadi [24,161], A. Dimitrievska [17a], J. Dingfelder [24], I-M. Dinu [27b], S.J. Dittmeier [63b], F. Dittus [36], F. Djama [102], T. Djobava [149b], J.I. Djuvsland [16], C. Doglioni [101,98], J. Dolejsi [133], Z. Dolezal [133], M. Donadelli [82c], B. Dong [107], J. Donini [40], A. D'Onofrio [77a,77b], M. D'Onofrio [92], J. Dopke [134], A. Doria [72a], M.T. Dova [90], A.T. Doyle [59], M.A. Draguet [126], E. Drechsler [142], E. Dreyer [169], I. Drivas-koulouris [10], A.S. Drobac [158], M. Drozdova [56], D. Du [62a], T.A. du Pree [114], F. Dubinin [37], M. Dubovsky [28a], E. Duchovni [169], G. Duckeck [109], O.A. Ducu [27b], D. Duda [110], A. Dudarev [36], E.R. Duden [26], M. D'uffizi [101], L. Duflot [66], M. Dührssen [36], C. Dülsen [171], A.E. Dumitriu [27b], M. Dunford [63a], S. Dungs [49], K. Dunne [47a,47b], A. Duperrin [102], H. Duran Yildiz [3a], M. Düren [58], A. Durglishvili [149b], B.L. Dwyer [115], G.I. Dyckes [17a], M. Dyndal [85a], S. Dysch [101], B.S. Dziedzic [86], Z.O. Earnshaw [146], B. Eckerova [28a], S. Eggebrecht [55], M.G. Eggleston[51], E. Egidio Purcino De Souza [127], L.F. Ehrke [56], G. Eigen [16], K. Einsweiler [17a], T. Ekelof [161], P.A. Ekman [98], Y. El Ghazali [35b], H. El Jarrari [35e,148], A. El Moussaouy [35a], V. Ellajosyula [161], M. Ellert [161], F. Ellinghaus [171], A.A. Elliot [94], N. Ellis [36], J. Elmsheuser [29], M. Elsing [36], D. Emeliyanov [134], A. Emerman [41], Y. Enari [153], I. Ene [17a], S. Epari [13], J. Erdmann [49], P.A. Erland [86], M. Errenst [171], M. Escalier [66], C. Escobar [163], E. Etzion [151], G. Evans [130a], H. Evans [68], M.O. Evans [146], A. Ezhilov [37], S. Ezzarqtouni [35a], F. Fabbri [59], L. Fabbri [23b,23a], G. Facini [96], V. Fadeyev [136], R.M. Fakhrutdinov [37], S. Falciano [75a], L.F. Falda Ulhoa Coelho [36],

P.J. Falke[24], S. Falke[36], J. Faltova[133], Y. Fan[14a], Y. Fang[14a,14d], G. Fanourakis[46], M. Fanti[71a,71b], M. Faraj[69a,69b], Z. Farazpay[97], A. Farbin[8], A. Farilla[77a], T. Farooque[107], S.M. Farrington[52], F. Fassi[35e], D. Fassouliotis[9], M. Faucci Giannelli[76a,76b], W.J. Fawcett[32], L. Fayard[66], P. Federicova[131], O.L. Fedin[37,a], G. Fedotov[37], M. Feickert[170], L. Feligioni[102], A. Fell[139], D.E. Fellers[123], C. Feng[62b], M. Feng[14b], Z. Feng[114], M.J. Fenton[160], A.B. Fenyuk[37], L. Ferencz[48], R.A.M. Ferguson[91], S.I. Fernandez Luengo[137f], J. Ferrando[48], A. Ferrari[161], P. Ferrari[114,113], R. Ferrari[73a], D. Ferrere[56], C. Ferretti[106], F. Fiedler[100], A. Filipčič[93], E.K. Filmer[1], F. Filthaut[113], M.C.N. Fiolhais[130a,130c,b], L. Fiorini[163], F. Fischer[141], W.C. Fisher[107], T. Fitschen[101], I. Fleck[141], P. Fleischmann[106], T. Flick[171], L. Flores[128], M. Flores[33d], L.R. Flores Castillo[64a], F.M. Follega[78a,78b], N. Fomin[16], J.H. Foo[155], B.C. Forland[68], A. Formica[135], A.C. Forti[101], E. Fortin[102], A.W. Fortman[61], M.G. Foti[17a], L. Fountas[9], D. Fournier[66], H. Fox[91], P. Francavilla[74a,74b], S. Francescato[61], S. Franchellucci[56], M. Franchini[23b,23a], S. Franchino[63a], D. Francis[36], L. Franco[113], L. Franconi[19], M. Franklin[61], G. Frattari[26], A.C. Freegard[94], P.M. Freeman[20], W.S. Freund[82b], N. Fritzsche[50], A. Froch[54], D. Froidevaux[36], J.A. Frost[126], Y. Fu[62a], M. Fujimoto[118], E. Fullana Torregrosa[163,*], J. Fuster[163], A. Gabrielli[23b,23a], A. Gabrielli[155], P. Gadow[48], G. Gagliardi[57b,57a], L.G. Gagnon[17a], G.E. Gallardo[126], E.J. Gallas[126], B.J. Gallop[134], R. Gamboa Goni[94], K.K. Gan[119], S. Ganguly[153], J. Gao[62a], Y. Gao[52], F.M. Garay Walls[137a,137b], B. Garcia[29,af], C. García[163], J.E. García Navarro[163], M. Garcia-Sciveres[17a], R.W. Gardner[39], D. Garg[80], R.B. Garg[143], C.A. Garner[155], V. Garonne[29], S.J. Gasiorowski[138], P. Gaspar[82b], G. Gaudio[73a], V. Gautam[13], P. Gauzzi[75a,75b], I.L. Gavrilenko[37], A. Gavrilyuk[37], C. Gay[164], G. Gaycken[48], E.N. Gazis[10], A.A. Geanta[27b,27e], C.M. Gee[136], J. Geisen[98], C. Gemme[57b], M.H. Genest[60], S. Gentile[75a,75b], S. George[95], W.F. George[20], T. Geralis[46], L.O. Gerlach[55], P. Gessinger-Befurt[36], M.E. Geyik[171], M. Ghasemi Bostanabad[165], M. Ghneimat[141], K. Ghorbanian[94], A. Ghosal[141], A. Ghosh[160], A. Ghosh[7], B. Giacobbe[23b], S. Giagu[75a,75b], P. Giannetti[74a], A. Giannini[62a], S.M. Gibson[95], M. Gignac[136], D.T. Gil[85b], A.K. Gilbert[85a], B.J. Gilbert[41], D. Gillberg[34], G. Gilles[114], N.E.K. Gillwald[48], L. Ginabat[127], D.M. Gingrich[2,ac], M.P. Giordani[69a,69c], P.F. Giraud[135], G. Giugliarelli[69a,69c], D. Giugni[71a], F. Giuli[36], I. Gkialas[9,j], L.K. Gladilin[37], C. Glasman[99], G.R. Gledhill[123], M. Glisic[123], I. Gnesi[43b,f], Y. Go[29,af], M. Goblirsch-Kolb[26], B. Gocke[49], D. Godin[108], B. Gokturk[21a], S. Goldfarb[105], T. Golling[56], M.G.D. Gololo[33g], D. Golubkov[37], J.P. Gombas[107], A. Gomes[130a,130b], G. Gomes Da Silva[141], A.J. Gomez Delegido[163], R. Goncalves Gama[55], R. Gonçalo[130a,130c], G. Gonella[123], L. Gonella[20], A. Gongadze[38], F. Gonnella[20], J.L. Gonski[41], R.Y. González Andana[52], S. González de la Hoz[163], S. Gonzalez Fernandez[13], R. Gonzalez Lopez[92], C. Gonzalez Renteria[17a], R. Gonzalez Suarez[161], S. Gonzalez-Sevilla[56], G.R. Gonzalvo Rodriguez[163], L. Goossens[36], N.A. Gorasia[20], P.A. Gorbounov[37], B. Gorini[36], E. Gorini[70a,70b], A. Gorišek[93], A.T. Goshaw[51], M.I. Gostkin[38], S. Goswami[121], C.A. Gottardo[36], M. Gouighri[35b], V. Goumarre[48], A.G. Goussiou[138], N. Govender[33c], C. Goy[4], I. Grabowska-Bold[85a], K. Graham[34], E. Gramstad[125], S. Grancagnolo[18], M. Grandi[146], V. Gratchev[37,*], P.M. Gravila[27f], F.G. Gravili[70a,70b], H.M. Gray[17a], M. Greco[70a,70b], C. Grefe[24], I.M. Gregor[48], P. Grenier[143], C. Grieco[13], A.A. Grillo[136], K. Grimm[31,m], S. Grinstein[13,t], J.-F. Grivaz[66], E. Gross[169], J. Grosse-Knetter[55], C. Grud[106], J.C. Grundy[126], L. Guan[106], W. Guan[170], C. Gubbels[164], J.G.R. Guerrero Rojas[163], G. Guerrieri[69a,69b], F. Guescini[110], R. Gugel[100], J.A.M. Guhit[106], A. Guida[48], T. Guillemin[4], E. Guilloton[167,134], S. Guindon[36], F. Guo[14a,14d], J. Guo[62c], L. Guo[66], Y. Guo[106], R. Gupta[48], S. Gurbuz[24], S.S. Gurdasani[54], G. Gustavino[36], M. Guth[56],

P. Gutierrez [120], L.F. Gutierrez Zagazeta [128], C. Gutschow [96], C. Guyot [135], C. Gwenlan [126], C.B. Gwilliam [92], E.S. Haaland [125], A. Haas [117], M. Habedank [48], C. Haber [17a], H.K. Hadavand [8], A. Hadef [100], S. Hadzic [110], E.H. Haines [96], M. Haleem [166], J. Haley [121], J.J. Hall [139], G.D. Hallewell [102], L. Halser [19], K. Hamano [165], H. Hamdaoui [35e], M. Hamer [24], G.N. Hamity [52], J. Han [62b], K. Han [62a], L. Han [14c], L. Han [62a], S. Han [17a], Y.F. Han [155], K. Hanagaki [83], M. Hance [136], D.A. Hangal [41,aa], H. Hanif [142], M.D. Hank [39], R. Hankache [101], J.B. Hansen [42], J.D. Hansen [42], P.H. Hansen [42], K. Hara [157], D. Harada [56], T. Harenberg [171], S. Harkusha [37], Y.T. Harris [126], N.M. Harrison [119], P.F. Harrison[167], N.M. Hartman [143], N.M. Hartmann [109], Y. Hasegawa [140], A. Hasib [52], S. Haug [19], R. Hauser [107], M. Havranek [132], C.M. Hawkes [20], R.J. Hawkings [36], S. Hayashida [111], D. Hayden [107], C. Hayes [106], R.L. Hayes [164], C.P. Hays [126], J.M. Hays [94], H.S. Hayward [92], F. He [62a], Y. He [154], Y. He [127], M.P. Heath [52], N.B. Heatley [94], V. Hedberg [98], A.L. Heggelund [125], N.D. Hehir [94], C. Heidegger [54], K.K. Heidegger [54], W.D. Heidorn [81], J. Heilman [34], S. Heim [48], T. Heim [17a], J.G. Heinlein [128], J.J. Heinrich [123], L. Heinrich [110], J. Hejbal [131], L. Helary [48], A. Held [170], S. Hellesund [125], C.M. Helling [164], S. Hellman [47a,47b], C. Helsens [36], R.C.W. Henderson[91], L. Henkelmann [32], A.M. Henriques Correia[36], H. Herde [98], Y. Hernández Jiménez [145], L.M. Herrmann [24], T. Herrmann [50], G. Herten [54], R. Hertenberger [109], L. Hervas [36], N.P. Hessey [156a], H. Hibi [84], E. Higón-Rodriguez [163], S.J. Hillier [20], I. Hinchliffe [17a], F. Hinterkeuser [24], M. Hirose [124], S. Hirose [157], D. Hirschbuehl [171], T.G. Hitchings [101], B. Hiti [93], J. Hobbs [145], R. Hobincu [27e], N. Hod [169], M.C. Hodgkinson [139], B.H. Hodkinson [32], A. Hoecker [36], J. Hofer [48], D. Hohn [54], T. Holm [24], M. Holzbock [110], L.B.A.H. Hommels [32], B.P. Honan [101], J. Hong [62c], T.M. Hong [129], J.C. Honig [54], B.H. Hooberman [162], W.H. Hopkins [6], Y. Horii [111], S. Hou [148], A.S. Howard [93], J. Howarth [59], J. Hoya [6], M. Hrabovsky [122], A. Hrynevich [48], T. Hryn'ova [4], P.J. Hsu [65], S.-C. Hsu [138], Q. Hu [41], Y.F. Hu [14a,14d,ae], D.P. Huang [96], S. Huang [64b], X. Huang [14c], Y. Huang [62a], Y. Huang [14a], Z. Huang [101], Z. Hubacek [132], M. Huebner [24], F. Huegging [24], T.B. Huffman [126], M. Huhtinen [36], S.K. Huiberts [16], R. Hulsken [104], N. Huseynov [12,a], J. Huston [107], J. Huth [61], R. Hyneman [143], S. Hyrych [28a], G. Iacobucci [56], G. Iakovidis [29], I. Ibragimov [141], L. Iconomidou-Fayard [66], P. Iengo [72a,72b], R. Iguchi [153], T. Iizawa [56], Y. Ikegami [83], A. Ilg [19], N. Ilic [155], H. Imam [35a], T. Ingebretsen Carlson [47a,47b], G. Introzzi [73a,73b], M. Iodice [77a], V. Ippolito [75a,75b], M. Ishino [153], W. Islam [170], C. Issever [18,48], S. Istin [21a], H. Ito [168], J.M. Iturbe Ponce [64a], R. Iuppa [78a,78b], A. Ivina [169], J.M. Izen [45], V. Izzo [72a], P. Jacka [131,132], P. Jackson [1], R.M. Jacobs [48], B.P. Jaeger [142], C.S. Jagfeld [109], P. Jain [54], G. Jäkel [171], K. Jakobs [54], T. Jakoubek [169], J. Jamieson [59], K.W. Janas [85a], G. Jarlskog [98], A.E. Jaspan [92], M. Javurkova [103], F. Jeanneau [135], L. Jeanty [123], J. Jejelava [149a,z], P. Jenni [54,g], C.E. Jessiman [34], S. Jézéquel [4], C. Jia[62b], J. Jia [145], X. Jia [61], X. Jia [14a,14d], Z. Jia [14c], Y. Jiang[62a], S. Jiggins [52], J. Jimenez Pena [110], S. Jin [14c], A. Jinaru [27b], O. Jinnouchi [154], P. Johansson [139], K.A. Johns [7], J.W. Johnson [136], D.M. Jones [32], E. Jones [167], P. Jones [32], R.W.L. Jones [91], T.J. Jones [92], R. Joshi [119], J. Jovicevic [15], X. Ju [17a], J.J. Junggeburth [36], T. Junkermann [63a], A. Juste Rozas [13,t], S. Kabana [137e], A. Kaczmarska [86], M. Kado [75a,75b], H. Kagan [119], M. Kagan [143], A. Kahn[41], A. Kahn [128], C. Kahra [100], T. Kaji [168], E. Kajomovitz [150], N. Kakati [169], C.W. Kalderon [29], A. Kamenshchikov [155], S. Kanayama [154], N.J. Kang [136], D. Kar [33g], K. Karava [126], M.J. Kareem [156b], E. Karentzos [54], I. Karkanias [152,e], S.N. Karpov [38], Z.M. Karpova [38], V. Kartvelishvili [91], A.N. Karyukhin [37], E. Kasimi [152,e], C. Kato [62d], J. Katzy [48], S. Kaur [34], K. Kawade [140], K. Kawagoe [89], T. Kawamoto [135], G. Kawamura[55], E.F. Kay [165], F.I. Kaya [158], S. Kazakos [13], V.F. Kazanin [37], Y. Ke [145], J.M. Keaveney [33a], R. Keeler [165], G.V. Kehris [61], J.S. Keller [34], A.S. Kelly[96], D. Kelsey [146],

J.J. Kempster[146], K.E. Kennedy[41], P.D. Kennedy[100], O. Kepka[131], B.P. Kerridge[167], S. Kersten[171], B.P. Kerševan[93], S. Keshri[66], L. Keszeghova[28a], S. Ketabchi Haghighat[155], M. Khandoga[127], A. Khanov[121], A.G. Kharlamov[37], T. Kharlamova[37], E.E. Khoda[138], T.J. Khoo[18], G. Khoriauli[166], J. Khubua[149b], Y.A.R. Khwaira[66], M. Kiehn[36], A. Kilgallon[123], D.W. Kim[47a,47b], E. Kim[154], Y.K. Kim[39], N. Kimura[96], A. Kirchhoff[55], D. Kirchmeier[50], C. Kirfel[24], J. Kirk[134], A.E. Kiryunin[110], T. Kishimoto[153], D.P. Kisliuk[155], C. Kitsaki[10], O. Kivernyk[24], M. Klassen[63a], C. Klein[34], L. Klein[166], M.H. Klein[106], M. Klein[92], S.B. Klein[56], U. Klein[92], P. Klimek[36], A. Klimentov[29], F. Klimpel[110], T. Klioutchnikova[36], P. Kluit[114], S. Kluth[110], E. Kneringer[79], T.M. Knight[155], A. Knue[54], D. Kobayashi[89], R. Kobayashi[87], M. Kocian[143], P. Kodyš[133], D.M. Koeck[146], P.T. Koenig[24], T. Koffas[34], M. Kolb[135], I. Koletsou[4], T. Komarek[122], K. Köneke[54], A.X.Y. Kong[1], T. Kono[118], N. Konstantinidis[96], B. Konya[98], R. Kopeliansky[68], S. Koperny[85a], K. Korcyl[86], K. Kordas[152,e], G. Koren[151], A. Korn[96], S. Korn[55], I. Korolkov[13], N. Korotkova[37], B. Kortman[114], O. Kortner[110], S. Kortner[110], W.H. Kostecka[115], V.V. Kostyukhin[141], A. Kotsokechagia[135], A. Kotwal[51], A. Koulouris[36], A. Kourkoumeli-Charalampidi[73a,73b], C. Kourkoumelis[9], E. Kourlitis[6], O. Kovanda[146], R. Kowalewski[165], W. Kozanecki[135], A.S. Kozhin[37], V.A. Kramarenko[37], G. Kramberger[93], P. Kramer[100], M.W. Krasny[127], A. Krasznahorkay[36], J.A. Kremer[100], T. Kresse[50], J. Kretzschmar[92], K. Kreul[18], P. Krieger[155], S. Krishnamurthy[103], M. Krivos[133], K. Krizka[17a], K. Kroeninger[49], H. Kroha[110], J. Kroll[131], J. Kroll[128], K.S. Krowpman[107], U. Kruchonak[38], H. Krüger[24], N. Krumnack[81], M.C. Kruse[51], J.A. Krzysiak[86], O. Kuchinskaia[37], S. Kuday[3a], D. Kuechler[48], J.T. Kuechler[48], S. Kuehn[36], R. Kuesters[54], T. Kuhl[48], V. Kukhtin[38], Y. Kulchitsky[37,a], S. Kuleshov[137d,137b], M. Kumar[33g], N. Kumari[102], A. Kupco[131], T. Kupfer[49], A. Kupich[37], O. Kuprash[54], H. Kurashige[84], L.L. Kurchaninov[156a], Y.A. Kurochkin[37], A. Kurova[37], M. Kuze[154], A.K. Kvam[103], J. Kvita[122], T. Kwan[104], K.W. Kwok[64a], N.G. Kyriacou[106], L.A.O. Laatu[102], C. Lacasta[163], F. Lacava[75a,75b], H. Lacker[18], D. Lacour[127], N.N. Lad[96], E. Ladygin[38], B. Laforge[127], T. Lagouri[137e], S. Lai[55], I.K. Lakomiec[85a], N. Lalloue[60], J.E. Lambert[120], S. Lammers[68], W. Lampl[7], C. Lampoudis[152,e], A.N. Lancaster[115], E. Lançon[29], U. Landgraf[54], M.P.J. Landon[94], V.S. Lang[54], R.J. Langenberg[103], A.J. Lankford[160], F. Lanni[36], K. Lantzsch[24], A. Lanza[73a], A. Lapertosa[57b,57a], J.F. Laporte[135], T. Lari[71a], F. Lasagni Manghi[23b], M. Lassnig[36], V. Latonova[131], A. Laudrain[100], A. Laurier[150], S.D. Lawlor[95], Z. Lawrence[101], M. Lazzaroni[71a,71b], B. Le[101], B. Leban[93], A. Lebedev[81], M. LeBlanc[36], T. LeCompte[6], F. Ledroit-Guillon[60], A.C.A. Lee[96], G.R. Lee[16], S.C. Lee[148], S. Lee[47a,47b], T.F. Lee[92], L.L. Leeuw[33c], H.P. Lefebvre[95], M. Lefebvre[165], C. Leggett[17a], K. Lehmann[142], G. Lehmann Miotto[36], M. Leigh[56], W.A. Leight[103], A. Leisos[152,s], M.A.L. Leite[82c], C.E. Leitgeb[48], R. Leitner[133], K.J.C. Leney[44], T. Lenz[24], S. Leone[74a], C. Leonidopoulos[52], A. Leopold[144], C. Leroy[108], R. Les[107], C.G. Lester[32], M. Levchenko[37], J. Levêque[4], D. Levin[106], L.J. Levinson[169], M.P. Lewicki[86], D.J. Lewis[4], A. Li[5], B. Li[62b], C. Li[62a], C-Q. Li[62c], H. Li[62a], H. Li[62b], H. Li[14c], H. Li[62b], J. Li[62c], K. Li[138], L. Li[62c], M. Li[14a,14d], Q.Y. Li[62a], S. Li[14a,14d], S. Li[62d,62c,d], T. Li[62b], X. Li[104], Z. Li[62b], Z. Li[126], Z. Li[104], Z. Li[92], Z. Li[14a,14d], S. Liang[14a,14d], Z. Liang[14a], M. Liberatore[48], B. Liberti[76a], K. Lie[64c], J. Lieber Marin[82b], H. Lien[68], K. Lin[107], R.A. Linck[68], R.E. Lindley[7], J.H. Lindon[2], A. Linss[48], E. Lipeles[128], A. Lipniacka[16], A. Lister[164], J.D. Little[4], B. Liu[14a], B.X. Liu[142], D. Liu[62d,62c], J.B. Liu[62a], J.K.K. Liu[32], K. Liu[62d,62c], M. Liu[62a], M.Y. Liu[62a], P. Liu[14a], Q. Liu[62d,138,62c], X. Liu[62a], Y. Liu[14c,14d], Y.L. Liu[106], Y.W. Liu[62a], M. Livan[73a,73b], J. Llorente Merino[142], S.L. Lloyd[94], E.M. Lobodzinska[48], P. Loch[7], S. Loffredo[76a,76b],

T. Lohse [18], K. Lohwasser [139], M. Lokajicek [131], J.D. Long [162], I. Longarini [160], L. Longo [70a,70b], R. Longo [162], I. Lopez Paz [67], A. Lopez Solis [48], J. Lorenz [109], N. Lorenzo Martinez [4], A.M. Lory [109], X. Lou [47a,47b], X. Lou [14a,14d], A. Lounis [66], J. Love [6], P.A. Love [91], J.J. Lozano Bahilo [163], G. Lu [14a,14d], M. Lu [80], S. Lu [128], Y.J. Lu [65], H.J. Lubatti [138], C. Luci [75a,75b], F.L. Lucio Alves [14c], A. Lucotte [60], F. Luehring [68], I. Luise [145], O. Lukianchuk [66], O. Lundberg [144], B. Lund-Jensen [144], N.A. Luongo [123], M.S. Lutz [151], D. Lynn [29], H. Lyons[92], R. Lysak [131], E. Lytken [98], F. Lyu [14a], V. Lyubushkin [38], T. Lyubushkina [38], M.M. Lyukova [145], H. Ma [29], L.L. Ma [62b], Y. Ma [96], D.M. Mac Donell [165], G. Maccarrone [53], J.C. MacDonald [139], R. Madar [40], W.F. Mader [50], J. Maeda [84], T. Maeno [29], M. Maerker [50], H. Maguire [139], D.J. Mahon [41], A. Maio [130a,130b,130d], K. Maj [85a], O. Majersky [48], S. Majewski [123], N. Makovec [66], V. Maksimovic [15], B. Malaescu [127], Pa. Malecki [86], V.P. Maleev [37], F. Malek [60], D. Malito [43b,43a], U. Mallik [80], C. Malone [32], S. Maltezos[10], S. Malyukov[38], J. Mamuzic [13], G. Mancini [53], G. Manco [73a,73b], J.P. Mandalia [94], I. Mandić [93], L. Manhaes de Andrade Filho [82a], I.M. Maniatis [169], J. Manjarres Ramos [50], D.C. Mankad [169], A. Mann [109], B. Mansoulie [135], S. Manzoni [36], A. Marantis [152], G. Marchiori [5], M. Marcisovsky [131], C. Marcon [71a,71b], M. Marinescu [20], M. Marjanovic [120], E.J. Marshall [91], Z. Marshall [17a], S. Marti-Garcia [163], T.A. Martin [167], V.J. Martin [52], B. Martin dit Latour [16], L. Martinelli [75a,75b], M. Martinez [13,t], P. Martinez Agullo [163], V.I. Martinez Outschoorn [103], P. Martinez Suarez [13], S. Martin-Haugh [134], V.S. Martoiu [27b], A.C. Martyniuk [96], A. Marzin [36], S.R. Maschek [110], D. Mascione [78a,78b], L. Masetti [100], T. Mashimo [153], J. Masik [101], A.L. Maslennikov [37], L. Massa [23b], P. Massarotti [72a,72b], P. Mastrandrea [74a,74b], A. Mastroberardino [43b,43a], T. Masubuchi [153], T. Mathisen [161], N. Matsuzawa[153], J. Maurer [27b], B. Maček [93], D.A. Maximov [37], R. Mazini [148], I. Maznas [152,e], M. Mazza [107], S.M. Mazza [136], C. Mc Ginn [29], J.P. Mc Gowan [104], S.P. Mc Kee [106], E.F. McDonald [105], A.E. McDougall [114], J.A. Mcfayden [146], G. Mchedlidze [149b], R.P. Mckenzie [33g], T.C. Mclachlan [48], D.J. Mclaughlin [96], K.D. McLean [165], S.J. McMahon [134], P.C. McNamara [105], C.M. Mcpartland [92], R.A. McPherson [165,w], T. Megy [40], S. Mehlhase [109], A. Mehta [92], B. Meirose [45], D. Melini [150], B.R. Mellado Garcia [33g], A.H. Melo [55], F. Meloni [48], E.D. Mendes Gouveia [130a], A.M. Mendes Jacques Da Costa [20], H.Y. Meng [155], L. Meng [91], S. Menke [110], M. Mentink [36], E. Meoni [43b,43a], C. Merlassino [126], L. Merola [72a,72b], C. Meroni [71a], G. Merz[106], O. Meshkov [37], J. Metcalfe [6], A.S. Mete [6], C. Meyer [68], J-P. Meyer [135], M. Michetti [18], R.P. Middleton [134], L. Mijović [52], G. Mikenberg [169], M. Mikestikova [131], M. Mikuž [93], H. Mildner [139], A. Milic [36], C.D. Milke [44], D.W. Miller [39], L.S. Miller [34], A. Milov [169], D.A. Milstead[47a,47b], T. Min[14c], A.A. Minaenko [37], I.A. Minashvili [149b], L. Mince [59], A.I. Mincer [117], B. Mindur [85a], M. Mineev [38], Y. Mino [87], L.M. Mir [13], M. Miralles Lopez [163], M. Mironova [126], M.C. Missio [113], T. Mitani [168], A. Mitra [167], V.A. Mitsou [163], O. Miu [155], P.S. Miyagawa [94], Y. Miyazaki[89], A. Mizukami [83], J.U. Mjörnmark [98], T. Mkrtchyan [63a], M. Mlinarevic [96], T. Mlinarevic [96], M. Mlynarikova [36], T. Moa [47a,47b], S. Mobius [55], K. Mochizuki [108], P. Moder [48], P. Mogg [109], A.F. Mohammed [14a,14d], S. Mohapatra [41], G. Mokgatitswane [33g], B. Mondal [141], S. Mondal [132], K. Mönig [48], E. Monnier [102], L. Monsonis Romero[163], J. Montejo Berlingen [83], M. Montella [119], F. Monticelli [90], N. Morange [66], A.L. Moreira De Carvalho [130a], M. Moreno Llácer [163], C. Moreno Martinez [56], P. Morettini [57b], S. Morgenstern [167], M. Morii [61], M. Morinaga [153], A.K. Morley [36], F. Morodei [75a,75b], L. Morvaj [36], P. Moschovakos [36], B. Moser [36], M. Mosidze[149b], T. Moskalets [54], P. Moskvitina [113], J. Moss [31,n], E.J.W. Moyse [103], O. Mtintsilana [33g], S. Muanza [102], J. Mueller [129], D. Muenstermann [91], R. Müller [19], G.A. Mullier [161], J.J. Mullin[128], D.P. Mungo [155], J.L. Munoz Martinez [13], D. Munoz Perez [163],

F.J. Munoz Sanchez [101], M. Murin [101], W.J. Murray [167,134], A. Murrone [71a,71b], J.M. Muse [120], M. Muškinja [17a], C. Mwewa [29], A.G. Myagkov [37,a], A.J. Myers [8], A.A. Myers[129], G. Myers [68], M. Myska [132], B.P. Nachman [17a], O. Nackenhorst [49], A. Nag [50], K. Nagai [126], K. Nagano [83], J.L. Nagle [29,af], E. Nagy [102], A.M. Nairz [36], Y. Nakahama [83], K. Nakamura [83], H. Nanjo [124], R. Narayan [44], E.A. Narayanan [112], I. Naryshkin [37], M. Naseri [34], C. Nass [24], G. Navarro [22a], J. Navarro-Gonzalez [163], R. Nayak [151], A. Nayaz [18], P.Y. Nechaeva [37], F. Nechansky [48], L. Nedic [126], T.J. Neep [20], A. Negri [73a,73b], M. Negrini [23b], C. Nellist [113], C. Nelson [104], K. Nelson [106], S. Nemecek [131], M. Nessi [36,h], M.S. Neubauer [162], F. Neuhaus [100], J. Neundorf [48], R. Newhouse [164], P.R. Newman [20], C.W. Ng [129], Y.S. Ng[18], Y.W.Y. Ng [48], B. Ngair [35e], H.D.N. Nguyen [108], R.B. Nickerson [126], R. Nicolaidou [135], J. Nielsen [136], M. Niemeyer [55], N. Nikiforou [36], V. Nikolaenko [37,a], I. Nikolic-Audit [127], K. Nikolopoulos [20], P. Nilsson [29], I. Ninca [48], H.R. Nindhito [56], G. Ninio [151], A. Nisati [75a], N. Nishu [2], R. Nisius [110], J-E. Nitschke [50], E.K. Nkadimeng [33g], S.J. Noacco Rosende [90], T. Nobe [153], D.L. Noel [32], Y. Noguchi [87], T. Nommensen [147], M.A. Nomura[29], M.B. Norfolk [139], R.R.B. Norisam [96], B.J. Norman [34], J. Novak [93], T. Novak [48], O. Novgorodova [50], L. Novotny [132], R. Novotny [112], L. Nozka [122], K. Ntekas [160], N.M.J. Nunes De Moura Junior [82b], E. Nurse[96], F.G. Oakham [34,ac], J. Ocariz [127], A. Ochi [84], I. Ochoa [130a], S. Oerdek [161], J.T. Offermann [39], A. Ogrodnik [85a], A. Oh [101], C.C. Ohm [144], H. Oide [83], R. Oishi [153], M.L. Ojeda [48], Y. Okazaki [87], M.W. O'Keefe[92], Y. Okumura [153], A. Olariu[27b], L.F. Oleiro Seabra [130a], S.A. Olivares Pino [137e], D. Oliveira Damazio [29], D. Oliveira Goncalves [82a], J.L. Oliver [160], M.J.R. Olsson [160], A. Olszewski [86], J. Olszowska [86,*], Ö.O. Öncel [54], D.C. O'Neil [142], A.P. O'Neill [19], A. Onofre [130a,130e], P.U.E. Onyisi [11], M.J. Oreglia [39], G.E. Orellana [90], D. Orestano [77a,77b], N. Orlando [13], R.S. Orr [155], V. O'Shea [59], R. Ospanov [62a], G. Otero y Garzon [30], H. Otono [89], P.S. Ott [63a], G.J. Ottino [17a], M. Ouchrif [35d], J. Ouellette [29,af], F. Ould-Saada [125], M. Owen [59], R.E. Owen [134], K.Y. Oyulmaz [21a], V.E. Ozcan [21a], N. Ozturk [8], S. Ozturk [21d], J. Pacalt [122], H.A. Pacey [32], K. Pachal [51], A. Pacheco Pages [13], C. Padilla Aranda [13], G. Padovano [75a,75b], S. Pagan Griso [17a], G. Palacino [68], A. Palazzo [70a,70b], S. Palestini [36], J. Pan [172], T. Pan [64a], D.K. Panchal [11], C.E. Pandini [114], J.G. Panduro Vazquez [95], H. Pang [14b], P. Pani [48], G. Panizzo [69a,69c], L. Paolozzi [56], C. Papadatos [108], S. Parajuli [44], A. Paramonov [6], C. Paraskevopoulos [10], D. Paredes Hernandez [64b], T.H. Park [155], M.A. Parker [32], F. Parodi [57b,57a], E.W. Parrish [115], V.A. Parrish [52], J.A. Parsons [41], U. Parzefall [54], B. Pascual Dias [108], L. Pascual Dominguez [151], V.R. Pascuzzi [17a], F. Pasquali [114], E. Pasqualucci [75a], S. Passaggio [57b], F. Pastore [95], P. Pasuwan [47a,47b], P. Patel [86], J.R. Pater [101], T. Pauly [36], J. Pearkes [143], M. Pedersen [125], R. Pedro [130a], S.V. Peleganchuk [37], O. Penc [36], E.A. Pender[52], C. Peng [64b], H. Peng [62a], K.E. Penski [109], M. Penzin [37], B.S. Peralva [82d,82d], A.P. Pereira Peixoto [60], L. Pereira Sanchez [47a,47b], D.V. Perepelitsa [29,af], E. Perez Codina [156a], M. Perganti [10], L. Perini [71a,71b,*], H. Pernegger [36], S. Perrella [36], A. Perrevoort [113], O. Perrin [40], K. Peters [48], R.F.Y. Peters [101], B.A. Petersen [36], T.C. Petersen [42], E. Petit [102], V. Petousis [132], C. Petridou [152,e], A. Petrukhin [141], M. Pettee [17a], N.E. Pettersson [36], A. Petukhov [37], K. Petukhova [133], A. Peyaud [135], R. Pezoa [137f], L. Pezzotti [36], G. Pezzullo [172], T.M. Pham [170], T. Pham [105], P.W. Phillips [134], M.W. Phipps [162], G. Piacquadio [145], E. Pianori [17a], F. Piazza [71a,71b], R. Piegaia [30], D. Pietreanu [27b], A.D. Pilkington [101], M. Pinamonti [69a,69c], J.L. Pinfold [2], B.C. Pinheiro Pereira [130a], C. Pitman Donaldson[96], D.A. Pizzi [34], L. Pizzimento [76a,76b], A. Pizzini [114], M.-A. Pleier [29], V. Plesanovs[54], V. Pleskot [133], E. Plotnikova[38], G. Poddar [4], R. Poettgen [98], L. Poggioli [127], I. Pogrebnyak [107], D. Pohl [24], I. Pokharel [55], S. Polacek [133], G. Polesello [73a], A. Poley [142,156a], R. Polifka [132], A. Polini [23b],

C.S. Pollard [167], Z.B. Pollock [119], V. Polychronakos [29], E. Pompa Pacchi [75a,75b], D. Ponomarenko [113], L. Pontecorvo [36], S. Popa [27a], G.A. Popeneciu [27d], D.M. Portillo Quintero [156a], S. Pospisil [132], P. Postolache [27c], K. Potamianos [126], P.P. Potepa [85a], I.N. Potrap [38], C.J. Potter [32], H. Potti [1], T. Poulsen [48], J. Poveda [163], M.E. Pozo Astigarraga [36], A. Prades Ibanez [163], M.M. Prapa [46], J. Pretel [54], D. Price [101], M. Primavera [70a], M.A. Principe Martin [99], R. Privara [122], M.L. Proffitt [138], N. Proklova [128], K. Prokofiev [64c], G. Proto [76a,76b], S. Protopopescu [29], J. Proudfoot [6], M. Przybycien [85a], J.E. Puddefoot [139], D. Pudzha [37], P. Puzo[66], D. Pyatiizbyantseva [37], J. Qian [106], D. Qichen [101], Y. Qin [101], T. Qiu [94], A. Quadt [55], M. Queitsch-Maitland [101], G. Quetant [56], G. Rabanal Bolanos [61], D. Rafanoharana [54], F. Ragusa [71a,71b], J.L. Rainbolt [39], J.A. Raine [56], S. Rajagopalan [29], E. Ramakoti [37], K. Ran [48,14d], N.P. Rapheeha [33g], V. Raskina [127], D.F. Rassloff [63a], S. Rave [100], B. Ravina [55], I. Ravinovich [169], M. Raymond [36], A.L. Read [125], N.P. Readioff [139], D.M. Rebuzzi [73a,73b], A. Redelbach [166], G. Redlinger [29], K. Reeves [45], J.A. Reidelsturz [171], D. Reikher [151], A. Rej [141], C. Rembser [36], A. Renardi [48], M. Renda [27b], M.B. Rendel[110], F. Renner [48], A.G. Rennie [59], S. Resconi [71a], M. Ressegotti [57b,57a], E.D. Resseguie [17a], S. Rettie [36], J.G. Reyes Rivera [107], B. Reynolds[119], E. Reynolds [17a], M. Rezaei Estabragh [171], O.L. Rezanova [37], P. Reznicek [133], N. Ribaric [91], E. Ricci [78a,78b], R. Richter [110], S. Richter [47a,47b], E. Richter-Was [85b], M. Ridel [127], S. Ridouani [35d], P. Rieck [117], P. Riedler [36], M. Rijssenbeek [145], A. Rimoldi [73a,73b], M. Rimoldi [48], L. Rinaldi [23b,23a], T.T. Rinn [29], M.P. Rinnagel [109], G. Ripellino [144], I. Riu [13], P. Rivadeneira [48], J.C. Rivera Vergara [165], F. Rizatdinova [121], E. Rizvi [94], C. Rizzi [56], B.A. Roberts [167], B.R. Roberts [17a], S.H. Robertson [104,w], M. Robin [48], D. Robinson [32], C.M. Robles Gajardo[137f], M. Robles Manzano [100], A. Robson [59], A. Rocchi [76a,76b], C. Roda [74a,74b], S. Rodriguez Bosca [63a], Y. Rodriguez Garcia [22a], A. Rodriguez Rodriguez [54], A.M. Rodríguez Vera [156b], S. Roe[36], J.T. Roemer [160], A.R. Roepe-Gier [120], J. Roggel [171], O. Røhne [125], R.A. Rojas [103], B. Roland [54], C.P.A. Roland [68], J. Roloff [29], A. Romaniouk [37], E. Romano [73a,73b], M. Romano [23b], A.C. Romero Hernandez [162], N. Rompotis [92], L. Roos [127], S. Rosati [75a], B.J. Rosser [39], E. Rossi [4], E. Rossi [72a,72b], L.P. Rossi [57b], L. Rossini [48], R. Rosten [119], M. Rotaru [27b], B. Rottler [54], C. Rougier [102], D. Rousseau [66], D. Rousso [32], G. Rovelli [73a,73b], A. Roy [162], S. Roy-Garand [155], A. Rozanov [102], Y. Rozen [150], X. Ruan [33g], A. Rubio Jimenez [163], A.J. Ruby [92], V.H. Ruelas Rivera [18], T.A. Ruggeri [1], F. Rühr [54], A. Ruiz-Martinez [163], A. Rummler [36], Z. Rurikova [54], N.A. Rusakovich [38], H.L. Russell [165], J.P. Rutherfoord [7], K. Rybacki[91], M. Rybar [133], E.B. Rye [125], A. Ryzhov [37], J.A. Sabater Iglesias [56], P. Sabatini [163], L. Sabetta [75a,75b], H.F-W. Sadrozinski [136], F. Safai Tehrani [75a], B. Safarzadeh Samani [146], M. Safdari [143], S. Saha [104], M. Sahinsoy [110], M. Saimpert [135], M. Saito [153], T. Saito [153], D. Salamani [36], G. Salamanna [77a,77b], A. Salnikov [143], J. Salt [163], A. Salvador Salas [13], D. Salvatore [43b,43a], F. Salvatore [146], A. Salzburger [36], D. Sammel [54], D. Sampsonidis [152,e], D. Sampsonidou [62d,62c], J. Sánchez [163], A. Sanchez Pineda [4], V. Sanchez Sebastian [163], H. Sandaker [125], C.O. Sander [48], J.A. Sandesara [103], M. Sandhoff [171], C. Sandoval [22b], D.P.C. Sankey [134], T. Sano [87], A. Sansoni [53], L. Santi [75a,75b], C. Santoni [40], H. Santos [130a,130b], S.N. Santpur [17a], A. Santra [169], K.A. Saoucha [139], J.G. Saraiva [130a,130d], J. Sardain [7], O. Sasaki [83], K. Sato [157], C. Sauer[63b], F. Sauerburger [54], E. Sauvan [4], P. Savard [155,ac], R. Sawada [153], C. Sawyer [134], L. Sawyer [97], I. Sayago Galvan[163], C. Sbarra [23b], A. Sbrizzi [23b,23a], T. Scanlon [96], J. Schaarschmidt [138], P. Schacht [110], D. Schaefer [39], U. Schäfer [100], A.C. Schaffer [66,44], D. Schaile [109], R.D. Schamberger [145], E. Schanet [109], C. Scharf [18], M.M. Schefer [19], V.A. Schegelsky [37], D. Scheirich [133], F. Schenck [18], M. Schernau [160], C. Scheulen [55], C. Schiavi [57b,57a], Z.M. Schillaci [26], E.J. Schioppa [70a,70b], M. Schioppa [43b,43a],

B. Schlag [100], K.E. Schleicher [54], S. Schlenker [36], J. Schmeing [171], M.A. Schmidt [171], K. Schmieden [100], C. Schmitt [100], S. Schmitt [48], L. Schoeffel [135], A. Schoening [63b], P.G. Scholer [54], E. Schopf [126], M. Schott [100], J. Schovancova [36], S. Schramm [56], F. Schroeder [171], H-C. Schultz-Coulon [63a], M. Schumacher [54], B.A. Schumm [136], Ph. Schune [135], H.R. Schwartz [136], A. Schwartzman [143], T.A. Schwarz [106], Ph. Schwemling [135], R. Schwienhorst [107], A. Sciandra [136], G. Sciolla [26], F. Scuri [74a], F. Scutti [105], C.D. Sebastiani [92], K. Sedlaczek [49], P. Seema [18], S.C. Seidel [112], A. Seiden [136], B.D. Seidlitz [41], C. Seitz [48], J.M. Seixas [82b], G. Sekhniaidze [72a], S.J. Sekula [44], L. Selem [4], N. Semprini-Cesari [23b,23a], S. Sen [51], D. Sengupta [56], V. Senthilkumar [163], L. Serin [66], L. Serkin [69a,69b], M. Sessa [77a,77b], H. Severini [120], F. Sforza [57b,57a], A. Sfyrla [56], E. Shabalina [55], R. Shaheen [144], J.D. Shahinian [128], D. Shaked Renous [169], L.Y. Shan [14a], M. Shapiro [17a], A. Sharma [36], A.S. Sharma [164], P. Sharma [80], S. Sharma [48], P.B. Shatalov [37], K. Shaw [146], S.M. Shaw [101], Q. Shen [62c,5], P. Sherwood [96], L. Shi [96], C.O. Shimmin [172], Y. Shimogama [168], J.D. Shinner [95], I.P.J. Shipsey [126], S. Shirabe [60], M. Shiyakova [38], J. Shlomi [169], M.J. Shochet [39], J. Shojaii [105], D.R. Shope [125], S. Shrestha [119,ag], E.M. Shrif [33g], M.J. Shroff [165], P. Sicho [131], A.M. Sickles [162], E. Sideras Haddad [33g], A. Sidoti [23b], F. Siegert [50], Dj. Sijacki [15], R. Sikora [85a], F. Sili [90], J.M. Silva [20], M.V. Silva Oliveira [36], S.B. Silverstein [47a], S. Simion [66], R. Simoniello [36], E.L. Simpson [59], H. Simpson [146], L.R. Simpson [106], N.D. Simpson [98], S. Simsek [21d], S. Sindhu [55], P. Sinervo [155], S. Singh [142], S. Singh [155], S. Sinha [48], S. Sinha [33g], M. Sioli [23b,23a], I. Siral [36], S.Yu. Sivoklokov [37,*], J. Sjölin [47a,47b], A. Skaf [55], E. Skorda [98], P. Skubic [120], M. Slawinska [86], V. Smakhtin [169], B.H. Smart [134], J. Smiesko [36], S.Yu. Smirnov [37], Y. Smirnov [37], L.N. Smirnova [37,a], O. Smirnova [98], A.C. Smith [41], E.A. Smith [39], H.A. Smith [126], J.L. Smith [92], R. Smith [143], M. Smizanska [91], K. Smolek [132], A. Smykiewicz [86], A.A. Snesarev [37], H.L. Snoek [114], S. Snyder [29], R. Sobie [165,w], A. Soffer [151], C.A. Solans Sanchez [36], E.Yu. Soldatov [37], U. Soldevila [163], A.A. Solodkov [37], S. Solomon [54], A. Soloshenko [38], K. Solovieva [54], O.V. Solovyanov [40], V. Solovyev [37], P. Sommer [36], A. Sonay [13], W.Y. Song [156b], J.M. Sonneveld [114], A. Sopczak [132], A.L. Sopio [96], F. Sopkova [28b], V. Sothilingam [63a], S. Sottocornola [68], R. Soualah [116b], Z. Soumaimi [35e], D. South [48], S. Spagnolo [70a,70b], M. Spalla [110], F. Spanò [95], D. Sperlich [54], G. Spigo [36], M. Spina [146], S. Spinali [91], D.P. Spiteri [59], M. Spousta [133], E.J. Staats [34], A. Stabile [71a,71b], R. Stamen [63a], M. Stamenkovic [114], A. Stampekis [20], M. Standke [24], E. Stanecka [86], M.V. Stange [50], B. Stanislaus [17a], M.M. Stanitzki [48], M. Stankaityte [126], B. Stapf [48], E.A. Starchenko [37], G.H. Stark [136], J. Stark [102], D.M. Starko [156b], P. Staroba [131], P. Starovoitov [63a], S. Stärz [104], R. Staszewski [86], G. Stavropoulos [46], J. Steentoft [161], P. Steinberg [29], A.L. Steinhebel [123], B. Stelzer [142,156a], H.J. Stelzer [129], O. Stelzer-Chilton [156a], H. Stenzel [58], T.J. Stevenson [146], G.A. Stewart [36], M.C. Stockton [36], G. Stoicea [27b], M. Stolarski [130a], S. Stonjek [110], A. Straessner [50], J. Strandberg [144], S. Strandberg [47a,47b], M. Strauss [120], T. Strebler [102], P. Strizenec [28b], R. Ströhmer [166], D.M. Strom [123], L.R. Strom [48], R. Stroynowski [44], A. Strubig [47a,47b], S.A. Stucci [29], B. Stugu [16], J. Stupak [120], N.A. Styles [48], D. Su [143], S. Su [62a], W. Su [62d,138,62c], X. Su [62a,66], K. Sugizaki [153], V.V. Sulin [37], M.J. Sullivan [92], D.M.S. Sultan [78a,78b], L. Sultanaliyeva [37], S. Sultansoy [3b], T. Sumida [87], S. Sun [106], S. Sun [170], O. Sunneborn Gudnadottir [161], M.R. Sutton [146], M. Svatos [131], M. Swiatlowski [156a], T. Swirski [166], I. Sykora [28a], M. Sykora [133], T. Sykora [133], D. Ta [100], K. Tackmann [48,u], A. Taffard [160], R. Tafirout [156a], J.S. Tafoya Vargas [66], R.H.M. Taibah [127], R. Takashima [88], K. Takeda [84], E.P. Takeva [52], Y. Takubo [83], M. Talby [102], A.A. Talyshev [37], K.C. Tam [64b], N.M. Tamir [151], A. Tanaka [153], J. Tanaka [153], R. Tanaka [66], M. Tanasini [57b,57a], J. Tang [62c], Z. Tao [164], S. Tapia Araya [137f], S. Tapprogge [100], A. Tarek Abouelfadl Mohamed [107],

S. Tarem[150], K. Tariq[62b], G. Tarna[102,27b], G.F. Tartarelli[71a], P. Tas[133], M. Tasevsky[131], E. Tassi[43b,43a], A.C. Tate[162], G. Tateno[153], Y. Tayalati[35e,v], G.N. Taylor[105], W. Taylor[156b], H. Teagle[92], A.S. Tee[170], R. Teixeira De Lima[143], P. Teixeira-Dias[95], J.J. Teoh[155], K. Terashi[153], J. Terron[99], S. Terzo[13], M. Testa[53], R.J. Teuscher[155,w], A. Thaler[79], O. Theiner[56], N. Themistokleous[52], T. Theveneaux-Pelzer[18], O. Thielmann[171], D.W. Thomas[95], J.P. Thomas[20], E.A. Thompson[17a], P.D. Thompson[20], E. Thomson[128], E.J. Thorpe[94], Y. Tian[55], V. Tikhomirov[37,a], Yu.A. Tikhonov[37], S. Timoshenko[37], E.X.L. Ting[1], P. Tipton[172], S. Tisserant[102], S.H. Tlou[33g], A. Tnourji[40], K. Todome[23b,23a], S. Todorova-Nova[133], S. Todt[50], M. Togawa[83], J. Tojo[89], S. Tokár[28a], K. Tokushuku[83], O. Toldaiev[68], R. Tombs[32], M. Tomoto[83,111], L. Tompkins[143], K.W. Topolnicki[85b], P. Tornambe[103], E. Torrence[123], H. Torres[50], E. Torró Pastor[163], M. Toscani[30], C. Tosciri[39], M. Tost[11], D.R. Tovey[139], A. Traeet[16], I.S. Trandafir[27b], T. Trefzger[166], A. Tricoli[29], I.M. Trigger[156a], S. Trincaz-Duvoid[127], D.A. Trischuk[26], B. Trocmé[60], C. Troncon[71a], L. Truong[33c], M. Trzebinski[86], A. Trzupek[86], F. Tsai[145], M. Tsai[106], A. Tsiamis[152,e], P.V. Tsiareshka[37], S. Tsigaridas[156a], A. Tsirigotis[152,s], V. Tsiskaridze[145], E.G. Tskhadadze[149a], M. Tsopoulou[152,e], Y. Tsujikawa[87], I.I. Tsukerman[37], V. Tsulaia[17a], S. Tsuno[83], O. Tsur[150], D. Tsybychev[145], Y. Tu[64b], A. Tudorache[27b], V. Tudorache[27b], A.N. Tuna[36], S. Turchikhin[38], I. Turk Cakir[3a], R. Turra[71a], T. Turtuvshin[38,x], P.M. Tuts[41], S. Tzamarias[152,e], P. Tzanis[10], E. Tzovara[100], K. Uchida[153], F. Ukegawa[157], P.A. Ulloa Poblete[137c], E.N. Umaka[29], G. Unal[36], M. Unal[11], A. Undrus[29], G. Unel[160], J. Urban[28b], P. Urquijo[105], G. Usai[8], R. Ushioda[154], M. Usman[108], Z. Uysal[21b], L. Vacavant[102], V. Vacek[132], B. Vachon[104], K.O.H. Vadla[125], T. Vafeiadis[36], A. Vaitkus[96], C. Valderanis[109], E. Valdes Santurio[47a,47b], M. Valente[156a], S. Valentinetti[23b,23a], A. Valero[163], A. Vallier[102], J.A. Valls Ferrer[163], D.R. Van Arneman[114], T.R. Van Daalen[138], P. Van Gemmeren[6], M. Van Rijnbach[125,36], S. Van Stroud[96], I. Van Vulpen[114], M. Vanadia[76a,76b], W. Vandelli[36], M. Vandenbroucke[135], E.R. Vandewall[121], D. Vannicola[151], L. Vannoli[57b,57a], R. Vari[75a], E.W. Varnes[7], C. Varni[17a], T. Varol[148], D. Varouchas[66], L. Varriale[163], K.E. Varvell[147], M.E. Vasile[27b], L. Vaslin[40], G.A. Vasquez[165], F. Vazeille[40], T. Vazquez Schroeder[36], J. Veatch[31], V. Vecchio[101], M.J. Veen[103], I. Veliscek[126], L.M. Veloce[155], F. Veloso[130a,130c], S. Veneziano[75a], A. Ventura[70a,70b], A. Verbytskyi[110], M. Verducci[74a,74b], C. Vergis[24], M. Verissimo De Araujo[82b], W. Verkerke[114], J.C. Vermeulen[114], C. Vernieri[143], P.J. Verschuuren[95], M. Vessella[103], M.C. Vetterli[142,ac], A. Vgenopoulos[152,e], N. Viaux Maira[137f], T. Vickey[139], O.E. Vickey Boeriu[139], G.H.A. Viehhauser[126], L. Vigani[63b], M. Villa[23b,23a], M. Villaplana Perez[163], E.M. Villhauer[52], E. Vilucchi[53], M.G. Vincter[34], G.S. Virdee[20], A. Vishwakarma[52], C. Vittori[36], I. Vivarelli[146], V. Vladimirov[167], E. Voevodina[110], F. Vogel[109], P. Vokac[132], J. Von Ahnen[48], E. Von Toerne[24], B. Vormwald[36], V. Vorobel[133], K. Vorobev[37], M. Vos[163], K. Voss[141], J.H. Vossebeld[92], M. Vozak[114], L. Vozdecky[94], N. Vranjes[15], M. Vranjes Milosavljevic[15], M. Vreeswijk[114], R. Vuillermet[36], O. Vujinovic[100], I. Vukotic[39], S. Wada[157], C. Wagner[103], W. Wagner[171], S. Wahdan[171], H. Wahlberg[90], R. Wakasa[157], M. Wakida[111], V.M. Walbrecht[110], J. Walder[134], R. Walker[109], W. Walkowiak[141], A.M. Wang[61], A.Z. Wang[170], C. Wang[100], C. Wang[62c], H. Wang[17a], J. Wang[64a], R.-J. Wang[100], R. Wang[61], R. Wang[6], S.M. Wang[148], S. Wang[62b], T. Wang[62a], W.T. Wang[80], X. Wang[14c], X. Wang[162], X. Wang[62c], Y. Wang[62d], Y. Wang[14c], Z. Wang[106], Z. Wang[62d,51,62c], Z. Wang[106], A. Warburton[104], R.J. Ward[20], N. Warrack[59], A.T. Watson[20], H. Watson[59], M.F. Watson[20], G. Watts[138], B.M. Waugh[96], A.F. Webb[11], C. Weber[29], H.A. Weber[18], M.S. Weber[19], S.M. Weber[63a], C. Wei[62a], Y. Wei[126], A.R. Weidberg[126], J. Weingarten[49], M. Weirich[100], C. Weiser[54], C.J. Wells[48],

T. Wenaus [29], B. Wendland [49], T. Wengler [36], N.S. Wenke[110], N. Wermes [24], M. Wessels [63a], K. Whalen [123], A.M. Wharton [91], A.S. White [61], A. White [8], M.J. White [1], D. Whiteson [160], L. Wickremasinghe [124], W. Wiedenmann [170], C. Wiel [50], M. Wielers [134], C. Wiglesworth [42], L.A.M. Wiik-Fuchs [54], D.J. Wilbern[120], H.G. Wilkens [36], D.M. Williams [41], H.H. Williams[128], S. Williams [32], S. Willocq [103], P.J. Windischhofer [126], F. Winklmeier [123], B.T. Winter [54], J.K. Winter [101], M. Wittgen[143], M. Wobisch [97], R. Wölker [126], J. Wollrath[160], M.W. Wolter [86], H. Wolters [130a,130c], V.W.S. Wong [164], A.F. Wongel [48], S.D. Worm [48], B.K. Wosiek [86], K.W. Woźniak [86], K. Wraight [59], J. Wu [14a,14d], M. Wu [64a], M. Wu [113], S.L. Wu [170], X. Wu [56], Y. Wu [62a], Z. Wu [135,62a], J. Wuerzinger [126], T.R. Wyatt [101], B.M. Wynne [52], S. Xella [42], L. Xia [14c], M. Xia[14b], J. Xiang [64c], X. Xiao [106], M. Xie [62a], X. Xie [62a], S. Xin [14a,14d], J. Xiong [17a], I. Xiotidis[146], D. Xu [14a], H. Xu[62a], H. Xu [62a], L. Xu [62a], R. Xu [128], T. Xu [106], W. Xu [106], Y. Xu [14b], Z. Xu [62b], Z. Xu [14a], B. Yabsley [147], S. Yacoob [33a], N. Yamaguchi [89], Y. Yamaguchi [154], H. Yamauchi [157], T. Yamazaki [17a], Y. Yamazaki [84], J. Yan[62c], S. Yan [126], Z. Yan [25], H.J. Yang [62c,62d], H.T. Yang [62a], S. Yang [62a], T. Yang [64c], X. Yang [62a], X. Yang [14a], Y. Yang [44], Y. Yang[62a], Z. Yang [62a,106], W-M. Yao [17a], Y.C. Yap [48], H. Ye [14c], H. Ye [55], J. Ye [44], S. Ye [29], X. Ye [62a], Y. Yeh [96], I. Yeletskikh [38], B.K. Yeo [17a], M.R. Yexley [91], P. Yin [41], K. Yorita [168], S. Younas [27b], C.J.S. Young [54], C. Young [143], Y. Yu [62a], M. Yuan [106], R. Yuan [62b,k], L. Yue [96], X. Yue [63a], M. Zaazoua [35e], B. Zabinski [86], E. Zaid[52], T. Zakareishvili [149b], N. Zakharchuk [34], S. Zambito [56], J.A. Zamora Saa [137d,137b], J. Zang [153], D. Zanzi [54], O. Zaplatilek [132], S.V. Zeißner [49], C. Zeitnitz [171], J.C. Zeng [162], D.T. Zenger Jr [26], O. Zenin [37], T. Ženiš [28a], S. Zenz [94], S. Zerradi [35a], D. Zerwas [66], M. Zhai [14a,14d], B. Zhang [14c], D.F. Zhang [139], J. Zhang [62b], J. Zhang [6], K. Zhang [14a,14d], L. Zhang [14c], P. Zhang[14a,14d], R. Zhang [170], S. Zhang [106], T. Zhang [153], X. Zhang [62c], X. Zhang [62b], Y. Zhang [62c,5], Z. Zhang [17a], Z. Zhang [66], H. Zhao [138], P. Zhao [51], T. Zhao [62b], Y. Zhao [136], Z. Zhao [62a], A. Zhemchugov [38], X. Zheng [62a], Z. Zheng [143], D. Zhong [162], B. Zhou[106], C. Zhou [170], H. Zhou [7], N. Zhou [62c], Y. Zhou[7], C.G. Zhu [62b], C. Zhu [14a,14d], H.L. Zhu [62a], H. Zhu [14a], J. Zhu [106], Y. Zhu [62c], Y. Zhu [62a], X. Zhuang [14a], K. Zhukov [37], V. Zhulanov [37], N.I. Zimine [38], J. Zinsser [63b], M. Ziolkowski [141], L. Živković [15], A. Zoccoli [23b,23a], K. Zoch [56], T.G. Zorbas [139], O. Zormpa [46], W. Zou [41], L. Zwalinski [36].

[1]Department of Physics, University of Adelaide, Adelaide; Australia.
[2]Department of Physics, University of Alberta, Edmonton AB; Canada.
[3(a)]Department of Physics, Ankara University, Ankara;[(b)]Division of Physics, TOBB University of Economics and Technology, Ankara; Türkiye.
[4]LAPP, Univ. Savoie Mont Blanc, CNRS/IN2P3, Annecy; France.
[5]APC, Université Paris Cité, CNRS/IN2P3, Paris; France.
[6]High Energy Physics Division, Argonne National Laboratory, Argonne IL; United States of America.
[7]Department of Physics, University of Arizona, Tucson AZ; United States of America.
[8]Department of Physics, University of Texas at Arlington, Arlington TX; United States of America.
[9]Physics Department, National and Kapodistrian University of Athens, Athens; Greece.
[10]Physics Department, National Technical University of Athens, Zografou; Greece.
[11]Department of Physics, University of Texas at Austin, Austin TX; United States of America.
[12]Institute of Physics, Azerbaijan Academy of Sciences, Baku; Azerbaijan.
[13]Institut de Física d'Altes Energies (IFAE), Barcelona Institute of Science and Technology, Barcelona; Spain.
[14(a)]Institute of High Energy Physics, Chinese Academy of Sciences, Beijing;[(b)]Physics Department, Tsinghua University, Beijing;[(c)]Department of Physics, Nanjing University, Nanjing;[(d)]University of

Chinese Academy of Science (UCAS), Beijing; China.
[15]Institute of Physics, University of Belgrade, Belgrade; Serbia.
[16]Department for Physics and Technology, University of Bergen, Bergen; Norway.
[17(a)]Physics Division, Lawrence Berkeley National Laboratory, Berkeley CA;[(b)]University of California, Berkeley CA; United States of America.
[18]Institut für Physik, Humboldt Universität zu Berlin, Berlin; Germany.
[19]Albert Einstein Center for Fundamental Physics and Laboratory for High Energy Physics, University of Bern, Bern; Switzerland.
[20]School of Physics and Astronomy, University of Birmingham, Birmingham; United Kingdom.
[21(a)]Department of Physics, Bogazici University, Istanbul;[(b)]Department of Physics Engineering, Gaziantep University, Gaziantep;[(c)]Department of Physics, Istanbul University, Istanbul;[(d)]Istinye University, Sariyer, Istanbul; Türkiye.
[22(a)]Facultad de Ciencias y Centro de Investigaciónes, Universidad Antonio Nariño, Bogotá;[(b)]Departamento de Física, Universidad Nacional de Colombia, Bogotá; Colombia.
[23(a)]Dipartimento di Fisica e Astronomia A. Righi, Università di Bologna, Bologna;[(b)]INFN Sezione di Bologna; Italy.
[24]Physikalisches Institut, Universität Bonn, Bonn; Germany.
[25]Department of Physics, Boston University, Boston MA; United States of America.
[26]Department of Physics, Brandeis University, Waltham MA; United States of America.
[27(a)]Transilvania University of Brasov, Brasov;[(b)]Horia Hulubei National Institute of Physics and Nuclear Engineering, Bucharest;[(c)]Department of Physics, Alexandru Ioan Cuza University of Iasi, Iasi;[(d)]National Institute for Research and Development of Isotopic and Molecular Technologies, Physics Department, Cluj-Napoca;[(e)]University Politehnica Bucharest, Bucharest;[(f)]West University in Timisoara, Timisoara;[(g)]Faculty of Physics, University of Bucharest, Bucharest; Romania.
[28(a)]Faculty of Mathematics, Physics and Informatics, Comenius University, Bratislava;[(b)]Department of Subnuclear Physics, Institute of Experimental Physics of the Slovak Academy of Sciences, Kosice; Slovak Republic.
[29]Physics Department, Brookhaven National Laboratory, Upton NY; United States of America.
[30]Universidad de Buenos Aires, Facultad de Ciencias Exactas y Naturales, Departamento de Física, y CONICET, Instituto de Física de Buenos Aires (IFIBA), Buenos Aires; Argentina.
[31]California State University, CA; United States of America.
[32]Cavendish Laboratory, University of Cambridge, Cambridge; United Kingdom.
[33(a)]Department of Physics, University of Cape Town, Cape Town;[(b)]iThemba Labs, Western Cape;[(c)]Department of Mechanical Engineering Science, University of Johannesburg, Johannesburg;[(d)]National Institute of Physics, University of the Philippines Diliman (Philippines);[(e)]University of South Africa, Department of Physics, Pretoria;[(f)]University of Zululand, KwaDlangezwa;[(g)]School of Physics, University of the Witwatersrand, Johannesburg; South Africa.
[34]Department of Physics, Carleton University, Ottawa ON; Canada.
[35(a)]Faculté des Sciences Ain Chock, Réseau Universitaire de Physique des Hautes Energies - Université Hassan II, Casablanca;[(b)]Faculté des Sciences, Université Ibn-Tofail, Kénitra;[(c)]Faculté des Sciences Semlalia, Université Cadi Ayyad, LPHEA-Marrakech;[(d)]LPMR, Faculté des Sciences, Université Mohamed Premier, Oujda;[(e)]Faculté des sciences, Université Mohammed V, Rabat;[(f)]Institute of Applied Physics, Mohammed VI Polytechnic University, Ben Guerir; Morocco.
[36]CERN, Geneva; Switzerland.
[37]Affiliated with an institute covered by a cooperation agreement with CERN.
[38]Affiliated with an international laboratory covered by a cooperation agreement with CERN.
[39]Enrico Fermi Institute, University of Chicago, Chicago IL; United States of America.

[40]LPC, Université Clermont Auvergne, CNRS/IN2P3, Clermont-Ferrand; France.
[41]Nevis Laboratory, Columbia University, Irvington NY; United States of America.
[42]Niels Bohr Institute, University of Copenhagen, Copenhagen; Denmark.
[43(a)]Dipartimento di Fisica, Università della Calabria, Rende;[(b)]INFN Gruppo Collegato di Cosenza, Laboratori Nazionali di Frascati; Italy.
[44]Physics Department, Southern Methodist University, Dallas TX; United States of America.
[45]Physics Department, University of Texas at Dallas, Richardson TX; United States of America.
[46]National Centre for Scientific Research "Demokritos", Agia Paraskevi; Greece.
[47(a)]Department of Physics, Stockholm University;[(b)]Oskar Klein Centre, Stockholm; Sweden.
[48]Deutsches Elektronen-Synchrotron DESY, Hamburg and Zeuthen; Germany.
[49]Fakultät Physik , Technische Universität Dortmund, Dortmund; Germany.
[50]Institut für Kern- und Teilchenphysik, Technische Universität Dresden, Dresden; Germany.
[51]Department of Physics, Duke University, Durham NC; United States of America.
[52]SUPA - School of Physics and Astronomy, University of Edinburgh, Edinburgh; United Kingdom.
[53]INFN e Laboratori Nazionali di Frascati, Frascati; Italy.
[54]Physikalisches Institut, Albert-Ludwigs-Universität Freiburg, Freiburg; Germany.
[55]II. Physikalisches Institut, Georg-August-Universität Göttingen, Göttingen; Germany.
[56]Département de Physique Nucléaire et Corpusculaire, Université de Genève, Genève; Switzerland.
[57(a)]Dipartimento di Fisica, Università di Genova, Genova;[(b)]INFN Sezione di Genova; Italy.
[58]II. Physikalisches Institut, Justus-Liebig-Universität Giessen, Giessen; Germany.
[59]SUPA - School of Physics and Astronomy, University of Glasgow, Glasgow; United Kingdom.
[60]LPSC, Université Grenoble Alpes, CNRS/IN2P3, Grenoble INP, Grenoble; France.
[61]Laboratory for Particle Physics and Cosmology, Harvard University, Cambridge MA; United States of America.
[62(a)]Department of Modern Physics and State Key Laboratory of Particle Detection and Electronics, University of Science and Technology of China, Hefei;[(b)]Institute of Frontier and Interdisciplinary Science and Key Laboratory of Particle Physics and Particle Irradiation (MOE), Shandong University, Qingdao;[(c)]School of Physics and Astronomy, Shanghai Jiao Tong University, Key Laboratory for Particle Astrophysics and Cosmology (MOE), SKLPPC, Shanghai;[(d)]Tsung-Dao Lee Institute, Shanghai; China.
[63(a)]Kirchhoff-Institut für Physik, Ruprecht-Karls-Universität Heidelberg, Heidelberg;[(b)]Physikalisches Institut, Ruprecht-Karls-Universität Heidelberg, Heidelberg; Germany.
[64(a)]Department of Physics, Chinese University of Hong Kong, Shatin, N.T., Hong Kong;[(b)]Department of Physics, University of Hong Kong, Hong Kong;[(c)]Department of Physics and Institute for Advanced Study, Hong Kong University of Science and Technology, Clear Water Bay, Kowloon, Hong Kong; China.
[65]Department of Physics, National Tsing Hua University, Hsinchu; Taiwan.
[66]IJCLab, Université Paris-Saclay, CNRS/IN2P3, 91405, Orsay; France.
[67]Centro Nacional de Microelectrónica (IMB-CNM-CSIC), Barcelona; Spain.
[68]Department of Physics, Indiana University, Bloomington IN; United States of America.
[69(a)]INFN Gruppo Collegato di Udine, Sezione di Trieste, Udine;[(b)]ICTP, Trieste;[(c)]Dipartimento Politecnico di Ingegneria e Architettura, Università di Udine, Udine; Italy.
[70(a)]INFN Sezione di Lecce;[(b)]Dipartimento di Matematica e Fisica, Università del Salento, Lecce; Italy.
[71(a)]INFN Sezione di Milano;[(b)]Dipartimento di Fisica, Università di Milano, Milano; Italy.
[72(a)]INFN Sezione di Napoli;[(b)]Dipartimento di Fisica, Università di Napoli, Napoli; Italy.
[73(a)]INFN Sezione di Pavia;[(b)]Dipartimento di Fisica, Università di Pavia, Pavia; Italy.
[74(a)]INFN Sezione di Pisa;[(b)]Dipartimento di Fisica E. Fermi, Università di Pisa, Pisa; Italy.
[75(a)]INFN Sezione di Roma;[(b)]Dipartimento di Fisica, Sapienza Università di Roma, Roma; Italy.
[76(a)]INFN Sezione di Roma Tor Vergata;[(b)]Dipartimento di Fisica, Università di Roma Tor Vergata,

Roma; Italy.
[77(a)]INFN Sezione di Roma Tre;[(b)]Dipartimento di Matematica e Fisica, Università Roma Tre, Roma; Italy.
[78(a)]INFN-TIFPA;[(b)]Università degli Studi di Trento, Trento; Italy.
[79]Universität Innsbruck, Department of Astro and Particle Physics, Innsbruck; Austria.
[80]University of Iowa, Iowa City IA; United States of America.
[81]Department of Physics and Astronomy, Iowa State University, Ames IA; United States of America.
[82(a)]Departamento de Engenharia Elétrica, Universidade Federal de Juiz de Fora (UFJF), Juiz de Fora;[(b)]Universidade Federal do Rio De Janeiro COPPE/EE/IF, Rio de Janeiro;[(c)]Instituto de Física, Universidade de São Paulo, São Paulo;[(d)]Rio de Janeiro State University, Rio de Janeiro; Brazil.
[83]KEK, High Energy Accelerator Research Organization, Tsukuba; Japan.
[84]Graduate School of Science, Kobe University, Kobe; Japan.
[85(a)]AGH University of Science and Technology, Faculty of Physics and Applied Computer Science, Krakow;[(b)]Marian Smoluchowski Institute of Physics, Jagiellonian University, Krakow; Poland.
[86]Institute of Nuclear Physics Polish Academy of Sciences, Krakow; Poland.
[87]Faculty of Science, Kyoto University, Kyoto; Japan.
[88]Kyoto University of Education, Kyoto; Japan.
[89]Research Center for Advanced Particle Physics and Department of Physics, Kyushu University, Fukuoka ; Japan.
[90]Instituto de Física La Plata, Universidad Nacional de La Plata and CONICET, La Plata; Argentina.
[91]Physics Department, Lancaster University, Lancaster; United Kingdom.
[92]Oliver Lodge Laboratory, University of Liverpool, Liverpool; United Kingdom.
[93]Department of Experimental Particle Physics, Jožef Stefan Institute and Department of Physics, University of Ljubljana, Ljubljana; Slovenia.
[94]School of Physics and Astronomy, Queen Mary University of London, London; United Kingdom.
[95]Department of Physics, Royal Holloway University of London, Egham; United Kingdom.
[96]Department of Physics and Astronomy, University College London, London; United Kingdom.
[97]Louisiana Tech University, Ruston LA; United States of America.
[98]Fysiska institutionen, Lunds universitet, Lund; Sweden.
[99]Departamento de Física Teorica C-15 and CIAFF, Universidad Autónoma de Madrid, Madrid; Spain.
[100]Institut für Physik, Universität Mainz, Mainz; Germany.
[101]School of Physics and Astronomy, University of Manchester, Manchester; United Kingdom.
[102]CPPM, Aix-Marseille Université, CNRS/IN2P3, Marseille; France.
[103]Department of Physics, University of Massachusetts, Amherst MA; United States of America.
[104]Department of Physics, McGill University, Montreal QC; Canada.
[105]School of Physics, University of Melbourne, Victoria; Australia.
[106]Department of Physics, University of Michigan, Ann Arbor MI; United States of America.
[107]Department of Physics and Astronomy, Michigan State University, East Lansing MI; United States of America.
[108]Group of Particle Physics, University of Montreal, Montreal QC; Canada.
[109]Fakultät für Physik, Ludwig-Maximilians-Universität München, München; Germany.
[110]Max-Planck-Institut für Physik (Werner-Heisenberg-Institut), München; Germany.
[111]Graduate School of Science and Kobayashi-Maskawa Institute, Nagoya University, Nagoya; Japan.
[112]Department of Physics and Astronomy, University of New Mexico, Albuquerque NM; United States of America.
[113]Institute for Mathematics, Astrophysics and Particle Physics, Radboud University/Nikhef, Nijmegen; Netherlands.

[114]Nikhef National Institute for Subatomic Physics and University of Amsterdam, Amsterdam; Netherlands.
[115]Department of Physics, Northern Illinois University, DeKalb IL; United States of America.
[116(a)]New York University Abu Dhabi, Abu Dhabi;[(b)]University of Sharjah, Sharjah; United Arab Emirates.
[117]Department of Physics, New York University, New York NY; United States of America.
[118]Ochanomizu University, Otsuka, Bunkyo-ku, Tokyo; Japan.
[119]Ohio State University, Columbus OH; United States of America.
[120]Homer L. Dodge Department of Physics and Astronomy, University of Oklahoma, Norman OK; United States of America.
[121]Department of Physics, Oklahoma State University, Stillwater OK; United States of America.
[122]Palacký University, Joint Laboratory of Optics, Olomouc; Czech Republic.
[123]Institute for Fundamental Science, University of Oregon, Eugene, OR; United States of America.
[124]Graduate School of Science, Osaka University, Osaka; Japan.
[125]Department of Physics, University of Oslo, Oslo; Norway.
[126]Department of Physics, Oxford University, Oxford; United Kingdom.
[127]LPNHE, Sorbonne Université, Université Paris Cité, CNRS/IN2P3, Paris; France.
[128]Department of Physics, University of Pennsylvania, Philadelphia PA; United States of America.
[129]Department of Physics and Astronomy, University of Pittsburgh, Pittsburgh PA; United States of America.
[130(a)]Laboratório de Instrumentação e Física Experimental de Partículas - LIP, Lisboa;[(b)]Departamento de Física, Faculdade de Ciências, Universidade de Lisboa, Lisboa;[(c)]Departamento de Física, Universidade de Coimbra, Coimbra;[(d)]Centro de Física Nuclear da Universidade de Lisboa, Lisboa;[(e)]Departamento de Física, Universidade do Minho, Braga;[(f)]Departamento de Física Teórica y del Cosmos, Universidad de Granada, Granada (Spain);[(g)]Departamento de Física, Instituto Superior Técnico, Universidade de Lisboa, Lisboa; Portugal.
[131]Institute of Physics of the Czech Academy of Sciences, Prague; Czech Republic.
[132]Czech Technical University in Prague, Prague; Czech Republic.
[133]Charles University, Faculty of Mathematics and Physics, Prague; Czech Republic.
[134]Particle Physics Department, Rutherford Appleton Laboratory, Didcot; United Kingdom.
[135]IRFU, CEA, Université Paris-Saclay, Gif-sur-Yvette; France.
[136]Santa Cruz Institute for Particle Physics, University of California Santa Cruz, Santa Cruz CA; United States of America.
[137(a)]Departamento de Física, Pontificia Universidad Católica de Chile, Santiago;[(b)]Millennium Institute for Subatomic physics at high energy frontier (SAPHIR), Santiago;[(c)]Instituto de Investigación Multidisciplinario en Ciencia y Tecnología, y Departamento de Física, Universidad de La Serena;[(d)]Universidad Andres Bello, Department of Physics, Santiago;[(e)]Instituto de Alta Investigación, Universidad de Tarapacá, Arica;[(f)]Departamento de Física, Universidad Técnica Federico Santa María, Valparaíso; Chile.
[138]Department of Physics, University of Washington, Seattle WA; United States of America.
[139]Department of Physics and Astronomy, University of Sheffield, Sheffield; United Kingdom.
[140]Department of Physics, Shinshu University, Nagano; Japan.
[141]Department Physik, Universität Siegen, Siegen; Germany.
[142]Department of Physics, Simon Fraser University, Burnaby BC; Canada.
[143]SLAC National Accelerator Laboratory, Stanford CA; United States of America.
[144]Department of Physics, Royal Institute of Technology, Stockholm; Sweden.
[145]Departments of Physics and Astronomy, Stony Brook University, Stony Brook NY; United States of

America.
[146]Department of Physics and Astronomy, University of Sussex, Brighton; United Kingdom.
[147]School of Physics, University of Sydney, Sydney; Australia.
[148]Institute of Physics, Academia Sinica, Taipei; Taiwan.
[149(a)]E. Andronikashvili Institute of Physics, Iv. Javakhishvili Tbilisi State University, Tbilisi;[(b)]High Energy Physics Institute, Tbilisi State University, Tbilisi;[(c)]University of Georgia, Tbilisi; Georgia.
[150]Department of Physics, Technion, Israel Institute of Technology, Haifa; Israel.
[151]Raymond and Beverly Sackler School of Physics and Astronomy, Tel Aviv University, Tel Aviv; Israel.
[152]Department of Physics, Aristotle University of Thessaloniki, Thessaloniki; Greece.
[153]International Center for Elementary Particle Physics and Department of Physics, University of Tokyo, Tokyo; Japan.
[154]Department of Physics, Tokyo Institute of Technology, Tokyo; Japan.
[155]Department of Physics, University of Toronto, Toronto ON; Canada.
[156(a)]TRIUMF, Vancouver BC;[(b)]Department of Physics and Astronomy, York University, Toronto ON; Canada.
[157]Division of Physics and Tomonaga Center for the History of the Universe, Faculty of Pure and Applied Sciences, University of Tsukuba, Tsukuba; Japan.
[158]Department of Physics and Astronomy, Tufts University, Medford MA; United States of America.
[159]United Arab Emirates University, Al Ain; United Arab Emirates.
[160]Department of Physics and Astronomy, University of California Irvine, Irvine CA; United States of America.
[161]Department of Physics and Astronomy, University of Uppsala, Uppsala; Sweden.
[162]Department of Physics, University of Illinois, Urbana IL; United States of America.
[163]Instituto de Física Corpuscular (IFIC), Centro Mixto Universidad de Valencia - CSIC, Valencia; Spain.
[164]Department of Physics, University of British Columbia, Vancouver BC; Canada.
[165]Department of Physics and Astronomy, University of Victoria, Victoria BC; Canada.
[166]Fakultät für Physik und Astronomie, Julius-Maximilians-Universität Würzburg, Würzburg; Germany.
[167]Department of Physics, University of Warwick, Coventry; United Kingdom.
[168]Waseda University, Tokyo; Japan.
[169]Department of Particle Physics and Astrophysics, Weizmann Institute of Science, Rehovot; Israel.
[170]Department of Physics, University of Wisconsin, Madison WI; United States of America.
[171]Fakultät für Mathematik und Naturwissenschaften, Fachgruppe Physik, Bergische Universität Wuppertal, Wuppertal; Germany.
[172]Department of Physics, Yale University, New Haven CT; United States of America.
[a] Also Affiliated with an institute covered by a cooperation agreement with CERN.
[b] Also at Borough of Manhattan Community College, City University of New York, New York NY; United States of America.
[c] Also at Bruno Kessler Foundation, Trento; Italy.
[d] Also at Center for High Energy Physics, Peking University; China.
[e] Also at Center for Interdisciplinary Research and Innovation (CIRI-AUTH), Thessaloniki ; Greece.
[f] Also at Centro Studi e Ricerche Enrico Fermi; Italy.
[g] Also at CERN, Geneva; Switzerland.
[h] Also at Département de Physique Nucléaire et Corpusculaire, Université de Genève, Genève; Switzerland.
[i] Also at Departament de Fisica de la Universitat Autonoma de Barcelona, Barcelona; Spain.
[j] Also at Department of Financial and Management Engineering, University of the Aegean, Chios; Greece.
[k] Also at Department of Physics and Astronomy, Michigan State University, East Lansing MI; United

States of America.
[l] Also at Department of Physics, Ben Gurion University of the Negev, Beer Sheva; Israel.
[m] Also at Department of Physics, California State University, East Bay; United States of America.
[n] Also at Department of Physics, California State University, Sacramento; United States of America.
[o] Also at Department of Physics, King's College London, London; United Kingdom.
[p] Also at Department of Physics, University of Fribourg, Fribourg; Switzerland.
[q] Also at Department of Physics, University of Thessaly; Greece.
[r] Also at Department of Physics, Westmont College, Santa Barbara; United States of America.
[s] Also at Hellenic Open University, Patras; Greece.
[t] Also at Institucio Catalana de Recerca i Estudis Avancats, ICREA, Barcelona; Spain.
[u] Also at Institut für Experimentalphysik, Universität Hamburg, Hamburg; Germany.
[v] Also at Institute of Applied Physics, Mohammed VI Polytechnic University, Ben Guerir; Morocco.
[w] Also at Institute of Particle Physics (IPP); Canada.
[x] Also at Institute of Physics and Technology, Ulaanbaatar; Mongolia.
[y] Also at Institute of Physics, Azerbaijan Academy of Sciences, Baku; Azerbaijan.
[z] Also at Institute of Theoretical Physics, Ilia State University, Tbilisi; Georgia.
[aa] Also at Lawrence Livermore National Laboratory, Livermore; United States of America.
[ab] Also at The Collaborative Innovation Center of Quantum Matter (CICQM), Beijing; China.
[ac] Also at TRIUMF, Vancouver BC; Canada.
[ad] Also at Università di Napoli Parthenope, Napoli; Italy.
[ae] Also at University of Chinese Academy of Sciences (UCAS), Beijing; China.
[af] Also at University of Colorado Boulder, Department of Physics, Colorado; United States of America.
[ag] Also at Washington College, Maryland; United States of America.
[*] Deceased